(12) INTERNATIONAL APPLICATION PUBLISHED UNDER THE PATENT COOPERATION TREATY (PCT)

(19) World Intellectual Property Organization
International Bureau

(43) International Publication Date
22 October 2015 (22.10.2015)

WIPO | PCT

(10) International Publication Number
WO 2015/160470 A2

(51) International Patent Classification:
A61K 49/10 (2006.01)

(21) International Application Number:
PCT/US2015/021578

(22) International Filing Date:
19 March 2015 (19.03.2015)

(25) Filing Language: English

(26) Publication Language: English

(30) Priority Data:
61/968,036 20 March 2014 (20.03.2014) US

(71) Applicant *(for all designated States except US)*: **THE TRUSTEES OF PRINCETON UNIVERSITY** [US/US]; One Nassau Hall, Princeton, NJ 08544 (US).

(72) Inventors; and
(71) Applicants *(for US only)*: **RABINOWITZ, Joshua, D.** [US/US]; No. 2 Greenholm Street, Princeton, NJ 08450 (US). **FAN, Jing** [CN/US]; 334 S Yellowstone Dr., Apt. 4, Madison, WI 53705 (US). **DUCKER, Gregory, S.** [US/US]; 130 Washington St., Apt 5, Rocky Hill, NJ 08553 (US).

(74) Agents: **AUERBACH, Jeffrey, I.** et al.; AuerbachSchrot LLC, 2200 Research Blvd., Suite 560, Rockville, MD 20850 (US).

(81) Designated States *(unless otherwise indicated, for every kind of national protection available)*: AE, AG, AL, AM, AO, AT, AU, AZ, BA, BB, BG, BH, BN, BR, BW, BY, BZ, CA, CH, CL, CN, CO, CR, CU, CZ, DE, DK, DM, DO, DZ, EC, EE, EG, ES, FI, GB, GD, GE, GH, GM, GT, HN, HR, HU, ID, IL, IN, IR, IS, JP, KE, KG, KN, KP, KR, KZ, LA, LC, LK, LR, LS, LU, LY, MA, MD, ME, MG, MK, MN, MW, MX, MY, MZ, NA, NG, NI, NO, NZ, OM, PA, PE, PG, PH, PL, PT, QA, RO, RS, RU, RW, SA, SC, SD, SE, SG, SK, SL, SM, ST, SV, SY, TH, TJ, TM, TN, TR, TT, TZ, UA, UG, US, UZ, VC, VN, ZA, ZM, ZW.

(84) Designated States *(unless otherwise indicated, for every kind of regional protection available)*: ARIPO (BW, GH, GM, KE, LR, LS, MW, MZ, NA, RW, SD, SL, ST, SZ, TZ, UG, ZM, ZW), Eurasian (AM, AZ, BY, KG, KZ, RU, TJ, TM), European (AL, AT, BE, BG, CH, CY, CZ, DE, DK, EE, ES, FI, FR, GB, GR, HR, HU, IE, IS, IT, LT, LU, LV, MC, MK, MT, NL, NO, PL, PT, RO, RS, SE, SI, SK, SM, TR), OAPI (BF, BJ, CF, CG, CI, CM, GA, GN, GQ, GW, KM, ML, MR, NE, SN, TD, TG).

Published:

— *without international search report and to be republished upon receipt of that report (Rule 48.2(g))*

— *with sequence listing part of description (Rule 5.2(a))*

(54) **Title**: NADPH PRODUCTION BY THE 10-FORMYL-THF PATHWAY, AND ITS USE IN THE DIAGNOSIS AND TREATMENT OF DISEASE

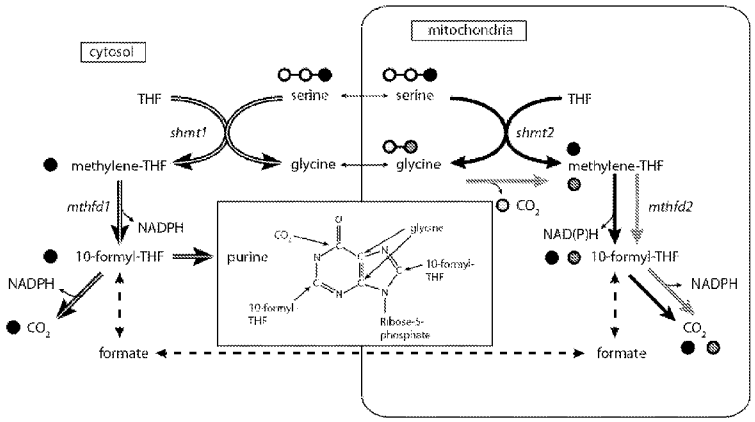

Figure 3A

(57) **Abstract**: The present invention relates to the recognition of a 10-formyl-THF pathway for producing NADPH, and to the use of that recognition in the diagnosis and treatment of cancer and metabolic disease, and in the development of new antineoplastic agents and/or regimens, and new therapeutics for treating metabolic disease.

WO 2015/160470 A2

Title of the Invention:

NADPH Production by the 10-Formyl-THF Pathway, and Its Use in the Diagnosis and Treatment of Disease

Cross-Reference to Related Applications:

[0001] This application claims priority to United States Patent Application Serial No. 61/968,036 (filed March 20, 2014; pending), which application is herein incorporated by reference in its entirety.

Statement Regarding Federally Sponsored Research or Development:

[0002] This invention was made with government support under AI097382 and CA105463, awarded by the National Institutes of Health. The government has certain rights in the invention.

Reference to Sequence Listing:

[0003] This application includes one or more Sequence Listings pursuant to 37 C.F.R. 1.821 *et seq*., which are disclosed in both paper and computer-readable media, and which paper and computer-readable disclosures are herein incorporated by reference in their entirety.

Background of the Invention:

Field of the Invention:

[0004] The present invention relates to the recognition of a 10-formyl-THF pathway for producing NADPH, and to the use of that recognition in the diagnosis and treatment of cancer and metabolic disease, and in the development of new antineoplastic agents and/or regimens, and new therapeutics for treating metabolic disease.

Description of Related Art:

[0005] Humans and other animals derive the energy needed to perform work by recovering chemical energy from ingested foods. Such energy, whether stored as sugar, starch or fat, is ultimately transferred to high-energy compounds for actual use. Adenosine triphosphate ("**ATP**") is the dominant high-energy compound for, *e.g.*,

muscle contraction and neuronal firing). However, an equally important role is played by nicotinamide adenine dinucleotide phosphate ("**NADPH**"), which powers redox defense and provides the energy needed for biosynthetic reactions (Voet, D.V. *et al.* (2004) BIOCHEMISTRY (3rd Ed.), John Wiley & Sons). NADPH differs from NADH in the possession of a phosphate group. However, this difference permits the two molecules to have independent regulation and independent functions. Most commonly, NADPH participates in reactions that consume energy in order build up or synthesize larger molecules ("**anabolic reactions**"); NADH participates in reactions that break down molecules to release energy ("**catabolic reactions**") (Agledal, L. *et al.* (2010) "*The Phosphate Makes A Difference: Cellular Functions Of NADP*," Redox Rep. 15(1):2-10).

[0006] ATP is produced both in the cellular cytosol, via the anaerobic conversion of glucose and glycerol to pyruvate ("**glycolysis**") and in the mitochondria via the aerobic conversion of glucose to water and CO_2 ("**respiration**"). NADPH is most directly produced from glucose in the cytosol via the oxidative pentose phosphate pathway ("**oxPPP**"); however a portion of the body's NAPDH is produced in both the cytosol and the mitochondria by decarboxylating malate dehydrogenases.

[0007] Cells can obtain ATP both from cytosolic and mitochondrial processes, and the relative proportion of cytosolic vs. mitochondrial production of ATP has been found to be correlated with the presence of disease, including cancer, a recognition now referred to as the "**Warburg Effect**" (Warburg, O. (1956) "*On The Origin* Of *Cancer Cells*," Science 123:309-314; Vander Heiden, M.G. *et al.* (2009) "*Understanding The Warburg Effect: The Metabolic Requirements Of Cell Proliferation*," Science 324:1029-1033; Razungles, J. *et al.* (2013) "[*The Warburg Effect: From Theory To Therapeutic Applications In Cancer*]," Med Sci (Paris). (11):1026-1033; Palsson-McDermott, E.M. *et al.* (2013) "*The Warburg Effect Then And Now: From Cancer To Inflammatory Diseases*," Bioessays 35(11):965-973; Jang, M. *et al.* (2013) "*Cancer Cell Metabolism: Implications For Therapeutic Targets*," Exp. Molec. Med. 45:e45. doi: 10.1038/emm.2013.85; Nam, S.O. *et al.* (2013) "*Possible Therapeutic Targets Among The Molecules Involved In The Warburg Effect In Tumor Cells*," Anticancer Res. 33(7):2855-2860; Upadhyay, M. *et al.* (2012) "*The*

Warburg Effect: Insights From The Past Decade," Pharmacol. Ther. 137(3):318-330; Dang, C.V. (2012) "*Links Between Metabolism And Cancer*," Genes Dev. 26(9):877-890; Ponisovskiy, M.R. (2011) "*Warburg Effect Mechanism As The Target For Theoretical Substantiation Of A New Potential Cancer Treatment*," Crit. Rev. Eukaryot. Gene. Expr. 21(1):13-28; Fogg, V.C. *et al.* (2011) "*Mitochondria In Cancer: At The Crossroads Of Life And Death*," Chin. J. Cancer 30(8):526-539; Dang, C.V. (2011) "*Therapeutic Targeting Of Cancer Cell Metabolism*," J. Molec. Med. (Berl) 89(3):205-212; Ferreira, L.M. (2010) "*Cancer Metabolism: The Warburg Effect Today*," Exp. Molec. Pathol. 89(3):372-380; Gogvadze, V. *et al.* (2009) "*The Warburg Effect And Mitochondrial Stability In Cancer Cells*," Molec. Aspects Med. 31(1):60-74).

[0008] Specifically, most cancer cells actively ferment glucose into lactic acid in the cytosol, thereby producing significantly more ATP via glycolysis than is the case in most normal cells (Alfarouk, K.O. *et al.* (2011) "*Tumor Acidity As Evolutionary Spite*," Cancers 3(4):408-414; Gatenby, R.A. *et al.* (2004) "*Why Do Cancers Have High Aerobic Glycolysis*?" Nature Reviews Cancer 4(11):891-899; Kim, J.W. (2006) "*Cancer's Molecular Sweet Tooth And The Warburg Effect*," Cancer Res. 66(18):8927-8930). Malignant, rapidly growing tumor cells typically have glycolytic rates up to 200 times higher than those of their normal tissues of origin, even in the presence of oxygen. Research has demonstrated that the Warburg Effect is caused by mutations in oncogenes and tumor suppressor genes.

[0009] The Warburg Effect has important medical applications as high aerobic glycolysis by malignant tumors may be used clinically to diagnose and monitor treatment responses of cancers (Lin, G. *et al.* (2014) "*Current Opportunities And Challenges Of Magnetic Resonance Spectroscopy, Positron Emission Tomography, And Mass Spectrometry Imaging For Mapping Cancer Metabolism in vivo*," Biomed. Res. Int. 2014:625095 doi: 10.1155/2014/625095; Boland, M.L. *et al.* (2013) "*Mitochondrial Dysfunction In Cancer*," Front. Oncol. 3:292; Witkiewicz, A.K. *et al.* (2012) "*Using The "Reverse Warburg Effect" To Identify High-Risk Breast Cancer Patients: Stromal MCT4 Predicts Poor Clinical Outcome In Triple-Negative Breast Cancers*," Cell Cycle 11(6):1108-1117).

[0010] The production of NADPH has also been found to differ in cancer cells relative to normal cells (D'Alessandro, A. *et al.* (2013) "*Proteomics And Metabolomics In Cancer Drug Development*," Expert Rev. Proteomics 10(5):473-488; Wen, S. *et al.* (2013) "*Targeting Cancer Cell Mitochondria As A Therapeutic Approach*," Future Med. Chem. 5(1):53-67; Dang, C.V. (2012) "*Links Between Metabolism And Cancer*," Genes Dev. 26(9):877-990; Cui, X. (2012) "*Reactive Oxygen Species: The Achilles' Heel Of Cancer Cells?*" Antioxid. Redox Signal. 16(11):1212-1214; Stanton, R.C. (2012) "*Glucose-6-Phosphate Dehydrogenase, NADPH, And Cell Survival*," IUBMB Life 64(5):362-369).

[0011] The production of NADPH in oxPPP has been found to be usually high in rapidly proliferating tumor cells (Patra, K.C. *et al.* (2014) "*The Pentose Phosphate Pathway And Cancer*," Trends Biochem. Sci. doi.org/10.1016/j.tibs.2014.06.005). Protection against oxidative stress is especially important for cancer cells. Thus, the enhanced production of NADPH in such cells may be a means for protecting cancer cells from oxidative stress. It can also contribute to drug resistance (Irwin, M.E. *et al.* (2013) "*Redox Control Of Leukemia: From Molecular Mechanisms To Therapeutic Opportunities*," Antioxid. Redox Signal. 18(11):1349-1383; Bonner, M.Y. *et al.* (2012) "*Targeting NADPH Oxidases For The Treatment Of Cancer And Inflammation*," Cell. Mol. Life Sci. 69(14):2435-2442).

[0012] An understanding of the routes of ATP production and consumption, first achieved more than a half century ago, has formed the foundation for much of subsequent metabolism research and has provided a means for discriminating between cancer cells and normal cells. (Warburg, O. (1956) "*On The Origin Of Cancer Cells*," Science 123:309-314). An analogous understanding of the routes of NADPH production and consumption is likewise central to a global understanding of metabolism. The ability to quantitatively analyze NADPH metabolism would thus provide a means for assessing the aggressiveness of a cancer, its amenability to treatment and its responsiveness to a treatment regimen. However, despite all prior work, a need remains for methods suitable for measuring, especially quantitatively, the respective contributions of NADPH production pathways to the total cellular NADPH production. The present invention is directed to these and other goals.

Summary of the Invention:

[0013] The present invention relates to the recognition of a 10-formyl-THF pathway for producing NADPH, and to the use of that recognition in the diagnosis and treatment of cancer and metabolic disease, and in the development of new antineoplastic agents and/or regimens, and new therapeutics for treating metabolic disease (Fan, K. *et al.* (2014) "*Quantitative Flux Analysis Reveals Folate-Dependent NADPH Production*," Nature 510(7504):298-302, herein incorporated by reference in its entirety).

[0014] As indicated above, although the relative contribution of glycolysis and oxidative phosphorylation to ATP production has been extensively analyzed, similar analysis of NADPH metabolism has been lacking. The present invention demonstrates the ability to directly track, by liquid chromatography-mass spectrometry, the passage of deuterium from labeled substrates into NADPH, and in combination with carbon labeling and mathematical modeling, permits the measurement of NADPH fluxes. In proliferating cells, the largest contributor to cytosolic NADPH is the oxPPP. Surprisingly, one finding of the present invention is that a nearly comparable contribution can come from serine-driven one-carbon metabolism, where oxidation of methylene-tetrahydrofolate to 10-formyl-tetrahydrofolate is coupled to the reduction of NADP+ to NADPH. Moreover, the tracing of mitochondrial one-carbon metabolism revealed complete oxidation of the one carbon unit to make NADPH.

[0015] Since folate metabolism has not previously been considered an NADPH producer, confirmation of its functional significance was undertaken through knockdown of methylene-tetrahydrofolate dehydrogenase (MTHFD) genes. Depletion of either the cytosolic or mitochondrial MTHFD isozyme resulted in decreased cellular ratios of NADPH to NADP+ and GSH to GSSG ratios and increased cell sensitivity to oxidative stress. Thus, while the importance of folate metabolism for proliferating cells has been long recognized and attributed to its function of producing one-carbon units for nucleic acid synthesis, another crucial function of this pathway is generating reducing power. This recognition points to novel therapies for cancer, including regimens that comprise an anti-folate drug and

one or more of the classical end products of folate metabolism as rescue agent(s), since provision of such an products will not obviate the need of the folate pathway to make NADPH and therefore the anti-folate may retain clinical efficacy despite provision of the classical pathways and products. Such therapies may have superior therapeutic indices, i.e., ratio of therapeutic benefits to side effects, or equivalently cancer specificity, than current treatment.

[0016] In detail, the invention provides a method of assessing the suitability of a cancer therapy for a particular cancer patient, wherein the cancer therapy comprises the administration of an anticancer agent, which method comprises:

(A) administering a deuterium-labeled substrate of a biomolecule and the anticancer agent to tumor cells of the patient; and

(B) determining the extent of deuterium labeling of the biomolecule by the tumor cells;

wherein a determination that the rate of the deuterium labeling is elevated relative to that of healthy cells, and is not substantially reduced over the course of the cancer therapy is indicative of the non-suitability of the therapy for the particular patient.

[0017] The invention further provides the embodiment of the above-described method wherein the deuterium-labeled substrate and the anticancer agent are administered to the patient, and wherein the rate of the deuterium labeling is determined *in vivo*.

[0018] The invention further provides the embodiment of the above-described method wherein the deuterium-labeled substrate and the anticancer agent are administered to tumor cells removed from the patient, and wherein the rate of the deuterium labeling is determined *in vitro*.

[0019] The invention further provides the embodiment of the above-described method wherein the anticancer agent is administered to the patient and the deuterium-labeled substrate is administered to tumor cells removed from the patient, and wherein the rate of the deuterium labeling is determined *in vitro*.

[0020] The invention further provides the embodiment of any of the above-described methods wherein the deuterium-labeled substrate is a substrate of a redox-active hydride of NADPH and the deuterium-labeled biomolecules comprise the redox-active hydride of NADH.

[0021] The invention further provides the embodiment of any of the above-described methods wherein the deuterium-labeled substrate is a substrate of a redox-active hydride of NADPH and the deuterium-labeled biomolecules comprise the redox-active hydride of NADPH.

[0022] The invention further provides the embodiment of any of the above-described methods wherein the deuterium-labeled substrate is a substrate of a molecule having a fatty acid moiety and the deuterium-labeled biomolecules comprise the molecule having the fatty acid moiety.

[0023] The invention further provides the embodiment of any of the above-described methods wherein the deuterium-labeled substrate is a substrate of a thymine moiety-containing biomolecule and the deuterium-labeled biomolecules comprise the thymine moiety-containing biomolecule.

[0024] The invention further provides the embodiment of any of the above-described methods wherein the cancer therapy comprises inhibiting cytosolic folate metabolism, wherein the deuterium-labeled substrate is a serine molecule that comprises deuteration at serine carbon C-3, and wherein the extent of deuterium labeling of the one or more biomolecules by the tumor cells is determined by measuring the ratio of M+1 to M+2 of deuterated thymine or of a molecule that comprises a deuterated thymine moiety.

[0025] The invention further provides the embodiment of any of the above-described methods wherein the cancer therapy comprises inhibiting mitochondrial folate metabolism, wherein the deuterium-labeled substrate is a serine molecule that comprises deuteration at serine carbon C-3, and wherein the extent of deuterium labeling of the one or more biomolecules by the tumor cells is determined by

measuring the ratio of M+1 to M+2 of deuterated thymine or of a molecule that comprises a deuterated thymine moiety.

[0026] The invention further provides the embodiment of any of the above-described methods wherein the cancer therapy comprises inhibiting cytosolic folate metabolism, wherein the deuterium-labeled substrate is a serine molecule that comprises deuteration at serine carbon C-3, and wherein the extent of deuterium labeling of the one or more biomolecules by the tumor cells is determined by measuring the production of a ^{2}H-labeled fatty acid moiety.

[0027] The invention further provides the embodiment of any of the above-described methods wherein the cancer therapy comprises inhibiting mitochondrial folate metabolism, wherein the deuterium-labeled substrate is a serine molecule that comprises deuteration at serine carbon C-3, and wherein the extent of deuterium labeling of the one or more biomolecules by the tumor cells is determined by measuring the production of a ^{2}H-labeled fatty acid moiety.

[0028] The invention further provides the embodiment of any of the above-described methods wherein the deuterium-labeled substrate is 2,3,3-^{2}H-serine or 3,3-^{2}H-serine.

[0029] The invention further provides the embodiment of any of the above-described methods wherein the extent of deuterium labeling is determined using magnetic resonance imaging (MRI).

[0030] The invention further provides the embodiment of any of the above-described methods wherein the extent of deuterium labeling is determined using Liquid Chromatography-Mass Spectroscopy (LC-MS), Gas Chromatography-Mass Spectroscopy (GC-MS) or Raman spectroscopy.

[0031] The invention further provides the embodiment of any of the above-described methods wherein the anticancer agent is selected from the group consisting of a Non-Specific Chemotherapeutic Agent and a Target Specific Chemotherapeutic Agent.

[0032] The invention further provides the embodiment of any of the above-described methods wherein the anticancer agent is an Immunotherapeutic Agent, and is selected from the group consisting of an antibody, a molecule that comprises an epitope-binding fragment of an antibody, and a diabody.

[0033] The invention further provides a method of treating cancer in a cancer patient, wherein the method comprises administering to the cancer patient a pharmaceutical composition comprising:

(A) an anti-folate anticancer agent; and

(B) one or more metabolic compounds selected from the group consisting of thymine, a molecule that comprises a thymine moiety, formate, a molecule that comprises a formate moiety, glycine and a purine; and

(C) a pharmaceutically acceptable excipient, carrier or diluent;

wherein the composition contains the anti-folate anticancer agent in an amount sufficient to treat the cancer and contains the metabolic compound(s) in amount(s) sufficient to remediate attenuation of the concentration of the metabolic compound(s) by the anti-folate anticancer agent or to attenuate an adverse side effect caused by the administered anti-folate anticancer agent.

[0034] The invention further provides the embodiment of such method wherein the one or more metabolic compounds is thymidine.

[0035] The invention further provides the embodiment of all such methods, wherein the tumor cells are tumor cells of: an adrenal gland tumor, an AIDS-associated cancer, an alveolar soft part sarcoma, an astrocytic tumor, bladder cancer, bone cancer, a brain and spinal cord cancer, a metastatic brain tumor, a breast cancer, a carotid body tumor, a cervical cancer, a chondrosarcoma, a chordoma, a chromophobe renal cell carcinoma, a clear cell carcinoma, a colon cancer, a colorectal cancer, a cutaneous benign fibrous histiocytoma, a desmoplastic small round cell tumor, an ependymoma, a Ewing's tumor, an extraskeletal myxoid chondrosarcoma, a fibrogenesis imperfecta ossium, a fibrous dysplasia of the bone, a gallbladder or bile duct cancer, gastric cancer, a gestational trophoblastic disease, a germ cell tumor, a head and neck cancer, hepatocellular carcinoma, an islet cell tumor, a Kaposi's sarcoma, a kidney cancer, a

leukemia, a lipoma/benign lipomatous tumor, a liposarcoma/malignant lipomatous tumor, a liver cancer, a lymphoma, a lung cancer, a medulloblastoma, a melanoma, a meningioma, a multiple endocrine neoplasia, a multiple myeloma, a myelodysplastic syndrome, a neuroblastoma, a neuroendocrine tumors, an ovarian cancer, a pancreatic cancer, a papillary thyroid carcinoma, a parathyroid tumor, a pediatric cancer, a peripheral nerve sheath tumor, a phaeochromocytoma, a pituitary tumor, a prostate cancer, a posterior uveal melanoma, a rare hematologic disorder, a renal metastatic cancer, a rhabdoid tumor, a rhabdomysarcoma, a sarcoma, a skin cancer, a soft-tissue sarcoma, a squamous cell cancer, a stomach cancer, a synovial sarcoma, a testicular cancer, a thymic carcinoma, a thymoma, a thyroid metastatic cancer, or a uterine cancer.

Brief Description of the Drawings:

[0036] **Figures 1A-1H** show the quantitation of NADPH labeling via oxPPP and of total cytosolic NADPH production. **Figure 1A** provides an oxPPP pathway schematic diagram. **Figure 1B** shows mass spectra of NADPH (**Figure 1B, Panel (A)**) and NADP+ (**Figure 1B, Panel (B)**) from cells labeled with 1-^{2}H-glucose (iBMK-parental cells, 20 min). **Figure 1C** shows the kinetics of NADPH labeling from 1-^{2}H-glucose (iBMK-parental cells). **Figure 1D** shows NADPH labeling from 1-^{2}H-glucose (20 min). **Figure 1E** shows that 1-^{2}H-glucose and 3-^{2}H-glucose yield similar NADPH labeling (iBMK-parental cells, 20 min). Substrate labeling is reported for glucose-6-phosphate for 1-^{2}H-glucose and 6-phosphogluconate for 3-^{2}H-glucose. **Figure 1F** provides a schematic illustrating that the total cytosolic NADP+ reduction flux is the absolute oxPPP flux (measured based on ^{14}CO2 excretion) divided by the fractional oxPPP contribution (measured based on NADPH ^{2}H-labeling). **Figure 1G** shows OxPPP flux based on difference in 14C-CO2 release from 1-^{14}C- and 6-^{14}C-glucose. **Figure 1H** shows total cytosolic NADP+ reduction flux. All results are mean ± SD, N≥ 2 biological replicates from a single experiment and were confirmed in multiple experiments.

[0037] **Figures 2A-2F** show pathways contributing to NADPH production. **Figure 2A** shows canonical NADPH production pathways. **Figure 2B** shows NADPH and NADP+ isotopic distribution (without correction for natural isotope abundances) after

incubation with 2,3,3,4,4-^{2}H-glutamine tracer to probe NADPH production via glutamate dehydrogenase and malic enzyme (HEK293T cells, 20 min). See also **Figures 8A-8H**. **Figure 2C** shows NADPH and NADP+ isotopic distribution as in **Figure 2B** using 2,3,3-^{2}H–aspartate tracer to probe NADPH production via IDH. See also **Figures 8A-8H**. **Figure 2D** shows NADPH production routes predicted by experimentally-constrained genome-scale flux balance analysis. **Figure 2E** shows NADPH and NADP+ isotopic distribution as in **Figure 2B** using 2,3,3-^{2}H-serine tracer to probe NADPH production via folate metabolism (no glycine in the media). See also **Figures 9A-9D**. **Figure 2F** shows the relative NADPH to NADP+ ratio in HEK293T cells with knockdown of various potential NADPH-producing enzymes: glucose-6-phosphate dehydrogenase (G6PD), cytosolic malic enzyme (ME1), cytosolic and mitochondrial isocitrate dehydrogenase (IDH1 and IDH2), transhydrogenase (NNT), and cytosolic and mitochondrial methylene-tetrahydrofolate dehydrogenase (MTHFD1 and MTHFD2). Plotted ratios are relative to vector control knockdown. Results are mean ± SD, N ≥ 2 biological replicates from a single experiment and were confirmed in multiple experiments.

[0038] **Figures 3A-3J** show the quantitation of folate-dependent NADPH production. **Figure 3A** shows a pathway schematic depicting the role played by serine and glycine in NADPH production. **Figure 3B** shows the glycine and ATP labeling pattern after incubation with U-^{13}C-glycine (HEK293T cells, 24 h). The lack of M+3 and M+4 ATP indicates that no glycine-derived one-carbon units contributed to purine synthesis. **Figure 3C** shows the fraction of NADPH labeled at the redox-active hydrogen after 24 h incubation with 2,3,3-^{2}H-serine in HEK293T cells with stable MTHFD1 or MTHFD2 knockdown. The same cells were used also in **Figures 3F-3I**. **Figure 3D** shows the absolute rate of cytosolic folate-dependent NADPH production. **Figure 3E** shows the CO_2 release rate from glycine C1 and glycine C2. **Figure 3F** shows the GSH/GSSG ratio. **Figure 3G** shows the relative growth, normalized to untreated samples, during 48 h exposure to H_2O_2. **Figure 3H** shows the fractional death observed after 24 h exposure to 250 μM H2O2. **Figure 3I** shows the fractional death observed after 24 h exposure to 300 μM diamide. **Figure 3J** shows the relative reactive oxygen species ("**ROS**") levels measured using DCFH assay. Mean ± SD, N=3.

[0039] **Figures 4A-4B** show a comparison of NADPH production and consumption. **Figure 4A** shows the major NADPH consumption pathways. **Figure 4B** shows cytosolic NADPH production and consumption fluxes. Mean ± SD, with error bar showing the variation of total production or consumption, N = 3.

[0040] **Figures 5A-5G** probe the fractional contribution of the oxPPP to NADPH production with ^{2}H-glucose. **Figure 5A** shows an example of LC-MS chromatogram of M+0 and M+1 forms of NADPH (**Figure 5A, Panel (A)**) and NADP+ (**Figure 5A, Panel (B)**) Plotted values are 5 ppm mass window around each compound. **Figure 5B** shows that the extent of NADPH labeling should be corrected for the extent of glucose-6-phosphate labeling. Incomplete labeling can occur due to influx from glycogen or ^{1}H/^{2}H ("**H/D**") exchange. **Figure 5C** shows the labeling fraction of glucose-6-phosphate and fructose-1,6-phosphate in iBMK cells with and without activated Akt (20 min after switching into 1-^{2}H-glucose). **Figure 5D** shows the labeling fraction of fructose-1,6-phosphate and 6-phosphogluconate after feeding 1-^{2}H-glucose. The labeling fraction of fructose-1,6-phosphate reflects the labeling of glucose-6-phosphate, whose peak after addition of the ^{2}H-glucose was not sufficiently resolved from other LC-MS peaks in HEK293T and MDA-MB-468 cells to allow precise quantitation of its labeling directly. The difference in the labeling fraction between glucose-6-phosphate and 6-phosphogluconate reflects the fraction of deuterium labeling specifically at position 1 of glucose-6-phosphate. **Figure 5E** shows that due to the kinetic isotope effect, feeding of deuterium tracer can potentially alter pathway fluxes. To assess whether the feeding of 1-^{2}H-glucose creates a bottleneck in the oxPPP, the relative concentration of oxPPP intermediates glucose-6-phosphate (**Figure 5E, Panel (A)**) and 6-phospho-gluconate (**Figure 5E, Panel (B)**) with or without feeding of 1-^{2}H-glucose was measured. No significant changes were observed. **Figure 5F** shows the impact of different mechanisms of correcting for the deuterium kinetic isotope effect on fractional contribution of oxPPP to NADPH production. **Figure 5G** shows the impact of different mechanisms of correcting for the deuterium kinetic isotope effect on calculated total NADPH production rate. The correction mechanisms are: (i) no kinetic isotope effect (C_{KIE} = 1), (ii) no impact on total pathway flux but preferential utilization of ^{1}H over ^{2}H-labeled substrate (**Equation 4**) (the smallest reasonable correction, and the one

applied herein, where not otherwise indicated), or (iii) full kinetic isotope effect observed for the isolate enzyme with associated decrease in total pathway flux (**Equation 5**) (the largest reasonable correction). All results are mean ± SD, N ≥ 2 biological replicates from a single experiment and were confirmed in multiple experiments.

[0041] **Figures 6A-6G** show that two independent measurement methods give consistent oxPPP fluxes. **Figure 6A** provides a diagram of 1-^{14}C-glucose and 6-^{14}C-glucose metabolism through glycolysis and the pentose phosphate pathway. The oxPPP specifically releases glucose C1 as CO_2, whereas all other CO_2-releasing reactions are downstream of triose phosphate isomerase (TPI). As TPI renders C1 and C6 of glucose indistinguishable (both positions become C3 of glyceraldehyde-3-phosphate), the difference in CO_2 release from C1 versus C6, multiplied by two, gives the absolute rate of NADPH production via oxPPP. A potential complication involves carbon scrambling via the reactions of the non-oxidative PPP, but this was insignificant (see **Figures 7A-7F**). **Figure 6B** shows the complete carbon labeling of glucose-6-phosphate. Glucose-6-phosphate labeled completely (> 99%) within 2 h of switching cells into U-^{13}Cglucose. **Figure 6C** shows the CO_2 release rate from 1-^{14}C-glucose and 6-^{14}C-glucose. **Figure 6D** shows the pool size of 6-phosphogluconate. **Figure 6E** (**Panels A-D**) shows the kinetics of glucose-6-phosphate and 6-phosphogluconate labeling upon switching cells to U-^{13}C-glucose. **Figure 6F, Panels A-D** shows an overlay upon the 6-phosphogluconate data from **Figure 6E** of simulated labeling curves based on the flux that best fits the labeling kinetics (dashed) and the flux from $^{14}CO_2$ release measurements (solid). **Figure 6G** shows the calculated fluxes and 95% confidence intervals based on the kinetics of 6-phosphogluconate labeling from U-^{13}C- glucose, compared to radioactive CO_2 release from 1-^{14}C- glucose and 6-^{14}C- glucose. The two approaches give consistent results, with the $^{14}CO_2$ release data being more precise. Mean + SD, N=3.

[0042] **Figures 7A-7F** show the extent of carbon scrambling via non-oxPPP is insufficient to impact substantially oxPPP flux determination using 1-^{14}C and 6-^{14}C-glucose, with most carbon entering oxPPP directed towards nucleotide synthesis. **Figure 7A** provides a schematic of glycolysis and PPP showing fate of glucose C6.

Note that glucose C6 occupies the phosphorylated position (*i.e.*, the last carbon) in every intermediate. Thus, upon catabolism to pyruvate, glucose C6 always becomes pyruvate C3, irrespective of any potential scrambling reactions. **Figure 7B** provides a schematic of glycolysis and PPP showing the fate of glucose C1. Glucose C1 can be scrambled via the non-oxPPP, moving to C3 (black dashed boxes) or C6, as shown in the Figure. The forms shown in the gray dashed boxes were not experimentally observed. As glucose C3 becomes pyruvate C1 (the carboxylic acid carbon of pyruvate), which is selectively released as CO_2 by pyruvate dehydrogenase, scrambling of C1 to C3 can potentially increase CO_2 release from glucose C1 relative to C6. This is ruled out in **Figure 7D** and **Figure 7E**. **Figure 7C** shows that feeding 1-^{13}C-glucose or 6-^{13}C-glucose results in 50% labeling of 3-phosphoglycerate without any double labeling (*i.e.*, M+2), as expected in the absence of scrambling. **Figure 7D** shows the use of the MS/MS method to analyze positional labeling of 1-labeled pyruvate. Collision induced dissociation breaks pyruvate to release the carboxylic acid group as CO_2. If the daughter peak of 1-labeled pyruvate does not contain labeled carbon (M/z = 43), the labeling is at the C1 position; otherwise, it is at C2 or C3. **Figure 7E** shows that after feeding 1-^{13}C-glucose or 6-^{13}C-glucose, pyruvate is not labeled at the C1 position (<0.5%), ruling out extensive scrambling. **Figure 7F** shows that the OxPPP flux is similar to or smaller than ribose demand for nucleotide synthesis. Mean + SD, N=3.

[0043] **Figures 8A-8H** probe the contribution of alternative NADPH-producing pathways. **Figure 8A** provides a pathway diagram showing the potential for 2,3,3,4,4-^{2}H-glutamine to label NADPH via glutamate dehydrogenase and via malic enzyme. Labeled hydrogens are shown in bold. **Figure 8B** shows NADP+ and NADPH labeling patterns (without correction for natural 13C-abundance) after 48 h incubation with 2,3,3,4,4-^{2}H-glutamine. The indistinguishable labeling of NADP+ and NADPH implies lack of NADPH redox-active hydrogen labeling. **Figure 8C** provides a pathway diagram showing the potential for 2,3,3-^{2}H-aspartate to label NADPH via isocitrate dehydrogenase. **Figure 8D** shows NADP+ and NADPH labeling patterns (without correction for natural ^{13}C-abundance) after 48 h incubation with 2,3,3-^{2}H-aspartate. The indistinguishable labeling of NADP+ and NADPH implies lack of redox-active hydrogen labeling. Lack of detectable labeling may be

due to insufficient substrate labeling or H/D exchange. **Figure 8E** provides a diagram of 2,3,3,4,4-^{2}H-glutamine metabolism through TCA cycle, tracing labeled hydrogen. Hydrogen atoms shown in lighter shade indicate potential H/D exchange with water. **Figure 8F** shows the malate labeling fraction after cells were fed 2,3,3,4,4-^{2}H-glutamine for 48 h. **Figure 8G** provides a pathway diagram showing the potential for 1,2,3-^{13}C-malate (made by feeding U-^{13}C-glutamine) to label pyruvate and lactate via malic enzyme. **Figure 8H** shows the extent of malate (**Figure 8H (Panel (A))** and pyruvate/lactate (**Figure 8H (Panel (B))** ^{13}C-labeling. Cells were incubated with U-^{13}C-glutamine for 48 h. M+3 pyruvate indicates malic enzyme flux, which may generate either NADH or NADPH. Similar results were also obtained for M+3 lactate (which was used as a surrogate for pyruvate, in cases where lactate was better detected). The corresponding maximal possible malic enzyme-driven NADPH production rate ranges, depending on the cell line, from < 2 nmol μL-1 h-1 to 6 nmol μL-1 h-1. Mean ± SD, N ≥ 2.

[0044] **Figures 9A-9D** show computational and experimental evidence for THF-dependent NADPH production. **Figure 9A** shows the contribution of folate metabolism to NADPH production predicted herein based on flux balance analysis, using minimization of total flux as the objective function, across different biomass compositions. The biomass fraction of cell dry weight consisting of protein, nucleic acid, and lipid was varied as follows: protein 50% - 90% with a step size of 10%; RNA/DNA 3%-20% with step size of 1%, and lipids 3% - 20% with step size of 1% (considering only those combinations that sum to no more than 100%). With this range of physiologically possible biomass compositions, the model predicts a median contribution of folate metabolism of 24%. Note that with the constraint of experimentally measured biomass composition, yet without constraining the uptake rate of amino acids other than glutamine to be ≤ 1/3 of the glutamine uptake rate, the contribution of folate pathway to total NADPH production is predicted to be 23%. **Figure 9B** shows the range of feasible flux through NADPH-producing reactions in Recon1 model computed via Flux Variability Analysis under the constraint of maximal growth rate. As shown, the model predicts that each NADPH-producing reaction can theoretically have zero flux, with all NADPH production proceeding through alternative pathways. Only reactions whose flux upper bound is greater than

zero are shown. Reactions producing NADPH via a thermodynamically infeasible futile cycle were manually removed. As shown, among all NADPH-producing reactions, MTHFD has the highest flux consistent with maximal growth. **Figure 9C** provides a pathway diagram showing the potential for 2,3,3-^{2}H-serine to label NADPH via methylene-tetrahydrofolate dehydrogenase. **Figure 9D** shows the NADP+ and NADPH labeling pattern after 48 h incubation with 2,3,3-^{2}H-serine (no glycine present in the media). The greater abundance of more heavily labeled forms of NADPH relative to NADP+ indicates redox-active hydrogen labeling. Results are mean ± SD, N ≥ 2 biological replicates from a single experiment and were confirmed in N ≥ 2 experiments. Based on the data in **Figure 9D**, the contribution of MTHFD1 to cytosolic NADPH production spans a broad range (10% - 40%) of total NADPH; the range is due to variation across cell lines, experimental noise, and the large KIE (Pawelek, P.D. *et al.* (1998) "*Methenyltetrahydrofolate Cyclohydrolase Is Rate Limiting For The Enzymatic Conversion Of 10-Formyltetrahydrofolate To 5,10-Methylenetetrahydrofolate In Bifunctional Dehydrogenase-Cyclohydrolase Enzymes*," Biochemistry 37:1109-1115). This range includes the flux calculated based on purine biosynthetic rate and $^{14}CO_2$ release from serine (**Figure 3D**). Note that the total contribution of the cytosolic folate metabolism to NADPH production can exceed that of MTHFD1, as 10-formyl-THF dehydrogenase also produces NADPH.

[0045] **Figures 10A-10F** show that one-carbon units used in purine and thymidine synthesis are derived from serine. **Figure 10A** shows the serine and ATP labeling pattern after 24 h incubation of HEK293T cells with U-^{13}C-serine. The presence of M+1 to M+4 ATP indicates that serine contributes carbon to purines both through glycine and through one-carbon units derived from serine C3. **Figure 10B** provides a quantitative analysis of cytosolic one-carbon unit labeling from measured the intracellular ATP, glycine, and serine labeling that reveals that most cytosolic 10-formyl-THF assimilated into purines comes from serine. **Figure 10C** shows that U-^{13}C- serine labels the methyl group that distinguishes dTTP from dUTP. **Figure 10D** shows that U-^{13}C-glycine does not label dTTP. **Figure 10E** shows that the extent of dTTP labeling mirrors the extent of intracellular serine labeling. **Figure 10F** shows that methionine does not label from U-^{13}C-glycine. In all experiments, cells were grown in U-13C-serine or glycine for 48 h. Mean ± SD, N = 3.

[0046] **Figures 11A-11H** show a measurement of the CO_2 release rate from serine and glycine by combination of ^{14}C- and ^{13}C-labeling. **Figure 11A** shows the $^{14}CO_2$ release rate when cells are fed medium with a trace amount of 3-^{14}C-serine, 1-^{14}C-glycine or 2-^{14}C-glycine. **Figure 11B** shows the fraction of intracellular serine labeled in cells grown in DMEM medium containing 0.4 mM 3-^{13}C-serine in place of unlabeled serine. The residual unlabeled serine is presumably from de novo synthesis. **Figure 11C** shows the fraction of intracellular glycine labeled in cells grown in DMEM medium containing 0.4 mM U-13C-glycine in place of unlabeled glycine. **Figure 11D** shows the CO_2 release rates from serine C3, glycine C1 or C2. **Figure 11E** shows a potential alternative pathway to metabolize glycine or serine into CO_2 via pyruvate. **Figure 11F** shows the pyruvate labeling fraction after 48 h labeling with U-^{13}C-serine or U-^{13}C-glycine. The lack of labeling in pyruvate indicates that serine and glycine are not metabolized through this pathway. **Figure 11G** shows that knockdown of MTHFD2 (**Figure 11G, Panel (A)**) or ALDH1L2 (**Figure 11G, Panel (B)**) decreases CO_2 release from glycine C2. **Figure 11H** shows that knockdown of ALDH1L2 decreases the GSH/GSSG ratio. Mean + SD, N=3.

[0047] **Figures 12A-12E** show that in the absence of serine, elevated concentrations of glycine inhibit cell growth and decrease the NADPH/NADP+ ratio. **Figure 12A** provides a schematic of the serine hydroxymethyltransferase reaction. High glycine may either inhibit forward flux (product inhibition) or drive reserve flux. **Figure 12B** shows the relative cell number observed after culturing HEK293T cells for 3 days in regular DMEM, DMEM with no serine, and DMEM with no serine and 12.5-times the normal concentration of glycine (5 mM instead of 0.4 mM). **Figure 12C** shows the relative NADPH/NADP+ ratio (normalized to cells grown in DMEM) after culturing HEK293T cell for 3 days in regular DMEM, DMEM with no serine, and DMEM with no serine and 12.5-times the normal concentration of glycine. **Figures 12D** and **12E** show that the labeling of serine and glycine after feeding HEK293T cells (**Figures 12D-12E, Panel (A)**) MDA-MB-498 cells (**Figures 12D-12E, Panel (B)**), iBMK-parental cells (**Figures 12D-12E, Panel (C)**) or iBMK-Akt cells (**Figures 12D-12E, Panel (D)**) U-^{13}C-serine (**Figure 12D**) or U-^{13}C-glycine (**Figure 12E**) reveals reverse serine hydroxymethyltransferase flux. Mean + SD, N=3.

[0048] **Figures 13A-13H** show a quantitative analysis of NADPH consumption for biomass production and antioxidant defense. **Figure 13A** shows cell doubling times, which are inversely proportional to biomass production rates. **Figure 13B** shows cellular protein content. **Figure 13C** shows cellular fatty acid content (from saponification of total cellular lipid). **Figure 13D** shows quantitation of fatty acid synthesis versus import, with synthesis but not import requiring NADPH. HEK293T cells were cultured in U-^{13}C-glucose and U-^{13}C-glutamine until pseudo-steady-state, and fatty acids saponified from total cellular lipids and their labeling patterns measured (light bars), and production versus import of each fatty acid was stimulated based on this experimental data. The fractional contribution of each route was determined by least square fitting, with the theoretical labeling pattern based on the elucidated routes shown (dark bars). **Figure 13D, Panel (A)**: C16:0; **Figure 13D, Panel (B)**: C16:1; **Figure 13D, Panel (C)**: C18:0; **Figure 13D, Panel (D)**: C18:1. Similar data were obtained also for MD-MBA-468, iBMK-parental, and iBMK-Akt cells and used to calculate associated NADPH consumption by fatty acid synthesis. **Figure 13E** shows cellular DNA and RNA contents. **Figure 13F** shows NADPH consumption by *de novo* DNA synthesis. **Figure 13G** shows glutamate (**Panel (A)**) and proline (**Panel (B)**) labeling patterns after 24 h in U-^{13}C-glutamine media, which was used to quantitate different proline synthesis routes and associated NADPH consumption. **Figure 13H** shows a quantitative analysis of cytosolic NADPH consumption in normally growing HEK293T cells (control) and non-growing cell under oxidative stress (150 μM H_2O_2, 5 h). Total cytosolic NADPH turnover was measured based on the absolute oxPPP flux divided by the fractional contribution of the oxPPP to total NADPH as measured using NADP2H formation from 1-^{2}H-glucose. Mean ± SD, N=3. **Figure 13H, Panel (A)**: oxPPP flux; **Figure 13H, Panel (B)**: hexose-phosphate 1-^{2}H-labeled fraction; **Figure 13H, Panel (C)**: NADPH-^{2}H-labeled fraction; **Figure 13H, Panel (D)**: NADPH production [nmole/h/μl cells].

[0049] **Figures 14A-14G** show confirmation of knockdown efficiency by Western blot or Q-PCR. **Figure 14A** shows a Western blot for G6PD knockdown. **Figure 14B** shows a Western blot for MTHFD1 and MTHFD2 knockdown. **Figure 14C** shows the mRNA level for ME1 knockdown. **Figure 14D** shows the mRNA level for NNT knockdown. **Figure 14E** shows the Western blot for IDH1 and IDH2

knockdown. **Figure 14F** shows a Western blot for ALDH1L2 knockdown. **Figure 14G** shows cell doubling times of HEK293T cells with stable knockdown of indicated genes (results for different hairpins of the same gene were indistinguishable).

[0050] **Figures 15A-15F** show the tracing of hydride flux through malic enzyme and total adipocyte central metabolic activity. **Figure 15A** is a schematic of [2,2,3,3-2H]dimethyl-succinate metabolism. As shown in the Figure, ^{2}H at malate position 2 is transferred to NADPH and lipid via malic enzyme (thick black arrows). Glc, glucose; Pyr, pyruvate; ME, malic enzyme; Suc, succinate; Mal, malate. **Figure 15B** shows the differential fate of ^{2}H at malate position 2 versus 3, and the potential for exchange between the two positions due to the symmetry of fumarate. MDH, malate dehydrogenase; GOT, glutamate-oxaloacetate transaminase; Asp, aspartate. **Figure 15C** shows NADP(H) ^{2}H-labeling in 3T3-L1 adipocytes (day 0 or day 5) fed [2,2,3,3-^{2}H] dimethyl succinate for 24 hours. **Figure 15D** shows the results of mass spectroscopy analysis of palmitic acid in 3T3-L1 adipocytes fed [2,2,3,3-^{2}H] dimethyl succinate for 5 days. In the proliferating condition, cells were maintained at $\leq$ 80% confluency with no differentiating reagents. In the differentiating condition, cells were provided with a differentiation cocktail with tracer added starting on day 0. **Figure 15E** shows the extent of ^{2}H-labeling of malate and aspartate in 3T3-L1 adipocytes at day 5. **Figure 15F** shows labeling in 3T3-L1 adipocytes (at day 5) of malate (fraction labeled at redox-active hydride at position 2, whether or not also labeled at other positions, see **Figure 5E**), whole cell NADPH (measured directly), and cytosolic NADPH (inferred from labeling of a set of abundant fatty acids).

[0051] **Figure 16** is a schematic of the pyruvate-citrate cycle driven by malate enzyme 1 (ME1) to promote fatty acid synthesis.

Detailed Description of the Invention:

[0052] The present invention relates to the recognition of a 10-formyl-THF pathway for producing NADPH, and to the use of that recognition in the diagnosis and treatment of cancer and metabolic disease, and in the development of new antineoplastic agents and/or regimens, and new therapeutics for treating metabolic disease (Fan, K. *et al.* (2014) "*Quantitative Flux Analysis Reveals Folate-Dependent*

NADPH Production," Nature 510(7504):298-302, herein incorporated by reference in its entirety).

I. Nomenclature

[0053] As used herein, the terms "**subject**" and "**patient**" refer to an animal (*e.g.*, a bird, a reptile or a mammal), preferably a mammal including a non-primate (*e.g.*, a camel, donkey, zebra, cow, pig, horse, goat, sheep, cat, dog, rat or mouse) and a primate (*e.g.*, a monkey, chimpanzee, or a human) and, most preferably, a human.

[0054] An atom of glucose or any of its derivatives is described hereon with reference to the carbon backbone of D-glucose molecule, with carbon atoms being numbered from 1 to 6, starting from the carbonyl carbon. Thus, for example, reference to "**3-H**" denotes a hydrogen atom pendant from the carbon that corresponds to carbon 3 of the D-glucose backbone. Likewise, reference to "**C1**," "**C2**," *etc.* with respect to a molecule denotes the first, second, *etc.* carbon atom of that molecule. Reference to "1-^{14}C" or "6-^{14}C" of a molecule denotes a ^{14}C-labeled carbon atom corresponding, respectively, to carbon 1 or carbon 6 of that molecule. Reference to "U" in the context of labeling denotes compounds that are uniformly or randomly labeled.

[0055] An atom of the amino acids serine and glycine is likewise described with reference to the carbon backbone of such molecules, with carbon atoms being numbered from 1 to 3 (for serine) or 1 to 2 for glycine, with the carboxylic carbon being designated as carbon 1 (*i.e.*, 1-C). Thus, for example, "**3-^{2}H-serine**" denotes a serine molecule that has been labeled with deuterium (^{2}H) at serine carbon 3 (the carbon furthest from the α-carboxy carbon). Similarly, "**2,3,3-^{2}H-serine**" denotes a serine molecule that has been labeled with three deuterium atoms, one of which is pendant from serine carbon 3 and two of which are pendant from serine carbon 3. Similarly, "**3,3-^{2}H-serine**" denotes a serine molecule that has been labeled with two deuterium atoms, both being pendant from serine carbon 3. As used herein, a molecule that comprises "**deuteration**" at a recited carbon atom is intended to denote that at least one of the hydrogen atoms pendant from such carbon atom is deuterium. Thus, for example, the phrase "a serine molecule that comprises deuteration at serine

carbon C-3" is intended to denote a serine molecule in which at least one of the 3-C serine hydrogens is ^{2}H (for example, 3-^{2}H-serine; 2,3-^{2}H-serine, 2,3,3-^{2}H-serine, U-^{2}H-serine (uniformly labeled with ^{2}H).

[0056] A biomolecule that contains a single labeled deuterium atom is referred to herein as being "**M+1**" (i.e., mass of the biomolecule + 1, with the "1" being the differential weight of deuterium (^{2}H) relative to hydrogen (^{1}H)). A biomolecule that contains a two labeled deuterium atoms is thus referred to herein as being "**M+2**," *etc.*

[0057] The term "**fatty acid moiety**" refers to a carboxylic acid group (HO-C(O)-) bonded to a saturated or unsaturated aliphatic chain (R) (*i.e.*, HO-C(O)-R). The term "**thymine moiety**" refers to a 5-methylpyrimidine-2,4(1H,3H)-dione group. Examples of molecules comprising a thymine moiety include thymidine, thymidine, thymidine triphosphate, thymidine diphosphate, thymidine monophosphate, DNA, *etc.* The term "**formate moiety**" refers to a methanoate group (-C(O)OH). Examples of molecules comprising a formate moiety include formate esters (*e.g.,* ROC(O)H) such as ethyl formate, methyl formate, triethyl orthoformate, trimethyl orthoformate, *etc.*). The term "**glycine**" refers to NH_2CH_2COOH. The term "**purine**" refers a heterocyclic aromatic organic compound that comprises a pyrimidine ring fused to an imidazole ring (*e.g.*, adenine, caffeine, guanine, uric acid, xanthine, *etc.*). A "**pyrimidine**" is a 6 membered heterocyclic diazine having nitrogen atoms at positions 1 and 3 in the ring (*e.g.*, cytosine, thymine, uracil, *etc.*). An "imidazole" is a five membered ring having nitrogen atoms at positions 1 and 3 in the ring.

[0058] The term "**anti-folate anticancer agent**" is intended to refer to a compound that is an inhibitor of an enzyme of folate metabolism, for example, an inhibitor of dihydrofolate reductase (DHFR), an inhibitor of β-glycinamide ribonucleotide transformylase (GARFT), an inhibitor of 5′-amino-4′-imidazolecarboxamide ribonucleotide transformylase (AICARFT), an inhibitor of thymidylate synthetase (TYMS), an inhibitor of methylene tetrahydrofolate dehydrogenase 1 or 2 (MTHFD1 or MTHFD2), an inhibitor of serine hydroxymethyltransferase 1 or 2 (SHMT1 or SHMT2), formyltetrahydrofolate dehydrogenase 1 or 2 (ALDH1L1 or ALDH1L2), *etc.* In one embodiment, such anti-folate anticancer agents may be structural

analogues of a folate (pteroylglutamate). Examples of anti-folate anticancer agents include 2,4-diamino-pteroylglutamate (4-amino-folic acid; Aminopterin or "AMT"), its 10-methyl congener, methotrexate ("MTX"), Tomudex (D1694, raltitrexed), Pemetrexed (Alimta, Eli Lilly), Pralatrexate (PDX; 10′-propargyl 10′-deazaaminopterin), Lometrexol (LMTX), Edatrexate (EDX), Talotrexin (PT-523), TMQ, Piritrexim (PTX), Nolatrexed (Thymitaq, TM), *etc.* (see, *e.g.*, Hagner, N. *et al.* (2010) *Cancer Chemotherapy: Targeting Folic Acid Synthesis*," Cancer Manag. Res. 2:293-301; Surmont, V.F. *et al.* (2011) "*Raltitrexed in Mesothelioma*," Expert Rev. Anticancer Ther. 11(10):1481-1490; Tomao, F. *et al.* (2009) "*Emerging Role Of Pemetrexed In Ovarian Cancer*," Expert Rev. Anticancer Ther. 9(12):1727-1735; Joerger, M. *et al.* (2010) "*The Role Of Pemetrexed In Advanced Non Small-Cell Lung Cancer: Special Focus On Pharmacology And Mechanism Of Action*," Curr. Drug Targets 11(1):37-47; Calvert, A.H. (2004) "*Biochemical Pharmacology Of Pemetrexed*," Oncology (Williston Park) 18(13 Suppl 8):13-17; McGuire, J.J. (2003) "*Anticancer Antifolates: Current Status And Future Directions*," Curr. Pharm. Des. 9(31):2593-2613). As used herein, the term "**anti-folate anticancer agent**" also refers to prodrugs of folate inhibitors, for example, formate esters thereof.

II. Measurement of NADPH Production

[0059] Past examination of NADPH production during cell growth has analyzed metabolic fluxes in cells using ^{13}C and ^{14}C isotope tracers (Lee, W. N. et al. (1998) *Mass Isotopomer Study Of The Nonoxidative Pathways Of The Pentose Cycle With [1,2-^{13}C2]Glucose*," Am. J. Physiol. 274:E843-E851; Metallo, C.M. *et al.* (2009) "*Evaluation Of ^{13}C Isotopic Tracers For Metabolic Flux Analysis In Mammalian Cells*," J. Biotechnol. 144:167-174; Fan, T.W. *et al.* (2008) "*Rhabdomyosarcoma Cells Show An Energy Producing Anabolic Metabolic Phenotype Compared With Primary Myocytes*," Mol. Cancer 7:79 (pages 1-20); Brekke, E.M. *et al.* (2012) "*Quantitative Importance Of The Pentose Phosphate Pathway Determined By Incorporation Of ^{13}C From [2-^{13}C]- And [3-^{13}C]Glucose Into TCA Cycle Intermediates And Neurotransmitter Amino Acids In Functionally Intact Neurons*," J. Cereb. Blood Flow Metab. 32:1788-1799).

[0060] For NADPH metabolism, however, carbon tracers alone are insufficient, because they cannot determine whether a particular redox reaction is making reduced nicotinamide adenine dinucleotide ("**NADH**") versus NADPH or the reaction's fractional contribution to total cellular NADPH production. To address these limitations, a deuterium (^{2}H) tracer approach was developed and used in conjunction with improved methods for analyzing ^{13}C labeling.

A. Preferred Methods for the Measurement of NADPH Redox-Active Hydrogen Labeling

[0061] A deuterium tracer approach was developed that directly measures NADPH redox-active hydrogen labeling. To probe the oxPPP, cells were shifted from unlabeled to 1-^{2}H-glucose or 3-^{2}H-glucose (**Figure 1A**) and the resulting NADP+ and NADPH labeling was measured using liquid chromatography-mass spectrometry (Lu, W. *et al.* (2010) "*Metabolomic Analysis Via Reversed-Phase Ion-Pairing Liquid Chromatography Coupled To A Stand Alone Orbitrap Mass Spectrometer*," Analytical Chemistry 82:3212-3221). ^{2}H-labeling may be similarly used to directly observe NADPH production by other pathways by providing other labeled compounds. Exemplary compounds include: 2,3,3-^{2}H-Aspartate; 1-^{2}H-Citrate; 2,2-^{2}H-Citrate; 2,2,4,4-^{2}H-Citrate; 1-^{2}H Fructose-6-Phosphate; 3-^{2}H Fructose-1,6-Biphosphate; 1-^{2}H Glucose-6-Phosphate; 2,3,3,4,4-^{2}H-Glutamate; 2,3,3,4,4-^{2}H-Glutamine; 1,2,3-^{2}H-Malate; 2,2,3-^{2}H-Malate; 2,2-^{2}H-Oxaloacetate; 3-^{2}H 6-Phospho-Gluconate; 2,3,3-^{2}H-Serine; 3,3-^{2}H-Serine; *etc.* Uptake of the labeled compound may be facilitated by permeabilizing the cells (Aragón, J.J. *et al.* (1980) "*Permeabilization Of Animal Cells For Kinetic Studies Of Intracellular Enzymes: In Situ Behavior Of The Glycolytic Enzymes Of Erythrocytes*," Proc. Natl. Acad. Sci. (U.S.A.) 77(11):6324-6328), or a cell-free system may be used (Stoecklin, F.B. *et al.* (1986) "*Formation Of Hexose 6-Phosphates From Lactate + Pyruvate + Glutamate By A Cell-Free System From Rat Liver*," Biochem J. 236(1):61-70).

[0062] As shown in **Figure 1F**, the total pool of NADPH comprises molecules produced through the addition of a hydrogen atom from glucose-6-phosphate ("**G6P**") via a cytosolic glycolysis reaction that yields ribulose-5-phosphate:

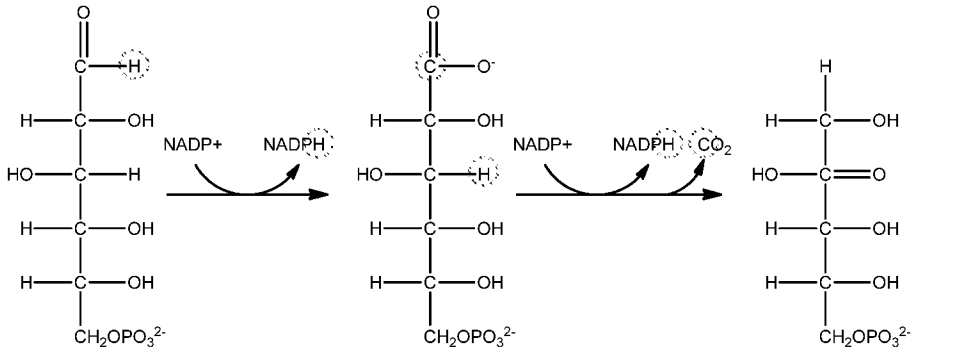

and CO_2, and molecules produced through the reduction of NADP to NADPH via other reactions. Since most NADPH production is cytosolic (Circu, M.L. *et al.* (2011) "*Disruption Of Pyridine Nucleotide Redox Status During Oxidative Challenge At Normal And Low-Glucose States: Implications For Cellular Adenosine Triphosphate, Mitochondrial Respiratory Activity, And Reducing Capacity In Colon Epithelial Cells*," Antioxid. Redox Signal 14:2151-2162), ^{2}H-glucose labeling results can be used to quantitate the fractional contribution of the oxPPP to total cytosolic NADPH production:

$$\text{Fraction}_{\text{NADPH from oxPPP}} = \frac{2 \times (\text{NADP}^2\text{H/Total NADPH})}{(^2\text{H-G6P/TotalG6P})} \times C_{KIE} \qquad \textbf{(Equation 1)}$$

wherein the parenthetical terms are the fractional ^{2}H-labeling of NADPH's redox-active hydrogen and the fractional ^{2}H-labeling of glucose-6-phosphate (G6P)'s targeted hydrogen (*i.e.*, the H pendant from the 1-C carbon of G6P) (**Figure 1E, Figures 5B-5D**). The term C_{KIE} accounts for the deuterium kinetic isotope effect (Shreve, D.S. *et al.* (1980) "*Kinetic Mechanism Of Glucose-6-Phosphate Dehydrogenase From The Lactating Rat Mammary Gland. Implications For Regulation*," J. Biol. Chem. 255:2670-2677; Price, N.E. *et al.* (1996) "*Kinetic And Chemical Mechanisms Of The Sheep Liver 6-Phosphogluconate Dehydrogenase*," Arch. Biochem. Biophys. 336:215-223) (**Figures 5E-5G**). Correction for the deuterium kinetic isotope effect was based on the assumption that total metabolic fluxes are not impacted. This correction was used as the default herein.

[0063] Let x be the fractional labeling of the relevant substrate hydrogen, F_U be the NADPH production flux from unlabeled substrate and F_L be the NADPH production flux from the labeled substrate, then:

$$\frac{F_L}{F_U} = \frac{x/(V_H/V_D)}{1-x} \quad \textbf{(Equation 2)}$$

$$F_{reaction} = F_L + F_U = F_L \frac{V_H/V_D + x(1-V_H/V_D)}{x} \quad \textbf{(Equation 3)}$$

wherein F_L/x is the flux in cases without a discernible kinetic isotope effect (e.g., for ^{13}C). The remaining term is the correction factor for the kinetic isotope effect:

$$C_{KIE} = V_H/V_D + x(1-V_H/V_D) \quad \textbf{(Equation 4)}$$

[0064] Alternatively, the largest reasonable correction for the deuterium kinetic isotope effect is based on the assumption that pathway flux is decreased by the introduction of ^2H-labeled tracer equivalent to the decrease in activity of the associated enzyme observed in vitro:

$$C_{KIE} = \frac{V_H/V_D}{1+N\times(V_H/V_D-1)\times X_{NADPH}} \quad \textbf{(Equation 5)}$$

where N is the number of NADPH produced per substrate molecule passing through the pathway. For the oxPPP, N = 2. Note that the impact of the kinetic isotope effect on NADP^{2}H production may be partially offset by an analogous (albeit smaller) kinetic isotope effect in NADP^{2}H consuming reactions. V_H/V_D for fatty acid synthetase is approximately 1.1 (Yuan, Z. *et al.* (1984) "*Elementary Steps In The Reaction Mechanism Of Chicken Liver Fatty Acid Synthase. pH Dependence Of NADPH Binding And Isotope Rate Effect For Beta-Ketoacyl Reductase*," J. Biol. Chem. 259:6748-6751). The impact of different mechanisms of correcting for the deuterium kinetic isotope is shown in **Figures 5A-5G**.

[0065] The kinetic isotope effect (V_H/V_D) for isolated NADPH-producing enzymes ranges from 1.8-4, with isolated G6PD and 6-phosphogluconate dehydrogenase having a V_H/V_D = 1.8 (Shreve, D.S. *et al.* (1980) "*Kinetic Mechanism Of Glucose-6-Phosphate Dehydrogenase From The Lactating Rat Mammary Gland. Implications*

For Regulation," J. Biol. Chem. 255:2670-2677; Price, N.E. *et al*. (1996) "*Kinetic And Chemical Mechanisms Of The Sheep Liver 6-Phosphogluconate Dehydrogenase*," Arch. Biochem. Biophys. 336:215-223). However, cellular homeostatic mechanisms (including flux control being distributed across multiple pathway enzymes) may result in a lesser impact on labeling patterns in cells.

[0066] The fractional NADPH redox-active site labeling (x) was measured from the observed NADPH and NADP+ labeling patterns from the same sample. x was calculated to best fit the steady-state mass distribution vectors of NADPH and NADP+ (MNADPH and MNADP+) by least square fitting in MATLAB (function: lsqcurvefit).

$$\mathrm{M}_{NADP+} = \begin{bmatrix} m_0 \\ m_1 \\ m_2 \\ \vdots \\ m_N \end{bmatrix} \begin{matrix} M+0 \\ M+1 \\ M+2 \\ \\ M+N \end{matrix}$$

$$\mathrm{M}_{NADPH} = \begin{bmatrix} m_0 \times (1-x) \\ m_1 \times (1-x) + m_0 \times x \\ m_2 \times (1-x) + m_1 \times x \\ \vdots \\ m_N \times (1-x) + m_{N-1} \times x \\ m_N \times x \end{bmatrix} \begin{matrix} M+0 \\ M+1 \\ M+2 \\ \\ M+N \\ M+N+1 \end{matrix} \qquad \textbf{(Equation 6)}$$

B. Preferred Methods for Deducing the Total Cytosolic NADPH Production Rate

[0067] The inferred fractional contribution of oxPPP to NADPH production can be used to deduce the total cytosolic NADPH production rate, which is equal to the absolute oxPPP flux divided by the fractional contribution of oxPPP to NADPH production (**Figure 1F**).

[0068] A first method for achieving this goal involves measuring $^{14}CO_2$ release from 1-^{14}C-glucose versus 6-^{14}C-glucose (**Figure 6A-6C**, **Figure 7A-7F**). Since oxPPP

converts glucose-6-phosphate to a phospho-pentose by removing carbon 1, use of 6-^{14}C-glucose (in which glucose carbon 6 is labeled) will not lead to the evolution of any labeled $^{14}CO_2$, whereas use of 1-^{14}C-glucose (in which glucose carbon 1 is labeled) results in the evolution of labeled $^{14}CO_2$ for glucose molecules that enter the oxPPP. Conversely, glycolysis of both 1-^{14}C-glucose and 6-^{14}C-glucose yields pyruvate, which then, via the TCA cycle, leads to the evolution of CO_2. Thus, by measuring the ratios of $^{14}CO_2$ released using 1-^{14}C-glucose or 6-^{14}C-glucose, one can determine the relative ratios of oxPPP and glycolytic processing of glucose.

$$\text{Fraction}_{\text{NADPH from oxPPP}} = 2 \times \left(\text{Fraction}_{CO_2 \text{ from Glucose C1}} - \text{Fraction}_{CO_2 \text{ from Glucose C6}} \right)$$

(Equation 7)

[0069] A second method for achieving this goal involves measuring the kinetics of 6-phosphogluconate labeling from U-^{13}C-glucose (**Figures 6D-6F**). U-^{13}C-glucose is converted, via oxPPP, into 6-phosphogluconate in a reaction that produces NADPH. Thus, for example, by monitoring the *reduction* in the percentage of *unlabeled* 6-phosphogluconate over time after provision of labeled U-^{13}C-glucose, one can calculate the contribution of oxPPP to NADPH production.

[0070] To quantify the absolute oxPPP flux, cells are switched to media containing U-^{13}C-glucose, and the kinetics glucose-6-phosphate and 6-phosphogluconate labeling were measured. Most preferably for such an analysis, cells are grown in Dulbecco's Modified Eagle's Medium (DMEM) without pyruvate (CELLGRO) with 10% dialyzed fetal bovine serum (Invitrogen) in 5% CO_2 at 37°C and harvested at approximately80% confluency. Preferably, for metabolite measurements, metabolism was quenched and metabolites were extracted by aspirating media and immediately adding -80°C 80:20 methanol:water. Supernatants from two rounds of extraction were combined, dried under N_2, resuspended in water, placed in a 4°C autosampler, and analyzed within 6 h by reversed-phase ion-pairing chromatography negative mode electrospray ionization high-resolution MS on a stand alone orbitrap (Thermo) (Lu, W. *et al.* (2010) "*Metabolomic Analysis Via Reversed-Phase Ion-Pairing Liquid Chromatography Coupled To A Stand Alone Orbitrap Mass Spectrometer*," Analytical Chemistry 82:3212-3221). Fluxes from ^{14}C-labeled substrates to CO_2 were measured by adding trace ^{14}C-labeled nutrient to normal culture media, quantifying

the radioactive CO_2 released (Folger, O. *et al.* (2011) "*Predicting Selective Drug Targets In Cancer Through Metabolic Networks*," Mol. Syst. Biol. 7:501 (pages 1-10), and correcting for intracellular substrate labeling according to the percentage of radioactive tracer in the media and the fraction of particular intracellular metabolite deriving from media uptake, as measured using ^{13}C-tracer.

[0071] The unlabeled fraction of 6-phosphoglucanate decays with time as:

$$\frac{d[6-phosphogluconate]^{unlabeled}}{dt} = -F_{oxPPP}\frac{[6-phosphogluconate]^{unlabeled}}{[6-phosphogluconate]^{total}} + F_{oxPPP} \times Fraction_{G6P}^{Unlabeled}(t)$$

(Equation 8)

wherein F_{oxPPP} is the flux of oxPPP, $[6\text{-}phosphogluconate]^{total}$ is the total cellular 6-phosphogluconate concentration, which was directly measured, and $Fraction_{G6P}^{Unlabeled}(t)$ is the unlabeled fraction of glucose-6-phosphate at time t, which decays exponentially. F_{oxPPP} is preferably obtained by lease square fitting (see, Yuan, J. *et al.* (2008) "*Kinetic Flux Profiling For Quantitation Of Cellular Metabolic Fluxes*," Nat. Protoc. 3:1328-1340).

[0072] Both methods gave consistent fluxes with the radioactive measurement more precise (**Figure 6G**). As confirmation of its specificity, elimination of glucose-6-phosphate dehydrogenase (via knock down) resulted in markedly reduced oxPPP $^{14}CO_2$ release, as expected (**Figure 1G**). Suitable knockdown cell lines may be generated using an shRNA-expressing lentivirus (see, *e.g.*, Alimperti, S. *et al.* (2012) "*A Novel Lentivirus For Quantitative Assessment Of Gene Knockdown In Stem Cell Differentiation*," Gene. Ther. 19(12):1123-1132) with puromycin selection. IDH1, IDH2 and ALDH1L2 knockdowns were generated by transfecting cells with siRNA. Knockdown was confirmed by Western blot (see **Figures 14A-14G**). In the absence of such knockdown, the oxPPP flux observed with some transformed cell lines ranged from 1-2.5 nmol μL^{-1} h^{-1} (where volume is the packed cell volume; **Figure 1G**). This flux is similar to, but slightly less than, the cellular ribose demand (**Figure 7F**). In combination with the fractional NADPH labeling, a total cytosolic NADPH production rate of approximately10 nmol uL^{-1} h^{-1} (**Figure 1H**) was determined using proliferating cells, which is 5-20% of the glucose uptake rate.

C. Identification and Analysis of NADPH-Producing Tetrahydrofolate Pathway (The "10-Formyl-THF Pathway")

[0073] A genome-scale human metabolic model (Duarte, N. C. *et al.* (2007) "*Global Reconstruction Of* The *Human Metabolic Network Based On Genomic And Bibliomic Data*," Proc. Natl. Acad. Sci. (U.S.A.) 104:1777-1782) was used in order to identify other potential NADPH-producing pathways. The model is biochemically, genetically, and genomically structured and accounts for the functions of 1,496 ORFs, 2,004 proteins, 2,766 metabolites, and 3,311 metabolic and transport reactions.

[0074] Preferably, the model is constrained based on the observed steady-state growth rate, biomass composition, and metabolite uptake and excretion rates of cancer cells without enforcing any constraints on NADPH production routes. The flux balance equations were solved in MATLAB with the objective function formulated to minimize the total sum of fluxes (Folger, O. *et al.* (2011) "*Predicting Selective Drug Targets In Cancer Through Metabolic Networks*," Mol. Syst. Biol. 7:501 (pages 1-10).

[0075] NADPH consumption by reductive biosynthesis is preferably determined based on reaction stoichiometries, experimentally measured cellular biomass composition, growth rate, fractional de novo synthesis of fatty acids (by ^{13}C-labeling from U-^{13}C-glucose and U-^{13}C-glutamine), and fractional synthesis of proline from glutamate versus arginine (by ^{13}C-labeling from U-^{13}C-glutamine).

[0076] This approach may be applied to a wide diversity of cell lines and other cells in culture, including immortalized baby mouse kidney cells (iBMK-parental cells) (Degenhardt, K. *et al.* (2002) "*BAX And BAK Mediate P53-Independent Suppression Of Tumorigenesis*," Cancer Cell 2:193-203). Similar results are obtained with many different transformed and/or cancerous proliferating cell lines.

[0077] The model, assessed via flux balance analysis with an objective of minimizing total enzyme expression requirements and hence flux (Folger, O. *et al.* (2011) "*Predicting Selective Drug Targets In Cancer Through Metabolic Networks*," Mol. Syst. Biol. 7:501 (pages 1-10), predicted that both the oxPPP and malic enzyme contribute approximately 30% of NADPH (**Figure 2D**). Surprisingly, however, an

even greater percentage (approximately 40%) of NADPH production was predicted to come from a mitochondrial folate-dependent pathway (**Figure 3A**)

[0078] In this mitochondrial pathway (the "**10-formyl-THF mitochondrial pathway**"), serine is converted to glycine via a reaction catalyzed by mitochondrial serine hydroxymethyltransferase ("**shmt2**") that transfers serine's 3-C carbon atom to tetrahydrofolate ("**THF**") thereby producing N^5,N^{10}-methylene-tetrahydrofolate ("**Methylene-THF**"). This reaction is distinct from the reaction, mediated by glycine decarboxylase, that produces methylene-THF from THF by decarboxylating the 2-C of glycine (and generating CO_2). Methylene-THF, produced from either reaction, is converted to 10-formyl-tetrahydrofolate ("**10-formyl-THF**") in a reaction catalyzed by the bifunctional methylene-tetrahydrofolate dehydrogenase/cyclohydrolase, mitochondrial enzyme ("**mthfd2**") (Peri, K.G. *et al.* (1989) "*Nucleotide Sequence Of The Human NAD-Dependent Methylene-Tetrahydrofolate Dehydrogenase-Cyclohydrolase*," Nucleic Acids Res 17(21):8853; Yang, X.M., *et al.* (1993) "*NAD-Dependent Methylenetetrahydrofolate Dehydrogenase-Methenyltetrahydrofolate Cyclohydrolase Is The Mammalian Homolog Of The Mitochondrial Enzyme Encoded By The Yeast MIS1 Gene*" Biochemistry 32(41):1118-1123). This reaction produces NADH or NADPH. An alternative objective function of maximizing growth rate further predicts a potentially substantial contribution of folate metabolism to NADPH production (**Figures 9A-9B**).

[0079] Similar to quantifying relative contribution of oxPPP to cytosolic NADPH production, the contribution of the 10-formyl-THF cytosolic pathway can be estimated from ^{2}H-serine labeling as follows:

$$Fraction_{NADPH(c)\ from\ MTHFD1} = \frac{NADP^2H(c)}{total\ NADP^2H(c)} \times \frac{total\ serine}{^2H-serine} \times C_{KIE}(MTHFD1)$$

(Equation 9)

[0080] Existing methods do not allow direct measurement of methylene-THF labeling, but such labeling can be approximated based on intracellular serine labeling (formally, the ^{2}H-serine labeling places an upper bound on ^{2}H-methylene-THF labeling):

$$Fraction_{NADPH(c)\ from\ MTHFD1} \geq \frac{NADP^2H(c)}{total\ NADP^2H(c)} \times \frac{total\ serine}{^2H-serine} \times C_{KIE}(MTHFD1)$$

(Equation 10)

wherein MTHFD1 has a deuterium kinetic isotope effect V_H/V_D of approximately 3.

[0081] The production of NADPH via a THF cycle is confirmed by Maddocks, O.D. *et al.* (2014) ("*Localization of NADPH Production: A Wheel within a Wheel*," Mol. Cell. 17;55(2):158-160).

D. Preferred Methods for Analyzing Fat Synthesis to Determine the NADPH Production Rate

[0082] The most NADPH-demanding biosynthetic activity in mammals is fat synthesis, which consumes a majority of cytosolic NADPH in typical transformed cells in culture (Fan, J. *et al.* (2014) "*Quantitative Flux Analysis Reveals Folate-Dependent NADPH Production*," Nature 510:298-302). In intact mammals, fat synthesis is thought to be localized primarily to liver and adipose (Nguyen, P. *et al.* (2008) "*Liver Lipid Metabolism*," J. Anim. Physiol. Anim. Nutr. (Berl). 92:272-283). Significant malic enzyme activity was described in adipose tissue more than 50 years ago, and malic enzyme is generally accepted to contribute to meeting the high NADPH needs of adipocytes; however, prior quantitative analysis of its contributions suggest that it is small relative to the oxPPP (Flatt, J.P. *et al.* (1964) "*Studies on the Metabolism of Adipose Tissue:* XV . AN EVALUATION OF THE MAJOR PATHWAYS OF GLUCOSE CATABOLISM AS INFLUENCED BY INSULIN AND EPINEPHRINE." J. Biol. Chem. 239:675-685). When desired, the observed rate of total cellular fatty acid accumulation may be corrected for the fraction of fatty acid synthesized *de novo*, which can be determined by administering [U-13C]glucose and [U-13C]glutamine and measuring the extent of fatty acid labeling by mass spectrometry.

[0083] In one embodiment, PPP activity is measured by incubating cultured adipocytes (*e.g.*, 3T3-L1 adipocytes) in the presence of [1-^{14}C]glucose versus [6-^{14}C]glucose and detecting the released $^{14}CO_2$. The oxPPP releases C1 of glucose as CO_2. The [6-^{14}C]glucose corrects for release of C1 by other pathways, because C1 and C6 are rendered identical by the triose phosphate isomerase step in glycolysis.

After determining the oxPPP flux, the cells are provided with [1-^{2}H]glucose, which selectively labels NADPH in the first step (G6PDH) of the PPP.

[0084] The ^{2}H-glucose labeling results can be used to quantitate the fractional contribution of the PPP to total cytosolic NADPH production. The inferred fractional contribution of the PPP to NADPH production can be used to deduce the total cytosolic NADPH production rate, which is equal to the absolute oxidative PPP flux divided by the fractional contribution of the PPP to NADPH production:

$$\text{Fraction}_{\text{NADPH from oxPPP}} = \frac{2 \text{ x } (\text{NADP}^{2}\text{H/Total NADPH})}{(^{2}\text{H-G6P/TotalG6P})} \text{ x } C_{\text{KIE}}$$

(Equation 1 (repeated))

$$\text{Fraction}_{\text{NADPH from oxPPP}} = 2 \times \frac{\text{NADP}^{2}\text{H}}{\text{NADPH}_{\text{total}}} \times \frac{\text{G6P}_{\text{total}}}{^{2}\text{H-G6P}} \times \text{Fraction}_{\text{NADPH from all cytosolic sources}} \times C_{\text{KIE}}$$

(Equation 11)

In **Equation 1**, the determination of CO_2 from glucose C1 is based on the measured release rates of ^{14}C-CO_2 corrected for the fractional radioactive labeling of glucose (and similarly for C6). These rates are multiplied by 2 to account for the stoichiometry of the oxPPP (2 NADPH per glucose). In **Equation 11**, the measured fractional ^{2}H-labeling of NADPH is corrected for the ^{2}H-labeling of glucose-6-phosphate and for the deuterium kinetic isotope effect (C_{KIE}) and multiplied by 2 to account for the [1-^{2}H]glucose tracer being labeled but that only one of the two hydrogens that are transferred to NADPH via the oxPPP.

[0085] The folate metabolic enzymes MTHFD and ALDH have NADPH-producing dehydrogenase activity. MTHFD is required for oxidizing methylene-THF into the key one-carbon donor formyl-tetrahydrofolate (formyl-THF), which is required for purine synthesis. In contrast, ALDH does not produce a useful one-carbon donor, but instead oxidizes formyl-THF into THF, CO_2, and NADPH (**Figure 3A**). To evaluate total malic enzyme flux (sum of NADPH- and NADH-dependent malic enzyme), cells may be provided with [U-^{13}C]glutamine, whose metabolism through the citric acid cycle and malic enzyme results in labeling of pyruvate.

$$\frac{\text{Fraction}_{\text{malic enzyme}}}{\text{Fraction}_{\text{glycolysis}}} = \frac{\text{Pyr}_{[M+2]}}{\text{Pyr}_{[M+0]}} \times \frac{\text{Malate}_{\text{total}}}{\text{Malate}_{[M+4]} + \text{Malate}_{[M+3]}} \quad \textbf{(Equation 12)}$$

This assay measures gross flux (the forward reaction flux from malate to pyruvate). Because malic enzyme is reversible, net flux (forward minus reverse flux) may be less.

[0086] Gross carbon flux through malic enzyme (ME) was quantified based on pyruvate labeling from [U-^{13}C]glutamine. Since the observed fraction of M+1 and M+2 pyruvate are small (sum of both is less than 0.5%) relative to M+3 pyruvate (3%), the analysis is based solely on the observed M+3 pyruvate signal relative corrected for the fractional proportion of malate capable of making M+3 pyruvate. Forward flux from [U-^{13}C]glutamine results in M+4 malate [1,2,3,4-^{13}C] (21%). Reductive carboxylation of glutamine coupled to citrate lyase can produce M+3 malate in the form [2,3,4-^{13}C], which produces M+2, not M+3, pyruvate. Malate M+3 (total fractional abundance 8%) exists also as [1,2,3-^{13}C], which produces M+3 pyruvate. Assuming rapid exchange between malate and fumarate (which is symmetric), the abundances of [1,2,3-^{13}C] and [2,3,4-^{13}C]malate will be equal; incomplete exchange will result in less [1,2,3-^{13}C]. This equation applies when malic enzyme flux is much less than glycolytic flux; otherwise, one would include a term to account for unlabeled pyruvate made via malic enzyme.

$$\frac{\text{Fraction}_{\text{Malic Enzyme}}}{\text{Fraction}_{\text{Glycolysis}}} = \frac{\text{Pyr}_{[M+3]}}{\text{Pyr}_{\text{unlabelled}}} \times \frac{\text{Malate}_{\text{total}}}{\text{Malate}_{[M+4]} + a * \text{Malate}_{[M+3]}} \quad \textbf{(Equation 13)}$$

where: $a = \frac{\text{Malate}_{[1,2,3\text{-}^{13}\text{C}]}}{\text{Malate}_{[1,2,3\text{-}^{13}\text{C}]} + \text{Malate}_{[2,3,4\text{-}^{13}\text{C}]}} \approx 0.5$

[0087] To more directly establish the contribution of malic enzyme to NADPH production, cells are provided with the ^{2}H-labeled succinate analogue [2,2,3,3-^{2}H]dimethyl-succinate, and deuterium labeling is followed through the C2 hydride of malate to NADPH and finally to newly synthesized fatty acid molecules (**Figures 15A-15F**). Although any suitable labeled molecule may be used to trace hydride flux from malate to NADPH and subsequently into fat, it is preferred to use [2,2,3,3-^{2}H]dimethyl-succinate for the above purpose.

[0088] NADPH labeling at its redox active hydride was analyzed by comparing the M+1 fraction of NADPH to NADP+. In the absence of [2,2,3,3-^{2}H]dimethyl succinate, the NADP+ and NADPH labeling patterns were identical; addition of tracer resulted in increased labeling of NADPH but not NADP+ selectively in differentiating (day 5) but not proliferating (day 0) 3T3-L1 cells, with 3.4% ± 0.3% of the total adipocyte NADPH labeled (**Figure 15C**). Analysis of fatty acids (which was corrected for the fraction of newly synthesized fatty acids based on carbon labeling, which reflects specifically cytosolic NADPH, similarly revealed selective 2H-labeling in the differentiating adipocytes (**Figure 15D**). Quantitative analysis of the mass isotope distribution of a set of abundant fatty acids revealed an average hydride 2H-labeling fraction of 2.87% ± 0.31%. Correction for the kinetic isotope effect in hydride transfer from NADPH to fat (approximately 1.1) yields an associated NADPH labeling fraction of 3.2% ± 0.5%, in excellent agreement with the directly measured whole cell NADPH labeling.

[0089] Converting the NADPH labeling fraction from [2,2,3,3-^{2}H] dimethyl-succinate into the fractional NADPH contribution of malic enzyme requires two important corrections: (i) fractional 2H-labeling of malate's C2 hydride and (ii) the malic enzyme deuterium kinetic isotope effect (approximately 1.5).

$$\text{Fraction}_{\text{NADPH from Malic Enzyme 1}} = \frac{\text{NADP}^2\text{H}}{\text{NADPH}} \times \frac{\text{Malate}}{\text{Malate}_{\text{C2-deuteron}}} \times \text{Fraction}_{\text{NADPH from all sources}} \times C_{\text{KIE}}$$

(Equation 14)

[0090] Forward flux from [2,2,3,3-^{2}H]succinate results in [2,3-^{2}H]malate, *i.e.*, M+2 malate (**Figure 15B**). The observed fraction of M+2 malate was, however, only 1.5%. The larger peak was M+1 malate (**Figure 15E**). Reverse flux through malate dehydrogenase can produce M+1 malate labeled at the C3 hydride ([3-^{2}H]malate). As fumarate is symmetric, fumarase will interconvert [3-^{2}H] and [2-^{2}H]malate (**Figure 15B**). Because malic enzyme will produce NADP^{2}H selectively from malate labeled at the C2 hydride, the relative abundance of [2-^{2}H] versus [3-^{2}H]malate was determined. [3-^{2}H]malate (and also [2,3-^{2}H]malate) yields M+1 oxaloacetate and hence M+1 aspartate, whereas [2-^{2}H]-malate yields unlabeled oxaloacetate and

aspartate. Hence, subtracting the fraction of M+1 aspartate from that of M+1 plus M+2 malate gives the fraction of [2-^{2}H]malate (**Figure 15E**), which was approximately 6.4%. Summing [2-^{2}H]malate and [2,3-^{2}H]malate, the fraction of malate that is capable of making NADP^{2}H was 7.9% (**Figure 15F**).

$$\frac{\text{Mal}_{\text{C2-deuteron}}}{\text{Mal}} = \frac{[2\text{-}^2\text{H}]\text{Mal}}{\text{Mal}} + \frac{[2,3\text{-}^2\text{H}]\text{Mal}}{\text{Mal}} = \left(\frac{\text{Mal}_{[\text{M+1}]} + \text{Mal}_{[\text{M+2}]}}{\text{Mal}}\right) - \left(\frac{\text{Asp}_{[\text{M+1}]}}{\text{Asp}} - \frac{\text{Mal}_{[\text{M+2}]}}{\text{Mal}}\right) \quad \textbf{(Equation 15)}$$

[0091] Correction for the isotope effect is:

$$\frac{F_D}{F_H} = \frac{x}{(1-x)} * \frac{v_D}{v_H} \quad \textbf{(Equation 16)}$$

[0092] Thus, while [2,2,3,3-^{2}H]dimethyl succinate labeled only approximately 3.2% of NADPH, after correction for the extent of malate labeling and the malic enzyme kinetic isotope effect, the fraction of NADPH generated via malic enzyme is approximately 60%. Thus, the deuterium tracer studies directly demonstrate that malic enzyme is the predominant NADPH source in 3T3-L1 adipocytes.

[0093] **Figure 16** shows the pyruvate-citrate cycle driven by ME1 to promote fatty acid synthesis.

III. Preferred Methods

A. Cell Lines and Culture Conditions

[0094] HEK293T and MDA-MB-468 cells may be purchased from ATCC. Immortalized baby mouse kidney epithelial cells (iBMK) with or without myr-AKT are obtainable from E. White (see, *e.g.*, Degenhardt, K. *et al.* (2002) "*BAX And BAK Mediate P53-Independent Suppression Of Tumorigenesis*," Cancer Cell 2:193-203; Mathew, R. (2008) "*Immortalized Mouse Epithelial Cell Models To Study The Role Of Apoptosis In Cancer*," Methods Enzymol. 446:77-106). All cell lines are preferably grown in Dulbecco's Modified Eagle's Medium (DMEM) without

pyruvate (CELLGRO), supplemented with 10% dialyzed fetal bovine serum (Invitrogen) in a 5% CO_2 incubator at 37°C.

[0095] Knockdown of enzymes is preferably accomplished by infection with lentivirus expressing the corresponding shRNA (**Table 1**) and puromycin selection.

Table 1

Gene	shRNA	Sequence	SEQ ID NO.
MTHFD1	#1	ccgggctgaa gagattggga tcaaactcga gtttgatccc aatctcttca gctttttg	**1**
	#2	ccgggccatt gatgctcgga tatttctcga gaaatatccg agcatcaatg gctttttg	**2**
MTHFD2	#1	ccgggcagtt gaagaaacat acaatctcga gattgtatgt ttcttcaact gctttttg	**3**
	#2	ccgggctggg tatatcactc cagttctcga gaactggagt gatataccca gctttttg	**4**
G6PD	#1	ccggcaacag atacaagaac gtgaactcga gttcacgttc ttgtatctgt tgttttg	**5**
	#2	ccgggctgat gaagagagtg ggtttctcga gaaacccact ctcttcatca gctttttg	**6**
NNT	#1	ccggccctat ggttaatcca acattctcga gaatgttgga ttaaccatag ggttttg	**7**
ME1	#1	ccgggccttc aatgaacggc ctattctcga gaataggccg ttcattgaag gctttttg	**8**
	#2	ccggccaaca atatagtttg gtgttctcga gaacaccaaa ctatattgtt ggttttg	**9**

[0096] To obtain the shRNA-expressing virus, pLKO-shRNA vectors (Sigma-Aldrich) are cotransfected with the third generation lentivirus packaging plasmids (pMDLg, pCMV-VSV-G and pRsv-Rev) into HEK293T cells using FuGENE 6 Transfection Reagent (Promega), fresh media added after 24 h, and viral supernatants collected at 48 h. Target cells are infected by viral supernatant (preferably diluted 1:1 with DMEM; 6 μg/ml polybrene), fresh DMEM is added after 24 h, and selection with 3 μg/ml puromycin initiated at 48 h and allowed to proceed for 2-3 days. Thereafter, cells are preferably maintained in DMEM with 1 μg/ml puromycin. For IDH1, IDH2 and ALDH1L2 knockdown, siRNA targeting IDH1 or IDH2 (Thermo Scientific, 40 nM) or ALDH1L2 (Santa Cruz, 30 nM) are transfected into H293T cells using LIPOFECTAMINE™ RNAiMAX (Invitrogen).

[0097] Knockdown of enzymes is preferably confirmed by immunoblotting using, for example, commercial antibodies: G6PD (Bethyl Laboratories), MTHFD1 and MTHFD2 (Abgent), IDH1 (Proteintech Group), IDH2 (Abcam) and ALDH1L2

(Santa Cruz) or quantitative RT-PCR probes (ME1 and NNT, Applied Biosystems) (**Figures 14A-14G**).

B. Measurement of Metabolite Concentrations and Labeling Patterns

[0098] Cells are preferably harvested at a consistent confluency, *e.g.*, approximately 80% confluency. For metabolomic experiments, medium is preferably replaced on a regular schedule, *e.g.*, every 2 days and additionally 2 h before metabolome harvesting and/or isotope tracer addition. Metabolism is quenched and metabolites extracted, *e.g.*, by aspirating media and immediately adding -80°C 80:20 methanol:water. Supernatants from two rounds of methanol:water extraction are then preferably combined, dried under N_2, resuspended in HPLC water, placed in a 4°C autosampler, and analyzed, preferably within 6 h to avoid NADPH degradation.

[0099] One suitable LC-MS method involves reversed-phase ion-pairing chromatography coupled by negative mode electrospray ionization to a standalone orbitrap mass spectrometer (Thermo Scientific) scanning from m/z 85-1000 at 1 Hz at 100,000 resolution (Lu, W. *et al.* (2010) "*Metabolomic Analysis Via Reversed-Phase Ion-Pairing Liquid Chromatography Coupled To A Stand Alone Orbitrap Mass Spectrometer*," Analytical Chemistry 82:3212-3221; Munger, J. *et al.* (2008) "*Systems-Level Metabolic Flux Profiling Identifies Fatty Acid Synthesis As A Target For Antiviral Therapy*," Nat. Biotechnol. 26:1179-1186; Lemons, J.M. *et al.* (2010) "*Quiescent Fibroblasts Exhibit High Metabolic Activity*," PLoS Biol. 8:e1000514 (pages 1-10) with LC separation on a Synergy Hydro-RP column (100 mm × 2 mm, 2.5 μm particle size, Phenomenex, Torrance, CA) using a gradient of solvent A (97:3 H_2O/MeOH with 10 mM tributylamine and 15 mM acetic acid), and solvent B (100% MeOH). A preferred gradient is: 0 min, 0% B; 2.5 min, 0% B; 5 min, 20% B; 7.5 min, 20% B; 13 min, 55% B; 15.5 min, 95% B; 18.5 min, 95% B; 19 min, 0% B; 25 min, 0% B. Injection volume was 10 μL, flow rate 200μl/min, and column temperature 25 °C. Data is preferably analyzed using the MAVEN software suite (Melamud, E. *et al.* (2010) "*Metabolomic Analysis And Visualization Engine For LC-MS Data*," Anal. Chem. 82:9818-9826). Other suitable methods are known in the art.

[00100] Data from ^{13}C-labeling experiments are preferably adjusted for natural ^{13}C abundance and impurity of labeled substrate; those from ^{2}H-labeling are preferably not adjusted (natural ^{2}H abundance is negligible) (Millard, P. *et al.* (2012) "*IsoCor: Correcting MS Data In Isotope Labeling Experiments*," Bioinformatics 28:1294-1296).

[00101] The absolute concentration of 6-phosphogluconate may be quantified by comparing the signal of ^{13}C-labeled intracellular compound (from feeding U-^{13}C-glucose) to the signal of unlabeled internal standard.

C. Network Analysis of Potential NADPH-Producing Pathways

[00102] To assess the potential contribution of various metabolic pathways to NADPH production, feasible steady-state fluxes of a genome-scale human metabolic network model (Duarte, N. C. *et al.* (2007) "*Global Reconstruction Of The Human Metabolic Network Based On Genomic And Bibliomic Data*," Proc. Natl. Acad. Sci. (U.S.A.) 104:1777-1782) is analyzed. The glucose (98 nmol/(μL*h)), glutamine (40 nmol/(μL*h)), and oxygen uptake rates (21 nmol/(μL*h)), and lactate (143 nmol/(μL*h)), alanine (2 nmol/(μL*h)), pyruvate (15 nmol/(μL*h)), and formate (< 0.25 nmole/(μL*h)) excretion rates are preferably set to experimental measured fluxes in the iBMK cell line (such values from exemplary experimental measurements of iBMK cells are written in parentheses above), as measured by a combination of electrochemistry (glucose, glutamine, lactate on YSI7200 instrument, YSI, Yellow Springs, OH), LC-MS (alanine, pyruvate with isotopic internal standards), fluorometry (oxygen on XF24 flux analyzer, Seahorse Bioscience, North Billerica, MA), and nuclear magnetic resonance (NMR) (formate by 1H 500 MHz, Bruker, 10 μM limit of detection). The uptake of amino acids from DMEM media can be measured directly or may be assumed to be bounded by a reasonable limit based on the cell type being studied, *e.g.*, to not more than a third of that of glutamine, which is a loose constraint relative to experimental observations in iBMK cells and in NCI-60 cells (Jain, M. *et al.* (2012) "*Metabolite Profiling Identifies A Key Role For Glycine In Rapid Cancer Cell Proliferation*," Science 336:1040-1044). Biomass requirements are based on the experimentally determined growth rate of the cell line with protein, fatty acids and nucleotides accounting for 60%, 10% and 10% of the total cellular dry

mass, respectively, based on experimental measurements, in iBMK cells. Steady-state intracellular fluxes that best fit these experimental constraints are then selected by solving the flux balance equations in MATLAB with the objective function formulated to minimize the sum of total fluxes (Folger, O. *et al.* (2011) "*Predicting Selective Drug Targets In Cancer Through Metabolic Networks*," Mol. Syst. Biol. 7:501 (pages 1-10).

D. ROS Measurement, Cell Proliferation and Cell Death Assay

[00103] Cells constantly generate reactive oxygen species (ROS) during aerobic metabolism. ROS measurement may be accomplished as described by Eruslanov, E. *et al.* (2010) ("*Identification Of ROS Using Oxidized DCFDA And Flow-Cytometry*," Methods Molec. Biol. 594:57-72). Briefly, cells are incubated with 5 μM CM-H2DCFDA (Invitrogen) for 30 min. Cells are trypsinized, and mean FL1 fluorescence is measured by flow cytometry. Cell proliferation is measured by trypsinizing cells and counting, for example, using a Beckman Multisizer 4 Coulter Counter. To measure cell death, cells are preferably stained with Trypan Blue. The stained and unstained cells are counted and cell death percentages are tabulated.

E. Measurement of $^{14}CO_2$ Release

[00104] Radioactive CO_2 released by cells from positionally-labeled substrates is preferably measured by trapping the CO_2 in filter paper saturated with 10 M KOH as described by Folger, O. *et al.* (2011) ("*Predicting Selective Drug Targets In Cancer Through Metabolic Networks*," Mol. Syst. Biol. 7:501 (pages 1-10). Cells are preferably grown in tissue culture flasks with DMEM medium with less than normal bicarbonate (0.74 g/L) and addition of HEPES buffer (6 g/L, pH 7.4). At the beginning of experiment, trace amount of desired 14C-labeled tracer is preferably added to the media. For each cell line, the amount added is preferably selected to be the minimum that gives a sufficient radioactive CO_2 signal to quantitate accurately (for example, approximately 1 μCi/ml).

[00105] All knockdown lines are treated identically to their corresponding parental line. Then the flask is sealed (*e.g.*, with a rubber stopper with a central well (Kimble Chase) containing a piece of filter paper saturated with 10 M KOH solution). The

flasks are preferably incubated at 37°C for 24 h. CO_2 released by cells is absorbed by the base (*i.e.*, KOH) in the central well. Metabolism is preferably stopped by injection of 1 mL 3 M acetic acid solution through the rubber stopper. The flasks are then incubated, *e.g.*, at room temperature for 1 h, to ensure all the CO_2 dissolved in media has been released and absorbed into the central well. The filter paper and all the liquid in central well is then transferred to a scintillation vial containing 15 mL liquid scintillation cocktail (PerkinElmer Inc.). The central well is washed, *e.g.*, with 100 μL water twice, and the water is added to the same scintillation vial. Radioactivity is then measured by liquid scintillation counting. Most preferably, in parallel, the same experiments are performed using U-^{13}C-labeled nutrient (in amounts that fully replace the unlabeled nutrient in DMEM) and the extent of labeling of the intracellular metabolite that is the substrate of the CO_2-releasing reaction is measured by LC-MS. Absolute CO_2 release rates from the nutrients of interest are calculated as follows:

$$Rate_{CO_2\ from\ fource_i}\left[nmole/h/\mu l\ cells\right] = \frac{Rate_{CO_2\ from\ ^{14}C\text{-}labeled\text{-}tracer_i}\left[\mu Ci/h/\mu l\ cells\right]}{overall\ media\ tracer_i\ activity\left[\mu Ci/nmole\right]} \times \frac{1}{fraction_{intracellular\ compound_i\ from\ media}} \quad \textbf{(Equation 17)}$$

F. Fractional Labeling of Cytosolic Formyl Groups From U-^{13}C-Serine

[00106] To measure the fractional labeling of cytosolic formyl groups from U-^{13}C-serine, cells are cultured with media containing U-^{13}C-serine, *e.g.*, for 48 h, washed three times with cold PBS to remove extracellular serine, extracted, and the intracellular labeling pattern analyzed by LC-MS for ATP (representing purines; there is no labeling of ribose-phosphate based on LC-MS measurements), glycine, and serine. The purine ring has 5 carbons: 1 from CO_2, 2 from glycine, and 2 from formyl groups (from 10-formyl-THF). It is assumed that CO_2 labeling is negligible, which is realistic for cells grown in a 5% CO_2 incubator. Let $X_{ATP\text{-}i}$ and $X_{Gly\text{-}j}$ represent the experimentally observed fraction ATP and glycine with i and j labeled carbons. The cytosolic 10-formyl-THF labeling fraction, x, is then fit by least squares:

$$X_{ATP-0} = X_{Gly-0} * (1-x)^2$$
$$X_{ATP-1} = 2*X_{Gly-0} * x\ (1-x)$$
$$X_{ATP-2} = X_{Gly-2} * (1-x)^2 + X_{Gly-0} * x^2$$
$$X_{ATP-3} = 2*X_{Gly-2} * x\ (1-x)$$
$$X_{ATP-4} = X_{Gly-2} * x^2 \quad \textbf{(Equation 18)}$$

G. Cytosolic NADPH Production from 10-Formyl-THF Pathway

[00107] Cytosolic NADPH production from 10-formyl-THF pathway is preferably quantified by tracking its end products: 10-formyl-THF consumed by purine synthesis and CO_2, since formate excretion into media is typically below the detection limit of NMR. All 10-formyl-THF consumed by purine synthesis is generated in cytosol and associated with the production of 1 NADPH. For each CO_2 released from serine C3, assuming reaction happens in cytosol, one molecule of NADPH is produced from 10-formyl-THF oxidation, and a second molecule of NADPH is produced via MTHFD1. Total cytosolic NADPH production via the 10-formyl-THF pathway is:

$$Flux_{NADPH(c)\ from\ THF\text{-}pathway} = 2 \times Flux_{purine\ synthesis} + 2 \times Flux_{CO_2\ from\ serine\ C3}$$

(Equation 19)

[00108] If complete oxidation of serine C3 instead happens in mitochondria, there is no cytosolic NADPH production associated with CO_2 released from serine C3 (*i.e.*, no black bar in **Figure 3D**). Instead, one molecule of mitochondrial NADPH is produced from 10-formyl-THF oxidation, and zero to one other molecules of mitochondrial NADPH is produced from 5,10-methylene-THF oxidation, depending on the enzyme used to catalyze the reaction and its cofactor specificity. In mitochondria, this reaction can be catalyzed by MTHFD2, which (at least in the presence of high phosphate *in vitro*) preferentially uses NAD+, or it can be catalyzed by MTHFD2L, which uses NADP+).

[00109] The complete oxidation of 3C of serine is found to be a meaningful source (approximately 5-10%) of NADPH in adipose cells.

H. Quantitation of NADPH Consumption by Reductive Biosynthesis

[00110] The general strategy for measuring consumption fluxes is preferably as follows: (i) identifying the biomass components produced in cells grown in culture media (such as DMEM) by NADPH-driven reductive biosynthesis (these are DNA,

proline, and fatty acids); (ii) determining the biomass fraction of each component in each cell line; (iii) quantifying the cellular growth rate $R_{growth} = \ln(2)/t_{1/2}$; (iv) measuring the fractional contribution of different biosynthetic routes to each biomass component via experiments with ^{13}C-labeled glucose and/or glutamine and LC-MS analysis; (v) computing the average number of NADPH per unit of biomass component, which equals the sum of the fractional contribution of each route multiplied by the number of NADPH consumed by that route; and (vi) determining NADPH consumption as follows:

$$\text{Consumption flux} = (\text{product abundance/cell volume}) \times R_{growth} \times (\text{average NADPH/product})$$

(Equation 20)

[00111] The data employed in such a determination can be acquired as follows:

DNA: Cellular DNA and RNA are extracted and separated with TRIzol reagent (Invitrogen), purified, and quantified by Nanodrop spectrophotometer;

Fatty acids: Total cellular lipid is extracted and saponified after addition of isotope-labeled internal standards for the C16:0, C16:1, C18:0, and C18:1. Samples are analyzed by negative ESI-LC-MS with LC separation on a C8 column. Concentrations of other fatty acids, for which isotope-labeled internal standard are not available, are measured by comparison to the palmitate internal standard. The calculated fatty acid concentrations are multiplied with a correction factor to account for incomplete lipid recovery in the first step of the sample preparation procedure. This correction factor is empirically determined to be 1.9 by experiments in which lipid standards were spiked into extraction solution. The extent of fatty acid synthesis and elongation (both of which consume NADPH) is determined by feeding cells U-^{13}C-glucose and U-^{13}C-glutamine for multiple doublings to achieve pseudo-steady-state labeling of their lipid pools. Fatty acid labeling patterns were measured and computationally simulated to quantify the fraction of production versus import for each individual fatty acid species. **Figures 13A-13H** show the associated data for C16:0, C16:1, C18:0, and C18:1, which together account for approximately 80% of total cellular fatty acids and greater than 90% of non-essential fatty acids (essential fatty acids are imported, not synthesized, and

thus do not impact NADPH production). NADPH calculations include similar data for all measurable fatty acids.

Proline: Proline can be made from either arginine or glutamate. Proline synthesis from either substrate requires two high-energy electrons at the step catalyzed by pyrroline-5-carboxylate reductase, which may use NADH or NADPH (for simplicity, an equal contribution from each is assumed). Proline synthesis from glutamate consumes one additional NADPH (Lorans, G. *et al.* (1981) "*Proline Synthesis And Redox Regulation: Differential Functions Of Pyrroline-5-Carboxylate Reductase In Human Lymphoblastoid Cell Lines*," Biochem. Biophys. Res. Commun. 101:1018-1025). To quantify the fraction of proline synthesized from each substrate, cells are labeled with U-13C-glutamine to steady-state, which labels glutamate but not arginine. Labeling of intracellular proline and glutamate are measured:

$$X_{Glu} = \frac{Fraction_{proline\ ^{13}C\text{-}labeled}}{Fraction_{glutamate\ ^{13}C\text{-}labeled}} \qquad \textbf{(Equation 21)}$$

$$Flux_{NADPH\ for\ proline} = \frac{growth\ rate \times protein\ content}{average\ formula\ weight\ per\ residue} \times proline\ frequency \times \left(1.5X_{Glu} + 0.5\left(1 - X_{Glu}\right)\right)$$

(Equation 22)

Proline synthesis enzymes are present in both the cytosol and mitochondria. For simplicity, exclusive cytosolic proline synthesis may be assumed (see, *e.g.*, **Figure 4A-4B**).

IV. Diagnostic Utility

[00112] As discussed above, cells obtain NADPH both from reactions occurring in the cytosol, such as those of the oxPPP, and from reactions occurring in the mitochondria, such as those mediated by malic enzyme. One finding of the present invention is that a second pathway (the "**10-formyl-THF pathway**") can be a major contributor of NADPH in proliferating cells. In selected embodiments of the invention, the extent to which the amount (or relative proportion) of NADPH produced in cancer cells via the 10-formyl-THF pathway is greater than the amount (or relative proportion) of NADPH produced in non-cancerous cells is indicative of the presence and/or aggressiveness of such cancer.

[00113] Thus, the methods of the present invention permit one to diagnose cancer or metabolic disease (especially diabetes) and/or to assess the prognosis of a patient (*i.e.*, a human or non-human mammal suspected or known to have cancer) having such disease by determining whether the contribution of its 10-formyl-THF pathway to cellular NADPH production is greater than that observed in normal, non-cancer cells.

[00114] The present invention thus provides a method for the diagnosis of cancer. Such method will most preferably be accomplished by administering a deuterium-labeled substrate of a biomolecule to actual or suspected tumor cells of a subject, and then determining the extent of deuterium labeling of the biomolecule by such cells. A determination that the rate of such deuterium labeling is elevated relative to that of healthy cells (preferably, of the same tissue type, and most preferably of the same tissue type and from the subject) is indicative of the presence of cancer. In one embodiment of such diagnostic method, the determination of the extent of deuterium labeling of the biomolecule is conducted *in vivo* (for example, using magnetic resonance imaging (MRI), **etc**.) or may be determined *in vitro* (for example, by first biopsying or otherwise obtaining a specimen of, the tumor or suspected tumor, and then subjecting the biomolecules produced by the cells of such biopsy or specimen to Liquid Chromatography-Mass Spectroscopy (LC-MS) analysis, Gas Chromatography-Mass Spectroscopy (GC-MS) analysis, *etc.*).

[00115] Although any suitable deuterium-labeled substrate may be employed, it is particularly preferred that such substrate be substrate of a redox-active hydride of NADPH, a substrate of a redox-active hydride of NADH, a substrate of a fatty acid molecule, or a substrate of a thymine moiety-containing biomolecule.

[00116] A particularly preferred deuterium-labeled substrate is 3,3-^{2}H-serine. Providing serine labeled at the hydrogens of carbon 3 (*i.e.*, the methanolic carbon) results in formation of methylene-tetrahydrofolate (THF) with the one-carbon unit labeled at these hydrogens. Use of this methylene-THF to donate its 1 carbon unit to dUMP to form dTMP (which contains a thymine moiety) results in the thymine moiety-containing 2 deuteriums (*i.e.*, mass is M+2). In contrast, if this methylene-THF first forms formyl-THF which then reforms methylene-THF, then one of the

deuteriums is lost and the resulting thymine moiety contains one deuterium (i.e., mass is M+1). When thymine is form solely via the cytosolic folate pathway, either M+1 or M+2 may be formed, depending on the extent of reversible flux through the enzyme MTHFD1. In addition, methylene-THF can directly exchange with formaldehyde (non-enzymatically or enzymatically), thereby losing label. In contrast when thymine is formed via feeding of 1 carbon units formed by the mitochondrial folate pathway into the cytosol, only M+1 thymine is formed. Hence, the extent of thymine labeling, or thymine labeling relative to serine labeling, can be used to ascertain whether cytosolic methylene-THF units contain one-carbon units formed originally in the mitochondrion versus cytosol. This in turn informs the relative activities of the cytosolic and mitochondrial folate pathways. Specifically, significant formation of thymine M+2 indicates a preference for inhibition of the cytosolic pathway for treatment of a tumor, whereas lack of thymine M+2 indicates the suitability of the inhibition of the mitochondrial pathway.

[00117] Although the presence or rate of production of any deuterium-labeled biomolecule formed from such substrate may be determined in accordance with the present invention, it is particularly preferred that such deuterium-labeled biomolecule be a product of NADPH, product of a redox-active hydride of NADPH, a product of a redox-active hydride of NADH, a fatty acid molecule, or a thymine moiety-containing biomolecule (such as thymidine, thymidine triphosphate, thymidine diphosphate, thymidine monophosphate, DNA, *etc.*).

[00118] Alternatively, such assessment may be conducted by incubating tumor cells of a patient in the presence of glycine having one or more isotopically-labeled carbon atoms, determining the rate of isotopically-labeled CO_2 release, and comparing the rate of such CO_2 release to the rate of isotopically-labeled CO_2 release by healthy cells of that individual, or by cells of a healthy individual, receiving the isotopically-labeled glycine. Alternatively, such assessment may be made by determining the rate of isotopically-labeled CO_2 release after administration of serine having one or more isotopically-labeled carbon atoms. Any detectable isotope of carbon may be used for such labeling, however, ^{13}C (detectable via NMR) and ^{14}C (detectable via beta particle emission) are preferred. In selected embodiments, a determination that the cells of the

patient exhibit a higher rate of isotopically-labeled CO_2 release than that exhibited by healthy cells is indicative of the presence of tumor cancer cells, or a determination that the tumor cells of the cancer patient exhibit a higher rate of isotopically-labeled CO_2 release than that exhibited by healthy cells is indicative of a poor cancer prognosis.

[00119] The present invention may also be used to diagnose cancer by measuring the amount (or relative proportion) of NADPH produced in cancer cells via oxPPP. In selected embodiments, a finding that such amount (or proportion) is lower or higher than the amount (or proportion) of NADPH produced in non-cancerous cells is indicative of the aggressiveness of such cancer.

[00120] The cancers that may be diagnosed in the above manners include a cancer such as: an adrenal gland tumor, an AIDS-associated cancer, an alveolar soft part sarcoma, an astrocytic tumor, a bladder cancer (*e.g.*, a squamous cell carcinoma and a transitional cell carcinoma), a bone cancer (*e.g.*, an adamantinoma, an aneurismal bone cyst, an osteochondroma, an osteosarcoma, *etc.*), a brain and spinal cord cancer, a metastatic brain tumor, a breast cancer, a carotid body tumor, a cervical cancer, a chondrosarcoma, a chordoma, a chromophobe renal cell carcinoma, a clear cell carcinoma, a colon cancer, a colorectal cancer, a cutaneous benign fibrous histiocytoma, a desmoplastic small round cell tumor, an ependymoma, a Ewing's tumor, an extraskeletal myxoid chondrosarcoma, a fibrogenesis imperfecta ossium, a fibrous dysplasia of the bone, a gallbladder and bile duct cancer, a gestational trophoblastic disease cancer, a germ cell tumor, a head and neck cancer, an islet cell tumor, a Kaposi's sarcoma, a kidney cancer (*e.g.*, a nephroblastoma, a papillary renal cell carcinoma, *etc.*), a leukemia, a lipoma/benign lipomatous tumor, a liposarcoma/malignant lipomatous tumor, a liver cancer (*e.g.*, a hepatoblastoma, a hepatocellular carcinoma), a lymphoma, a lung cancer (*e.g.*, a small cell carcinoma, a non-small cell carcinoma, an adenocarcinoma, a squamous cell carcinoma, a large cell carcinoma, *etc.*), a medulloblastoma, a melanoma, a meningioma, a multiple endocrine neoplasia, a multiple myeloma, a myelodysplastic syndrome cancer, a neuroblastoma, a neuroendocrine tumor, an ovarian cancer, a pancreatic cancer, a parathyroid tumor, a pediatric cancer, a peripheral nerve sheath tumor, a

phaeochromocytoma, a pituitary tumor, a prostate cancer, a posterious uveal melanoma, a rare hematologic disorder cancer, a renal metastatic cancer, a rhabdoid tumor, a rhabdomysarcoma, a sarcoma, a skin cancer, a soft-tissue sarcoma, a squamous cell cancer, a stomach cancer, a synovial sarcoma, a testicular cancer, a thymic carcinoma, a thymoma, a thyroid cancer (*e.g.*, a papillary thyroid carcinoma, a follicular thyroid carcinoma, a thyroid metastatic cancer, *etc.*) or a uterine cancer (*e.g.*, a carcinoma of the cervix, an endometrial carcinoma, a leiomyoma, *etc.*).

V. Prognostic Utility

[00121] The present invention also provides a method for determining the suitability of a cancer therapy that comprises the administration of an anticancer agent for a particular cancer patient. This embodiment of the invention will most preferably be accomplished by administering a deuterium-labeled substrate of a biomolecule and the anticancer agent to tumor cells of the cancer patient, and then determining the extent of deuterium labeling of the biomolecule by such cells over time (*i.e.*, upon 2 or more determinations made at different times) in the presence or absence of the anticancer agent. The present invention also provides a method for determining the suitability of a therapy for a metabolic disease (especially diabetes) that comprises the administration of a proposed therapeutic agent for a particular patient suffering from the metabolic disease. This embodiment of the invention will most preferably be accomplished by administering a deuterium-labeled substrate of a biomolecule to the patient, and then determining the extent of deuterium labeling of the biomolecule by such cells over time (*i.e.*, upon 2 or more determinations made at different times) in the presence or absence of the proposed therapeutic agent. A finding for such cancer therapy or such therapy for a metabolic disease that the rate of such deuterium labeling is elevated relative to that of healthy cells, and is not substantially reduced over the course of the cancer therapy or the therapy for the metabolic disease is indicative of the non-suitability of the therapy for the particular patient. In selected embodiments, a finding that the administration of such anticancer agent or such proposed therapeutic agent for the metabolic disease has decreased the contribution of the 10-formyl-THF pathway of such cells to cellular NADPH production is indicative of the likely success of the proposed therapy. Significantly, such an assessment may

be made prior to the initiation of any treatment, thus permitting doctors to rule out unsuitable therapies more quickly and at lower cost.

[00122] The deuterium-labeled substrate of a biomolecule and the anticancer agent may be concurrently administered, or may be administered at different times. In one embodiment, the deuterium-labeled substrate of a biomolecule and the anticancer agent are both administered to the patient. Alternatively, either of such reagents may be provided to the patient, after which a sample of tumor cells of the patient (*e.g.*, a biopsy or other specimen), may be removed and the second of such reagents may be administered to the removed sample, and the determination of the extent of deuterium labeling of the biomolecule is determined *in vitro*. Alternatively, both the deuterium-labeled substrate of a biomolecule and the anticancer agent are administered to the removed sample, and the determination of the extent of deuterium labeling of the biomolecule is determined *in vitro*.

[00123] As in the above-described diagnostic methods, the determination of the extent of deuterium labeling of the biomolecule may be conducted *in vivo* (for example, using magnetic resonance imaging (MRI), Raman spectroscopy, *etc.*) or may be determined *in vitro* (for example, by first obtaining a biopsy or other specimen of the tumor, or suspected tumor, and then subjecting the deuterium-labeled biomolecules produced by the cells of such biopsy or specimen to Liquid Chromatography-Mass Spectroscopy (LC-MS) analysis, Gas Chromatography-Mass Spectroscopy (GC-MS) analysis, magnetic resonance imaging (MRI), Raman spectroscopy, *etc.*).

[00124] Similarly to the above-described diagnostic methods, although any suitable deuterium-labeled substrate may be employed, it is particularly preferred that such substrate be a substrate of NADPH, a substrate of a redox-active hydride of NADPH, a substrate of a redox-active hydride of NADH, a substrate of a fatty acid molecule, or a substrate of a thymine moiety-containing biomolecule. A particularly preferred deuterium-labeled substrate is 3,3-^{2}H-serine.

[00125] Particularly when 3,3-^{2}H-serine is used as the deuterium-labeled substrate, such assessments may be made by measuring the production of M+2 deuterium-

labeled thymine or a molecule that comprises an M+2 deuterium-labeled thymine moiety, or by measuring the production of ^{2}H-labeled fatty acid molecules. The present invention is particularly amenable to assessing the suitability of a cancer therapy that comprises inhibiting cytosolic folate metabolism or inhibiting mitochondrial folate metabolism, especially by employing 3,3-^{2}H-serine as the deuterium-labeled substrate, and by measuring the production of M+2 deuterium-labeled thymine or a molecule that comprises an M+2 deuterium-labeled thymine moiety, or by measuring the production of ^{2}H-labeled fatty acid molecules.

[00126] Alternatively, as in the above-described diagnostic methods, although the presence or rate of production of any deuterium-labeled biomolecule formed from such substrate may be determined in accordance with the present invention, it is particularly preferred that such deuterium-labeled biomolecule compromise one or more atoms derived from a redox-active hydride of NADPH, a redox-active hydride of NADH, or that it be a fatty acid molecule, or a thymine moiety-containing biomolecule (such as thymidine, thymidine triphosphate, thymidine diphosphate, thymidine monophosphate, DNA, *etc.*). For example, the invention provides a method for determining the suitability of a cancer therapy that comprises the administration of an anticancer agent for a particular cancer patient in which the anticancer agent and a deuterium-labeled substrate of NADPH are administered to tumor cells of the patient and the rate of passage of deuterium from the labeled substrate into NADPH by the tumor cells in the presence and in the absence of the anticancer agent is measured. A determination that the anticancer agent decreases the rate of passage of deuterium from the labeled substrate into NADPH by the tumor cells is predictive of the effectiveness of the anticancer agent.

[00127] Alternatively, such assessment may be conducted by incubating tumor cells of a patient in the presence of glycine having one or more isotopically-labeled carbon atoms and in the presence and absence of the anticancer agent, determining the rate of isotopically-labeled CO_2 release, and comparing the rate of such CO_2 release to the rate of isotopically-labeled CO_2 release by healthy cells of that individual, or by cells of a healthy individual, receiving the isotopically-labeled glycine. Alternatively, such assessment may be made by determining the rate of isotopically-labeled CO_2 release

after administration of serine having one or more isotopically-labeled carbon atoms. Any detectable isotope of carbon may be used for such labeling, however, ^{13}C (detectable via NMR) and ^{14}C (detectable via beta particle emission) are preferred. In selected embodiments, a determination that the cells of the patient exhibit a higher rate of isotopically-labeled CO_2 release than that exhibited by healthy cells, and that such rate is not substantially reduced over the course of the cancer therapy is indicative of the non-suitability of the therapy for the particular patient.

[00128] The amount (or relative proportion) of NADPH produced by tumor cells via oxPPP may also be used to assess the suitability of a cancer therapy for a particular patient. In selected embodiments, a finding that such amount (or proportion) is lower than the amount (or proportion) of NADPH produced in non-cancerous cells and does not substantially decrease or increase over the course of the cancer therapy is indicative of the non-suitability of the therapy for the particular patient.

[00129] The cancers that may be evaluated in the above manners include a cancer such as: an adrenal gland tumor, an AIDS-associated cancer, an alveolar soft part sarcoma, an astrocytic tumor, a bladder cancer (*e.g.*, a squamous cell carcinoma and a transitional cell carcinoma), a bone cancer (*e.g.*, an adamantinoma, an aneurismal bone cyst, an osteochondroma, an osteosarcoma, *etc.*), a brain and spinal cord cancer, a metastatic brain tumor, a breast cancer, a carotid body tumor, a cervical cancer, a chondrosarcoma, a chordoma, a chromophobe renal cell carcinoma, a clear cell carcinoma, a colon cancer, a colorectal cancer, a cutaneous benign fibrous histiocytoma, a desmoplastic small round cell tumor, an ependymoma, a Ewing's tumor, an extraskeletal myxoid chondrosarcoma, a fibrogenesis imperfecta ossium, a fibrous dysplasia of the bone, a gallbladder and bile duct cancer, a gestational trophoblastic disease cancer, a germ cell tumor, a head and neck cancer, an islet cell tumor, a Kaposi's sarcoma, a kidney cancer (*e.g.*, a nephroblastoma, a papillary renal cell carcinoma, *etc.*), a leukemia, a lipoma/benign lipomatous tumor, a liposarcoma/malignant lipomatous tumor, a liver cancer (*e.g.*, a hepatoblastoma, a hepatocellular carcinoma), a lymphoma, a lung cancer (*e.g.*, a small cell carcinoma, a non-small cell carcinoma, an adenocarcinoma, a squamous cell carcinoma, a large cell carcinoma, *etc.*), a medulloblastoma, a melanoma, a meningioma, a multiple

endocrine neoplasia, a multiple myeloma, a myelodysplastic syndrome cancer, a neuroblastoma, a neuroendocrine tumor, an ovarian cancer, a pancreatic cancer, a parathyroid tumor, a pediatric cancer, a peripheral nerve sheath tumor, a phaeochromocytoma, a pituitary tumor, a prostate cancer, a posterious uveal melanoma, a rare hematologic disorder cancer, a renal metastatic cancer, a rhabdoid tumor, a rhabdomysarcoma, a sarcoma, a skin cancer, a soft-tissue sarcoma, a squamous cell cancer, a stomach cancer, a synovial sarcoma, a testicular cancer, a thymic carcinoma, a thymoma, a thyroid cancer (*e.g.*, a papillary thyroid carcinoma, a follicular thyroid carcinoma, a thyroid metastatic cancer, *etc.*) or a uterine cancer (*e.g.*, a carcinoma of the cervix, an endometrial carcinoma, a leiomyoma, *etc.*).

[00130] Notably, by periodic assessments of the contribution of the 10-formyl-THF pathway to the cellular NADPH production of tumors or of biopsied tumor cells, the present invention permits one to assess whether a particular therapeutic regimen remains suitable for use in the treatment of cancer in a particular patient. Thus, for example, assessments indicating that the contribution of the 10-formyl-THF pathway to the cellular NADPH production of a tumor or of biopsied tumor cells decreased upon initiation of a therapeutic regimen and has remained depressed (relative to baseline) is indicative of the continued efficacy of the therapeutic regimen. Conversely, assessments indicating that the contribution of the 10-formyl-THF pathway to the cellular NADPH production of biopsied tumor cells decreased upon initiation of a therapeutic regimen and but is rising back to baseline is indicative of a failed efficacy of the therapeutic regimen. Most preferably, such assessment is conducted by incubating a sample of such biopsied tumor cells in the presence of a deuterium-labeled substrate of a biomolecule as described above, and then determine the amount, rate or extent of the production of the labeled biomolecule. Thus, the methods of the present invention provide a general "companion" diagnostic suitable for use with a wide variety of therapeutic regimens, such as:

A. **Non-Specific Chemotherapeutic Agents**, such as an **alkylating agent** (*e.g.*, cyclophosphamide, mechlorethamine, chlorambucil, melphalan, nitrosoureas, temozolomide, *etc.*); an **anthracycline** (*e.g.*, daunorubicin, doxorubicin, epirubicin, idarubicin, mitoxantrone, valrubicin, *etc.*); a **cytoskeletal disruptor** (*e.g.*, paclitaxel, docetaxel, *etc.*); an **epothilone** (*e.g.*, epothilone A,

epothilone B, epothilone C, epothilone D, epothilone E, epothilone F, *etc.*); a **histone deacetylase inhibitor** (*e.g.*, vorinostat, romidepsin, *etc.*); **a nucleotide analogue or precursor analogue** (*e.g.*, azacitidine, azathioprine, capecitabine, cytarabine, doxifluridine, fluorouracil, gemcitabine, hydroxyurea, mercaptopurine, methotrexate, tioguanine (formerly thioguanine), *etc.*); **a peptide antibiotic** (*e.g.*, bleomycin, actinomycin, *etc.*); **a platinum-based antineoplastic agent** (*e.g.*, carboplatin, cisplatin, oxaliplatin, *etc.*); **a retinoid** (*e.g.*, tretinoin, alitretinoin, bexarotene, *etc.*); **a vinca alkaloid or derivative** (*e.g.*, vinblastine, vincristine, vindesine, vinorelbine, *etc.*);

B. **Target Specific Chemotherapeutic Agents**, such as a **topoisomerase inhibitor** (*e.g.*, irinotecan, topotecan, etoposide, teniposide, tafluposide, *etc.*), a **kinase inhibitor** (*e.g.*, bortezomib, erlotinib, gefitinib, imatinib, vemurafenib, vismodegib, *etc.*);

C. **Immunotherapeutic Agents** (*e.g.*, antibodies or their epitope-binding fragments, diabodies (*e.g.*, DARTs™, BiTEs™), *etc.*); or

D. **Radiotherapeutics** (*e.g.*, external beam radiation therapy, auger therapy, ionizing radiation therapy, particle therapy, brachytherapy, *etc.*).

[00131] Alternatively, such assessment may be conducted by incubating a sample of such biopsied tumor cells in the presence of carbon isotope-labeled glycine or serine and determining whether the administration of the potential therapeutic agent affects the rate of isotopically-labeled CO_2 release. In one embodiment, cells are transiently incubated in the absence of such agent, the rate of isotopically-labeled CO_2 release is measured and then the cells are further incubated in the presence of such agent with the rate of isotopically-labeled CO_2 release being measured again. Alternatively, two portions of the biopsied sample may be separately incubated, one in the absence of such agent and the second in the presence of such agent, and the observed rate of isotopically-labeled CO_2 release of such portions compared to determine the likely effect of the therapeutic agent. Any detectable isotope of carbon may be used for such labeling, however, ^{13}C (detectable via NMR) and ^{14}C (detectable via beta particle emission) are preferred.

VI. Therapeutic Utility

[00132] Anti-folate anticancer agents act to inhibit the growth of cancer cells by inhibiting the enzymes of folate metabolism, thereby inhibiting the synthesis DNA and RNA. Such agents likewise act to inhibit the synthesis of formate or of molecules that comprises a formate moiety, as well as acting to inhibit the synthesis of glycine and of purines. Since such syntheses are required for the growth and survival of both normal cells and cancer cells, the use of anti-folate anticancer agents are associated with significant side effects, such as:

Common severe side effects include: azotemia, bacterial infection of blood or tissues affecting the whole body, bleeding of the stomach or intestines, canker sores, decreased blood platelet counts, decreased white blood cell counts, intestinal ulcers, inflammation of the gums and mouth, inflammation of the lining of the stomach and intestines, and sun-sensitive skin;

Common less severe side effects include: vertigo, nausea, loss of appetite, fatigue, and general infirmity;

Infrequent severe side effects include: anemia, arachnoid membrane inflammation; disease in the white matter area of the brain, hardening of the liver, hepatitis, interstitial pneumonitis, liver tissue death, and lung fibrosis;

Infrequent less severe side effects include: liver function abnormalities, acne, chills, diarrhea, fever, hair loss, itching, skin boils, skin rashes, and throat irritation;

Rare severe side effects include: Leigh's disease, acquired decrease of all cells in the blood, acute liver failure, avascular necrosis of bone, deficiency of granulocytes, elevation of protein levels in the urine, erythema multiforme, excess liver fibrous tissue, increased uric acid in blood, increased eosinophils concentration in blood, increased spinal fluid pressure, inflammation of blood vessels in the skin, inflammation of the alveoli of the lungs, kidney disease, kidney failure, bone marrow failure, pulmonary failure, *Pneumocystis jirovecii*-associated pneumonia, seizures, skin rash with sloughing, Stevens-Johnson Syndrome, and toxic epidermal necrolysis; and

Rare less severe side effects include: bloody urine, inflammation of the bladder, and low sperm count.

[00133] The recognition that the 10-formyl-THF pathway contributes to cellular NADPH production additionally provides an improved method for using anti-folate anticancer agent to treat cancer. Such a method comprises administering to a cancer patient a pharmaceutical composition comprising:

(A) an anti-folate anticancer agent; and

(B) one or more metabolic compounds selected from the group consisting of thymine, a molecule that comprises a thymine moiety, formate, a molecule that comprises a formate moiety, glycine or a pro-drug thereof, and a purine or a pro-drug thereof; and

(C) a pharmaceutically acceptable excipient, carrier or diluent.

[00134] In accordance with the method, cells are at least partially rescued from the inhibition of thymine synthesis, formate synthesis, glycine synthesis and purine synthesis by the provision of one or more of such metabolic compounds. Accordingly, the effect of the anti-folate anticancer agent will be predominantly or completely focused on inhibiting cellular NADPH production via the 10-formyl-THF pathway. Since this pathway is particularly active in cancer cells (relative to non-cancer cells), the therapeutic index of the treatment (*i.e.*, it selectivity against cancer cells) is enhanced. Thus, the pharmaceutical composition acts to inhibit NADPH production without adversely affecting the concentration of desired metabolic compound(s).

[00135] Thus, the pharmaceutical composition is preferably provided in an amount sufficient to treat the cancer and the included metabolic compound(s) are preferably provided in an amount(s) sufficient to remediate the attenuation of the concentration of such metabolic compound(s) that would otherwise have been caused by the anti-folate anticancer agent. Preferably, the amount of each such included metabolic compound(s) will be independently determined and will be at least 0.25 μg/kg of the patient's body weight, at least 0.5 μg/kg of the patient's body weight, at least 1 μg/kg of the patient's body weight, at least 2 μg/kg of the patient's body weight, at least 3 μg/kg of the patient's body weight, at least 4 μg/kg of the patient's body weight, at least 5 μg/kg of the patient's body weight, at least 6 μg/kg of the patient's body weight, at least 7 μg/kg of the patient's body weight, at least 8 μg/kg of the patient's

body weight, at least 9 μg/kg of the patient's body weight, at least 10 μg/kg of the patient's body weight, at least 25 μg/kg of the patient's body weight, at least 50 μg/kg of the patient's body weight, at least 100 μg/kg of the patient's body weight, at least 250 μg/kg of the patient's body weight, at least 500 μg/kg of the patient's body weight, at least 1 mg/kg of the patient's body weight, at least 5 mg/kg of the patient's body weight, at least 6 mg/kg of the patient's body weight, at least 7 mg/kg of the patient's body weight, at least 8 mg/kg of the patient's body weight, at least 9 mg/kg of the patient's body weight, at least 10 mg/kg of the patient's body weight, at least 20 mg/kg of the patient's body weight, at least 30 mg/kg of the patient's body weight, at least 50 mg/kg of the patient's body weight, at least 100 mg/kg of the patient's body weight, at least 200 mg/kg of the patient's body weight, at least 300 mg/kg of the patient's body weight, at least 500 mg/kg of the patient's body weight, at least 1 g/kg of the patient's body weight, or more than 1 g/kg, or more than 1 g/kg of the patient's body weight.

[00136] Alternatively, the included metabolic compound(s) may be provided in an amount(s) sufficient to attenuate an adverse side effect that would otherwise have been caused by the administered anti-folate anticancer agent. In a preferred embodiment, the pharmaceutical composition is preferably provided in an amount sufficient to achieve one, two, three, four, or more of the following effects:

(i) reduce or ameliorate the severity of: azotemia, bacterial infection, intestinal or stomach ulcers, inflammation of the gums and mouth, inflammation of the lining of the stomach and intestines, or sun-sensitive skin;

(ii) increase blood platelet counts;

(iii) increase white blood cell counts;

(iv) reduce or ameliorate the severity of: anemia, arachnoid membrane inflammation; disease in the white matter area of the brain, hardening of the liver, hepatitis, interstitial pneumonitis, liver tissue death, or lung fibrosis;

(v) reduce or ameliorate the severity of: Leigh's disease, an acute liver failure, an avascular necrosis of bone, a deficiency of granulocytes, an elevation of protein level in the urine, erythema multiforme, excess liver fibrous tissue, increased uric acid in blood, increased eosinophils concentration in blood, increased spinal fluid pressure, inflammation of blood vessels in the skin,

inflammation of the alveoli of the lungs, kidney disease, kidney failure, bone marrow failure, pulmonary failure, Pneumocystis jirovecii-associated pneumonia, seizures, skin rash with sloughing, Stevens-Johnson Syndrome, or toxic epidermal necrolysis;

(vi) reduce or ameliorate the severity of: vertigo, nausea, loss of appetite, fatigue, or general infirmity; or

(vii) enhance or improve the prophylactic or therapeutic effect(s) of another therapy.

[00137] Such attenuation will preferably attenuate at least 20%, more preferably at least 25%, more preferably at least 30%, more preferably at least 35%, more preferably at least 40%, more preferably at least 45%, more preferably at least 50%, more preferably at least 55%, more preferably at least 60%, more preferably at least 65%, more preferably at least 70%, more preferably at least 75%, more preferably at least 80%, more preferably at least 85%, more preferably at least 90%, and most preferably at least 95% of at least one adverse side effect that would otherwise have been caused by the administered anti-folate anticancer agent.

[00138] In accordance with such methods, the anti-folate anticancer agent and the one or more metabolic compounds may be administered simultaneously to the patient, or may be administered to the patient at differing times. For example, the first of such two compositions (*i.e.*, either the anti-folate anticancer agent or the one or more metabolic compounds) can be administered at least 5 minutes prior to, at least 15 minutes prior to, at least 30 minutes prior to, at least 45 minutes prior to, at least 1 hour prior to, at least 2 hours prior to, at least 4 hour prior to, at least 6 hours prior to, at least 12 hours prior to, at least 24 hours prior to, at least 48 hours prior to, at least 96 hours prior to, at least 1 week prior to, at least 2 weeks prior to, at least 3 weeks prior to, at least 4 weeks prior to, at least 5 weeks prior to, at least 6 weeks prior to, at least 8 weeks prior to, or at least 12 weeks prior to the administration of the second of such compositions (*i.e.*, either the one or more metabolic compounds or the anti-folate anticancer agent).

[00139] The administration of the pharmaceutical composition (*i.e.*, the anti-folate anticancer agent, the one or more metabolic compounds, whether provided simultaneously or at different times) may be provided once, or the treatment may be repeated 2, 3, 4, 5, or more times in a course of treatment. Any temporal spacing between the administration of the anti-folate anticancer agent and the administration of the one or more metabolic compounds of a treatment may be maintained or altered in a subsequent treatment.

[00140] The anti-folate anticancer agent of the pharmaceutical composition may be any anti-folate anticancer agent, including in particular, any of those discussed above. Likewise, the cancers that may be treated in this manner include all of those discussed above.

VII. Pharmaceutical Compositions

[00141] Generally, the ingredients of the above-described pharmaceutical composition are supplied either separately or mixed together in unit dosage form, for example, as a dry lyophilized powder or water-free concentrate in a hermetically sealed container such as an ampoule or sachette indicating the quantity of active agent. Where the composition is to be administered by infusion, it can be dispensed with an infusion bottle containing sterile pharmaceutical grade water or saline. Where the composition is administered by injection, an ampoule of sterile water for injection or saline can be provided so that the ingredients may be conveniently mixed prior to administration.

[00142] The above-described pharmaceutical composition compositions may be formulated for oral administration and presented as discrete dosage forms, such as, but are not limited to, tablets (e.g., chewable tablets), caplets, capsules, and liquids (e.g., flavored syrups). Such dosage forms may be prepared by methods of pharmacy well known to those skilled in the art. See generally, Remington: The Science and Practice of Pharmacy (2000) Twentieth Edition, Lippincott Williams & Wilkins: Philadelphia, PA (Gennaro, A.R. ed.). Excipients suitable for use in oral liquid or aerosol dosage forms include, but are not limited to, water, glycols, oils, alcohols, flavoring agents, preservatives, and coloring agents. Excipients suitable for use in

solid oral dosage forms (*e.g.*, powders, tablets, capsules, and caplets) include, but are not limited to, starches, sugars, micro crystalline cellulose, diluents, granulating agents, lubricants, binders, and disintegrating agents.

[00143] Examples of excipients that can be used in oral dosage forms include, but are not limited to, binders, fillers, disintegrants, and lubricants. Binders suitable for use in pharmaceutical compositions and dosage forms include, but are not limited to, corn starch, potato starch, or other starches, gelatin, natural and synthetic gums such as acacia, sodium alginate, alginic acid, other alginates, powdered tragacanth, guar gum, cellulose and its derivatives (e.g., ethyl cellulose, cellulose acetate, carboxymethyl cellulose calcium, sodium carboxymethyl cellulose), polyvinyl pyrrolidone, methyl cellulose, pre gelatinized starch, hydroxypropyl methyl cellulose, (e.g., Nos. 2208, 2906, 2910), microcrystalline cellulose, and mixtures thereof.

[00144] Examples of fillers suitable for use in the pharmaceutical compositions and dosage forms provided herein include, but are not limited to, talc, calcium carbonate (e.g., granules or powder), microcrystalline cellulose, powdered cellulose, dextrates, kaolin, mannitol, silicic acid, sorbitol, starch, pre gelatinized starch, and mixtures thereof. The binder or filler in pharmaceutical compositions provided herein is typically present in from about 50 to about 99 weight percent of the pharmaceutical composition or dosage form.

[00145] Suitable forms of microcrystalline cellulose include, but are not limited to, the materials sold as AVICEL PH 101, AVICEL PH 103 AVICEL RC 581, AVICEL PH 105 (available from FMC Corporation, American Viscose Division, Avicel Sales, Marcus Hook, Pa.), and mixtures thereof. A specific binder is a mixture of microcrystalline cellulose and sodium carboxymethyl cellulose sold as AVICEL RC 581. Suitable anhydrous or low moisture excipients or additives include AVICEL PH 103.TM. and Starch 1500 LM.

[00146] A disintegrant may be used in the composition to provide tablets that disintegrate when exposed to an aqueous environment. The amount of disintegrant used varies based upon the type of formulation, and is readily discernible to those of ordinary skill in the art. Typical pharmaceutical compositions comprise from about

0.5 to about 15 weight percent of disintegrant, specifically from about 1 to about 5 weight percent of disintegrant. Disintegrants that can be used in pharmaceutical compositions and dosage forms provided herein include, but are not limited to, agar, alginic acid, calcium carbonate, microcrystalline cellulose, croscarmellose sodium, crospovidone, polacrilin potassium, sodium starch glycolate, potato or tapioca starch, pre gelatinized starch, other starches, clays, other algins, other celluloses, gums, and mixtures thereof.

[00147] Lubricants may be used in the composition if desired. Suitable lubricants include calcium stearate, magnesium stearate, mineral oil, light mineral oil, glycerin, sorbitol, mannitol, polyethylene glycol, other glycols, stearic acid, sodium lauryl sulfate, talc, hydrogenated vegetable oil (e.g., peanut oil, cottonseed oil, sunflower oil, sesame oil, olive oil, corn oil, and soybean oil), zinc stearate, ethyl oleate, ethyl laureate, agar, and mixtures thereof. Additional lubricants include, for example, a syloid silica gel (AEROSIL 200, manufactured by W.R. Grace Co. of Baltimore, Md.), a coagulated aerosol of synthetic silica (marketed by Degussa Co. of Plano, Tex.), CAB O SIL (a pyrogenic silicon dioxide product sold by Cabot Co. of Boston, Mass.), and mixtures thereof. If used at all, lubricants are typically used in an amount of less than about 1 weight percent of the pharmaceutical compositions or dosage forms into which they are incorporated.

[00148] The compounds of the pharmaceutical compositions can be formulated to permit their controlled release (see, *e.g.,* U.S. Patents. No. 3,845,770; 3,916,899; 3,536,809; 3,598,123; and 4,008,719, 5,674,533, 5,059,595, 5,591,767, 5,120,548, 5,073,543, 5,639,476, 5,354,556, and 5,733,566, each of which is incorporated herein by reference. Such dosage forms can be used to provide slow or controlled release of one or more active ingredients using, for example, hydropropylmethyl cellulose, other polymer matrices, gels, permeable membranes, osmotic systems, multilayer coatings, microparticles, liposomes, microspheres, or a combination thereof to provide the desired release profile in varying proportions. Suitable controlled release formulations known to those of ordinary skill in the art, including those described herein, can be readily selected for use with the active ingredients of the invention. The invention thus encompasses single unit dosage forms suitable for oral

administration such as, but not limited to, tablets, capsules, gelcaps, and caplets that are adapted for controlled release.

[00149] All controlled release pharmaceutical products have a common goal of improving drug therapy over that achieved by their non-controlled counterparts. Ideally, the use of an optimally designed controlled release preparation in medical treatment is characterized by a minimum of drug substance being employed to cure or control the condition in a minimum amount of time. Advantages of controlled release formulations include extended activity of the drug, reduced dosage frequency, and increased patient compliance. In addition, controlled release formulations can be used to affect the time of onset of action or other characteristics, such as blood levels of the drug, and can thus affect the occurrence of side (e.g., adverse) effects.

[00150] Most controlled release formulations are designed to initially release an amount of drug (active ingredient) that promptly produces the desired therapeutic effect, and gradually and continually release of other amounts of drug to maintain this level of therapeutic or prophylactic effect over an extended period of time. In order to maintain this constant level of drug in the body, the drug must be released from the dosage form at a rate that will replace the amount of drug being metabolized and excreted from the body. Controlled release of an active ingredient can be stimulated by various conditions including, but not limited to, pH, temperature, enzymes, water, or other physiological conditions or agents.

[00151] The pharmaceutical composition of the present invention may be formulated for parenteral administration. Parenteral dosage forms can be administered to patients by various routes including, but not limited to, subcutaneous, intravenous (including bolus injection), intramuscular, and intraarterial. Because their administration typically bypasses patients' natural defenses against contaminants, parenteral dosage forms are preferably sterile or capable of being sterilized prior to administration to a patient. Examples of parenteral dosage forms include, but are not limited to, solutions ready for injection, dry products ready to be dissolved or suspended in a pharmaceutically acceptable vehicle for injection, suspensions ready for injection, and emulsions. Suitable vehicles that can be used to provide parenteral dosage forms

provided herein are well known to those skilled in the art. Examples include, but are not limited to: Water for Injection USP; aqueous vehicles such as, but not limited to, Sodium Chloride Injection, Ringer's Injection, Dextrose Injection, Dextrose and Sodium Chloride Injection, and Lactated Ringer's Injection; water miscible vehicles such as, but not limited to, ethyl alcohol, polyethylene glycol, and polypropylene glycol; and non-aqueous vehicles such as, but not limited to, corn oil, cottonseed oil, peanut oil, sesame oil, ethyl oleate, isopropyl myristate, and benzyl benzoate.

[00152] Agents that increase the solubility of the compounds of the pharmaceutical compositions of the present invention can be incorporated into the parenteral dosage forms provided herein, if desired.

[00153] Transdermal, topical, and mucosal dosage forms of the pharmaceutical compositions of the present invention include, but are not limited to, ophthalmic solutions, sprays, aerosols, creams, lotions, ointments, gels, solutions, emulsions, suspensions, or other forms known to one of skill in the art. See generally, Remington: The Science and Practice of Pharmacy (2000) Twentieth Edition, Lippincott Williams & Wilkins: Philadelphia, PA (Gennaro, A.R. ed.). Dosage forms suitable for treating mucosal tissues within the oral cavity can be formulated as mouthwashes or as oral gels. Further, transdermal dosage forms include "reservoir type" or "matrix type" patches, which can be applied to the skin and worn for a specific period of time to permit the penetration of a desired amount of active ingredients.

[00154] Suitable excipients (*e.g.*, carriers and diluents) and other materials that can be used to provide transdermal, topical, and mucosal dosage forms provided herein are well known to those skilled in the pharmaceutical arts, and depend on the particular tissue to which a given pharmaceutical composition or dosage form will be applied. With that fact in mind, typical excipients include, but are not limited to, water, acetone, ethanol, ethylene glycol, propylene glycol, butane 1,3 diol, isopropyl myristate, isopropyl palmitate, mineral oil, and mixtures thereof to form lotions, tinctures, creams, emulsions, gels or ointments, which are non-toxic and pharmaceutically acceptable. Moisturizers or humectants can also be added to

pharmaceutical compositions and dosage forms if desired. Examples of such additional ingredients are well known in the art. See generally, Remington: The Science and Practice of Pharmacy (2000) Twentieth Edition, Lippincott Williams & Wilkins: Philadelphia, PA (Gennaro, A.R. ed.).

[00155] Depending on the specific tissue to be treated, additional components may be used prior to, in conjunction with, or subsequent to treatment with the pharmaceutical compositions of the present invention. For example, penetration enhancers can be used to assist in delivering the active ingredients to the tissue. Suitable penetration enhancers include, but are not limited to: acetone; various alcohols such as ethanol, oleyl, and tetrahydrofuryl; alkyl sulfoxides such as dimethyl sulfoxide; dimethyl acetamide; dimethyl formamide; polyethylene glycol; pyrrolidones such as polyvinylpyrrolidone; Kollidon grades (Povidone, Polyvidone); urea; and various water soluble or insoluble sugar esters such as Tween 80 (polysorbate 80) and Span 60 (sorbitan monostearate).

[00156] The pH of a pharmaceutical composition or dosage form, or of the tissue to which the pharmaceutical composition or dosage form is applied, may also be adjusted to improve delivery of the pharmaceutical compositions of the present invention. Similarly, the polarity of a solvent carrier, its ionic strength, or tonicity can be adjusted to improve delivery. Agents such as stearates can also be added to pharmaceutical compositions or dosage forms to advantageously alter the hydrophilicity or lipophilicity of the pharmaceutical compositions of the present invention so as to improve delivery. In this regard, stearates can serve as a lipid vehicle for the formulation, as an emulsifying agent or surfactant, and as a delivery enhancing or penetration enhancing agent. Different salts, hydrates or solvates of the Compounds can be used to further adjust the properties of the resulting composition.

[00157] In certain specific embodiments, the compositions are in oral, injectable, or transdermal dosage forms. In one specific embodiment, the compositions are in oral dosage forms. In another specific embodiment, the compositions are in the form of injectable dosage forms. In another specific embodiment, the compositions are in the form of transdermal dosage forms.

VIII. Use in Drug Discovery

[00158] The methods of the present invention also find utility in facilitating the discovery of new anticancer therapies. Thus, for example, the contribution of the 10-formyl-THF pathway to cellular NADPH production may be determined with respect to cancer cells (either primary or of an established cell line) in the absence or presence of one or more candidate therapeutic agents, to thereby assess whether any such candidate therapeutic agent decreases the contribution of the 10-formyl-THF pathway of such cells to cellular NADPH production. A finding of such a decrease is indicative that a candidate therapeutic agent possesses efficacy in the treatment of cancer. Such cancer may be any of those discussed above.

[00159] Most preferably, such assessment is conducted by incubating a sample of such cancer cells in the presence of isotopically-labeled glycine or serine and determining whether the administration of the candidate therapeutic agent affects the rate of isotopically-labeled CO_2 release. In one embodiment, cells are transiently incubated in the absence of any such agent, the rate of isotopically-labeled CO_2 release is measured and then the cells are further incubated in the presence of a candidate therapeutic agent with the rate of isotopically-labeled CO_2 release being measured again. Alternatively, portions of the cell sample may be separately incubated, one or more in the absence of any such agent and one or more in the presence of a candidate therapeutic agent, and the observed rate of isotopically-labeled CO_2 release of such portions compared to determine whether any of the candidate therapeutic agent have anticancer therapeutic potential. Any detectable isotope of carbon may be used for such labeling, however, ^{13}C (detectable via NMR) and ^{14}C (detectable via beta particle emission) are preferred. In other embodiments, the above approach is applied by using ^{2}H-tracers as described in the preceding sections as the readout.

IX. Kits

[00160] The present invention additionally includes diagnostic kits suitable for facilitating the above-described diagnostic methods. Such kits may comprise, for

example, one or more containers having filter paper, 10 M KOH, and other reagents suitable for collecting evolved CO_2 for subsequent quantitative measurement.

[00161] Having now generally described the invention, the same will be more readily understood through reference to the following examples, which are provided by way of illustration and are not intended to be limiting of the present invention unless specified.

Example 1
Use of Deuterium Tracer to Directly Measure NADPH Redox-Active Hydrogen Labeling

[00162] To probe the oxPPP, cells were shifted from unlabeled to 1-^{2}H-glucose or 3-^{2}H-glucose (**Figure 1A**) and the resulting NADP+ and NADPH labeling was measured using liquid chromatography-mass spectrometry (Lu, W. *et al.* (2010) "*Metabolomic Analysis Via Reversed-Phase Ion-Pairing Liquid Chromatography Coupled To A Stand Alone Orbitrap Mass Spectrometer*," Analytical Chemistry 82:3212-3221).

[00163] Results of such measurements are shown in the mass spectrum provided in **Figure 1B** and **Figure 5A**). The M+1 and M+2 peaks in NADP+ are natural isotope abundance, primarily from ^{13}C. The difference between NADP+ and NADPH reflects the redox-active hydrogen labeling. The labeling of NADPH's redox-active hydrogen is fast ($t_{1/2}$ approximately 5 min) (**Figure 1C**; in the Figure, all fractional labeling data are corrected for natural isotope abundance as opposed to relative mass intensities). NADPH labeling was similar across four different transformed mammalian cell lines. Knockdown of the committed enzyme of the oxPPP, glucose-6-phosphate dehydrogenase, eliminated most of the labeling, confirming that the NADPH-deuterium labeling reflects oxPPP flux (**Figure 1D**). Note that these ^{2}H-labeling experiments directly measure the fraction of NADPH made by the oxPPP without relying on measurement of the absolute pathway flux. Using either 1-^{2}H- or 3-^{2}H-glucose, we find that oxPPP accounts for 30-50% of overall NADP+ reduction.

Example 2
Use of Deuterium Tracer to Directly Measure NADPH Production from Other Pathways

[00164] To investigate whether ^{2}H-labeling could be used to directly observe NADPH production by other pathways (**Figure 2A**), cells were fed 2,3,3,4,4-^{2}H-glutamine and 2,3,3-^{2}H-aspartate. Downstream products of glutamine can potentially transfer ^{2}H to NADPH via glutamate dehydrogenase or malic enzyme, while downstream products of aspartate may do so via isocitrate dehydrogenase (**Figures 8A-8F**).

[00165] Malic enzyme can produce either NADH or NADPH. Thus, total malic enzyme flux puts an upper limit on the associated NADPH production. To probe overall malic enzyme activity, cells were incubated with U-^{13}C-glutamine for 48 h, which resulted in a majority of intracellular malate being uniformly labeled (4-^{13}C, denoting the labeling of all four of the malate carbon atoms, "$^{13}C_4$"), with a small portion being 3-^{13}C (denoting the labeling of 3 of the 4 malate carbon atoms). For simplicity, it is assumed that 3-^{13}C-malate is an equal mix of 1,2,3-^{13}C-malate and 2,3,4-^{13}C-malate (collectively designated as "$^{13}C_3$" malate) due to its rapid inter-conversion with fumarate (which is symmetric). Malic enzyme produces $^{13}C_3$-pyruvate from both 1,2,3,4-^{13}C malate and 1,2,3-^{13}C-malate, whereas glycolysis produces unlabeled pyruvate (**Figures 8A-8H**).

$$Flux_{NADPH\,ME} \leq \frac{Pyruvate(^{13}C_3)}{Total\ Pyruvate} \times \frac{Total\ Malate}{Malate(^{13}C_4) + 0.5Malate(^{13}C_3)} \times Flux_{glycolysis}$$

(Equation 23)

[00166] Identical mass spectra was observed for NADP+ and NADPH after feeding the deuterium-labeled glutamine and aspartate (**Figure 2B-2C**, **Figures 8B** and **8D**), and thus could not directly assign a fractional contribution to these pathways. Given recent evidence that malic enzyme is particularly important in cancer (Jiang, P. *et al.* (2013) "*Reciprocal Regulation Of P53 And Malic Enzymes Modulates Metabolism And Senescence*," Nature 493:689-693; Son, J. *et al.* (2013) "*Glutamine Supports Pancreatic Cancer Growth Through A KRAS-Regulated Metabolic Pathway*," Nature 496:101-105), an orthogonal approach based on feeding U-^{13}C-glutamine and

measuring labeling of pyruvate, lactate and citrate was used to evaluate its activity (**Figures 8G** and **8H**). While such carbon tracer studies cannot distinguish between NADH-dependent and NADPH-dependent malic enzyme, they put an upper bound on their collective activities, which ranged from 15% to 50% of cytosolic NADPH production depending on the cell line.

Example 3
Use of Deuterium Tracer to Directly Demonstrate the Presence of a Folate-Dependent Pathway for NADPH Production

[00167] A genome-scale human metabolic model (Duarte, N. C. *et al.* (2007) "*Global Reconstruction Of* The *Human Metabolic Network Based On Genomic And Bibliomic Data*," Proc. Natl. Acad. Sci. (U.S.A.) 104:1777-1782) predicted that the main folate-dependent NADPH-producing pathway involved the transfer of a one-carbon unit from serine to THF, followed by oxidation of the resulting product (methylene-THF) by the enzyme MTHFD to form the purine precursor formyl-THF with concomitant NADPH production. To assess whether this pathway indeed contributed to NADPH production, mouse kidney cells (iBMK-parental cells) (Degenhardt, K. *et al.* (2002) "*BAX And BAK Mediate P53-Independent Suppression Of Tumorigenesis*," Cancer Cell 2:193-203) were fed cells 2,3,3-^{2}H-serine, and labeling of both NADP+ and NADPH was observed. NADP+ labeling would result from the incorporation of the serine-derived formyl-THF one-carbon unit into NADP+'s adenine ring.

[00168] Relative to NADP+, the labeling pattern of NADPH was found to have been shifted towards more heavily labeled forms, indicating the specific labeling of NADPH's redox-active hydrogen (**Figure 2E**, **Figures 9C** and **9D**). Thus, the experimental results demonstrate that serine-driven folate metabolism contributed to NADP+ reduction.

[00169] To assess the functional significance of different pathways to NADPH homeostasis, a variety of potential NADPH-producing enzymes were knocked down in HEK293T cells, and the cellular NADPH to NADP+ ratio was measured (**Figure 2F**). While knockdown of malic enzyme 1 (ME1), cytosolic or mitochondrial NADP-dependent isocitrate dehydrogenase (IDH1 and IDH2), and transhydrogenase (NNT) did not significantly impact the NADPH to NADP+ ratio, knockdown of glucose-6-

phosphate dehydrogenase or either isozyme of methylene-tetrahydrofolate dehydrogenase (MTHFD1, cytosolic, or MTHFD2, mitochondrial) substantially decreased it. These observations further support the primacy of the oxPPP and folate-dependent pathways in NADPH production.

[00170] The importance of both isozymes of methylene-tetrahydrofolate dehydrogenase suggests that cytosolic and mitochondrial folate metabolism (**Figure 3A**) both contribute to NADPH homeostasis. The product of methylene-tetrahydrofolate dehydrogenase, 10-formyl-THF, is a required purine precursor, with each purine ring containing two formyl groups. Thus, the cytosolic 10-formyl-THF production rate must be at least twice the purine biosynthetic flux. The most direct path to cytosolic 10-formyl-THF is via MTHFD1 with concomitant NADPH production (**Figure 3A, striped lines**). Alternatively, 10-formyl-THF could potentially be made from formate initially generated in the mitochondrion (**Figure 3A, dashed lines**) (Tibbetts, A.S. *et al.* (2010) "*Compartmentalization Of Mammalian Folate-Mediated One-Carbon Metabolism*," Ann. Rev. Nutr. 30:57-81; Christensen, K.E. *et al.* (2008) "*Mitochondrial Methylenetetrahydrofolate Dehydrogenase, Methenyltetrahydrofolate Cyclohydrolase, And Formyltetrahydrofolate Synthetases*," Vitamins Hormones 79:393-410). To investigate these possibilities, U-^{13}C-glycine, which contributes selectively to mitochondrial one-carbon pools (**Figure 3A, gray lines**) was fed to cells. Glycine is assimilated intact into purines, resulting in M+2 labeling of ATP; however, labeling of M+1, M+3, or M+4 ATP was not detected, indicating that mitochondrial glycine-derived one-carbon units do not contribute to purine biosynthesis (**Figure 3B**). Consistent with this result, feeding of U-^{13}C-serine revealed that most one-carbon units assimilated into purines came from serine (**Figures 10A** and **10B**), and knockdown of MTHFD1 nearly eliminated NADPH redox-active hydrogen labeling from 2,3,3-^{2}H-serine (**Figure 3C**).

[00171] Assuming that all 10-formyl-THF production for purine synthesis is coupled to NADP+ reduction, the total NADPH production rate is approximately 2 nmol uL^{-1} h^{-1} (**Figure 3D**) or approximately 25% of total cytosolic NADPH flux. To probe potential further oxidation of serine, cells were fed 3-^{14}C-serine and release

of $^{14}CO2$ was observed, indicating that the THF pathway runs in excess of one-carbon demand so as to yield additional NADPH (**Figure 3D**, **Figures 11A-11H**).

[00172] The consequences of elimination of serine from the medium was also investigated (**Figures 12A-12E**). As has been observed previously both *in vitro* (Locasale, J.W. *et al.* (2011) "*Phosphoglycerate Dehydrogenase Diverts Glycolytic Flux And Contributes To Oncogenesis*," Nature Genetics 43:869-874; Possemato, R. *et al.* (2011) "*Functional Genomics Reveal That The Serine Synthesis Pathway Is Essential In Breast Cancer*," Nature 476:346-350) and in tumor models (Maddocks, O.D. *et al.* (2013) "*Serine Starvation Induces Stress And P53-Dependent Metabolic Remodelling In Cancer Cells*," Nature 493:542-546), serine depletion impaired cell growth (**Figure 12B**). Consistent with NADPH being an important downstream product of serine, serine removal decreased the NADPH to NADP+ ratio (**Figure 12C**). Glycine is both a product of serine metabolism, and itself a potential source of one-carbon units via the mitochondrial glycine cleavage system, whose expression has been linked to oncogenic transformation (Zhang, W.C. *et al.* (2012) "*Glycine Decarboxylase Activity Drives Non-Small Cell Lung Cancer Tumor-Initiating Cells And Tumorigenesis*," Cell 148:259-272). Accordingly, the conversion of serine and glycine were tested by ^{13}C labeling. It was found that flux through serine hydroxymethyltransferase is reversible, however, glycine-derived one-carbon unit cannot be used to synthesize serine in tested condition (**Figures 12B-12E**). Thus, increased glycine impairs methylene-THF production.

[00173] The above results establish that serine-driven, one-carbon metabolism plays a major role in NADPH homeostasis. Knockdown of MTHFD2 also alters the NADPH to NADP+ ratio, suggesting an additional role for mitochondrial one-carbon metabolism. Mitochondrial folate-dependent enzymes, especially MTHFD2, are overexpressed across human cancers (Nilsson, R. *et al.* (2014) "*Metabolic Enzyme Expression Highlights A Key Role For MTHFD2 And The Mitochondrial Folate Pathway In Cancer*," Nature Commun. 5:3128).

[00174] To probe specifically mitochondrial folate metabolism, cells were fed ^{14}C-labeled glycine and the release of radioactive CO_2 was monitored. The glycine

cleavage system releases the 1-C carbon of glycine as CO_2, while transferring glycine's 2-C carbon to THF (thereby forming methylene-THF). Notably, almost as much radioactive CO_2 was released from 2-^{14}C-glycine as from 1-^{14}C-glycine (**Figure 3E**), indicating that a majority of mitochondrial methylene-THF was being fully oxidized to CO_2. Consistent with such complete oxidation, when cells were fed ^{13}C-labeled glycine, the transfer of one-carbon units to the cytosol was not observed, based on the thymidine triphosphate (dTTP) or methionine labeling, with dTTP's one-carbon unit coming from serine (90-100%) and methionine coming from the medium (**Figures 10A-10F**). As expected based on the mitochondrial methylene-THF oxidation pathway, release of the 2-C carbon of glycine as CO_2 was decreased by knockdown of either MTHFD2 or ALDH1L2 (**Figure 11G**). Such complete one-carbon unit oxidation may be beneficial for reducing the cellular glycine concentration. In addition, it produces mitochondrial NADPH. Thus, two functions of mitochondrial folate metabolism are glycine detoxification and NADPH production.

Example 4
NADPH and Antioxidant Defense

[00175] One important role of NADPH is antioxidant defense. Consistent with folate metabolism being a significant NADPH producer, antifolates have been found to induce oxidative stress (Ayromlou, H. *et al.* (2011) "*Oxidative Effect Of Methotrexate Administration In Spinal Cord Of Rabbits*" J. Pakistan Med. Assoc. 61:1096-1099). To more directly link folate-mediated NADPH production with cellular redox defenses, glutathione, reactive oxygen species, and hydrogen peroxide sensitivity of MTHFD1 and MTHFD2 knockdown cells were measured. Knockdown of either isozyme decreased the ratio of reduced to oxidized glutathione (**Figure 3F**) and impaired resistance to oxidative stress induced by hydrogen peroxide (**Figures 3G** and **3H**) or diamide (**Figure 3I**). MTHFD2 knockdown specifically increased reactive oxygen species (**Figure 3J**), and ALDH1L2 knockdown decreased the ratio of reduced to oxidized glutathione (**Figure 11H**), demonstrating that the complete mitochondrial methylene-THF oxidation pathway is required for redox homeostasis.

[00176] To address the relative use of NADPH for biosynthesis versus redox defense total cytosolic NADPH production (as measured above) was compared to NADPH

consumption for biosynthesis (**Figure 4A**) based on the measured cellular content of DNA, amino acids, and lipids; their production routes (measured using a ^{13}C tracer); and cellular growth rate (**Figures 13A-13G**). The overall demand for NADPH for biosynthesis is > 80% of total cytosolic NADPH production (**Figure 4B**), with a majority of this NADPH consumed by fatty acid synthesis. Thus, in cells growing under aerobic conditions (and particularly transformed or cancerous cells) most cytosolic NADPH is devoted to biosynthesis, not redox defense.

[00177] To evaluate NADPH consumption for redox defense under overt redox stress, HEK293T cells were treated with hydrogen peroxide at a concentration that blocked growth without causing substantial cell death and the total cytosolic NADPH production rate was measured. The rate was found to be 5.5 nmol μL^{-1} $h^{-}1$, about half the rate observed in freely growing cells (**Figure 13H**). Thus, consistent with most cytosolic NADPH in growing cells being used for biosynthesis, growth-inhibiting oxidative stress decreased cytosolic NADPH production.

Example 5
Coupling of Nucleotide Synthesis with NADPH Production

[00178] The production of NADPH by the oxidative pentose phosphate pathway, which makes the nucleotide building block ribose, and by the 10-formyl-THF pathway, which contributes to purine synthesis, leads to an inherent coupling of nucleotide synthesis with NADPH production. These reactions together produce in growing cells roughly the amount of NADPH required for replication of cellular lipids (**Figure 4B**). Interruption of this intrinsic coordination by feeding of purines can impair cell growth (Bradley, K.K. *et al.* (2001) "*Purine Nucleoside-Dependent Inhibition Of Cellular Proliferation In 1321N1 Human Astrocytoma Cells*," J. Pharmacol. Exper. Therap. 299:748-752). In non-growing cells, or in other cases in which NADPH needs outstrip production coupled to nucleotide synthesis, it is likely that alternative pathways, *e.g.*, malic enzyme and IDH, will be of greater importance than was observed.

[00179] The contribution of the 10-formyl-THF pathway to NADPH production is particularly interesting in light of the importance of metabolism of serine and glycine,

the major carbon sources of this pathway, to cancer growth (Tedeschi, P.M. *et al.* (2013) "*Contribution Of Serine, Folate And Glycine Metabolism To The ATP, NADPH And Purine Requirements Of Cancer Cells*," Cell Death Dis. 4:e877 (pages 1-12). Serine synthesis is promoted by the cancer-associated M2 isozyme of pyruvate kinase (PKM2) and by amplification of 3-phosphoglycerate dehydrogenase (Locasale, J.W. *et al.* (2011) "*Phosphoglycerate Dehydrogenase Diverts Glycolytic Flux And Contributes To Oncogenesis*," Nature Genetics 43:869-874; Possemato, R. *et al.* (2011) "*Functional Genomics Reveal That The Serine Synthesis Pathway Is Essential In Breast Cancer*," Nature 476:346-350). The present data indicates that serine serves dual roles in providing both one-carbon units and NADPH. In this respect, it is significant that PKM2, in addition to sensing serine (Ye, J. *et al.* (2012) "*Pyruvate Kinase M2 Promotes De Novo Serine Synthesis To Sustain mTORC1 Activity And Cell Proliferation*," Proc. Natl. Acad. Sci. (U.S.A.) 109:6904-6909; Chaneton, B. *et al.* (2012) "*Serine Is A Natural Ligand And Allosteric Activator Of Pyruvate Kinase M2*," Nature 491:458-462), is inactivated by oxidative stress (Anastasiou, D. *et al.* (2011) "*Inhibition Of Pyruvate Kinase M2 By Reactive Oxygen Species Contributes To Cellular Antioxidant Responses*," Science 334:1278-1283). Such inactivation should increase 3-phosphoglycerate and thus potentially serine-driven NADPH production.

[00180] In addition to synthesizing serine, rapidly growing cells avidly consume glycine (Jain, M. *et al.* (2012) "*Metabolite Profiling Identifies A Key Role For Glycine In Rapid Cancer Cell Proliferation*," Science 336:1040-1044). Significantly, while only intact glycine (and not glycine-derived one-carbon units) is incorporated into purines, knockdown of the glycine cleavage system impairs cancer growth (Zhang, W.C. *et al.* (2012) "*Glycine Decarboxylase Activity Drives Non-Small Cell Lung Cancer Tumor-Initiating Cells And Tumorigenesis*," Cell 148:259-272). One aspect of the present invention relates to the finding that most glycine-derived one-carbon units are fully oxidized, arguing against the glycine cleavage system's primary role, at least in the tested cell lines, being to release one-carbon units to the cytosol. Instead, its function may be simultaneous elimination of unwanted glycine and production of mitochondrial NADPH.

[00181] Understanding NADPH's production and consumption routes is essential to global understanding of metabolism. The approaches provided herein will enable evaluation of these routes in different cell types and environmental conditions. Analogous measurements for ATP, achieved first more than a half century ago (Warburg, O. (1956) "*On The Origin Of Cancer Cells*," Science 123:309-314), have formed the foundation for much of subsequent metabolism research. Given NADPH's comparable role in medically important processes including lipogenesis, oxidative stress, and tumor growth (Vander Heiden, M.G. *et al.* (2009) "*Understanding the Warburg Effect: The Metabolic Requirements Of Cell Proliferation*," Science 324:1029-1033), quantitative analysis of its metabolism is of similar importance and provides a means for diagnosing and evaluating cancer and other diseases.

[00182] All publications and patents mentioned in this specification are herein incorporated by reference to the same extent as if each individual publication or patent application was specifically and individually indicated to be incorporated by reference in its entirety. While the invention has been described in connection with specific embodiments thereof, it will be understood that it is capable of further modifications and this application is intended to cover any variations, uses, or adaptations of the invention following, in general, the principles of the invention and including such departures from the present disclosure as come within known or customary practice within the art to which the invention pertains and as may be applied to the essential features hereinbefore set forth.

What Is Claimed Is:

Claim 1. A method of assessing the suitability of a cancer therapy for a particular cancer patient, wherein said cancer therapy comprises the administration of an anticancer agent, which method comprises:

(A) administering a deuterium-labeled substrate of a biomolecule and said anticancer agent to tumor cells of said patient; and

(B) determining the extent of deuterium labeling of said biomolecule by said tumor cells;

wherein a determination that the rate of said deuterium labeling is elevated relative to that of healthy cells, and is not substantially reduced over the course of said cancer therapy is indicative of the non-suitability of said therapy for said particular patient.

Claim 2. The method of claim 1, wherein said deuterium-labeled substrate and said anticancer agent are administered to said patient, and wherein said rate of said deuterium labeling is determined *in vivo*.

Claim 3. The method of claim 1, wherein said deuterium-labeled substrate and said anticancer agent are administered to tumor cells removed from said patient, and wherein said rate of said deuterium labeling is determined *in vitro*.

Claim 4. The method of claim 1, wherein said anticancer agent is administered to said patient and said deuterium-labeled substrate is administered to tumor cells removed from said patient, and wherein said rate of said deuterium labeling is determined *in vitro*.

Claim 5. The method of any of claims 1-4, wherein said deuterium-labeled substrate is a substrate of a redox-active hydride of NADPH and said deuterium-labeled biomolecules comprise said redox-active hydride of NADH.

Claim 6. The method of any of claims 1-4, wherein said deuterium-labeled substrate is a substrate of a redox-active hydride of NADPH and said deuterium-labeled biomolecules comprise said redox-active hydride of NADPH.

Claim 7. The method of any of claims 1-6, wherein said deuterium-labeled substrate is a substrate of a molecule having a fatty acid moiety and said deuterium-labeled biomolecules comprise said molecule having said fatty acid moiety.

Claim 8. The method of any of claims 1-6, wherein said deuterium-labeled substrate is a substrate of a thymine moiety-containing biomolecule and said deuterium-labeled biomolecules comprise said thymine moiety-containing biomolecule.

Claim 9. The method of any of claims 1-4, wherein said cancer therapy comprises inhibiting cytosolic folate metabolism, wherein said deuterium-labeled substrate is a serine molecule that comprises deuteration at serine carbon C-3, and wherein said extent of deuterium labeling of said one or more biomolecules by said tumor cells is determined by measuring the ratio of M+1 to M+2 of deuterated thymine or of a molecule that comprises a deuterated thymine moiety.

Claim 10. The method of any of claims 1-4, wherein said cancer therapy comprises inhibiting mitochondrial folate metabolism, wherein said deuterium-labeled substrate is a serine molecule that comprises deuteration at serine carbon C-3, and wherein said extent of deuterium labeling of said one or more biomolecules by said tumor cells is determined by measuring the ratio of M+1 to M+2 of deuterated thymine or of a molecule that comprises a deuterated thymine moiety.

Claim 11. The method of any of claims 1-4, wherein said cancer therapy comprises inhibiting cytosolic folate metabolism, wherein said deuterium-labeled substrate is a serine molecule that comprises

deuteration at serine carbon C-3, and wherein said extent of deuterium labeling of said one or more biomolecules by said tumor cells is determined by measuring the production of a ^{2}H-labeled fatty acid moiety.

Claim 12. The method of any of claims 1-4, wherein said cancer therapy comprises inhibiting mitochondrial folate metabolism, wherein said deuterium-labeled substrate is a serine molecule that comprises deuteration at serine carbon C-3, and wherein said extent of deuterium labeling of said one or more biomolecules by said tumor cells is determined by measuring the production of a ^{2}H-labeled fatty acid moiety.

Claim 13. The method of any of claims 9-12, wherein said deuterium-labeled substrate is 2,3,3-^{2}H-serine or 3,3-^{2}H-serine.

Claim 14. The method of any of claims 1-13, wherein said extent of deuterium labeling is determined using magnetic resonance imaging (MRI).

Claim 15. The method of any of claims 1-13, wherein said extent of deuterium labeling is determined using Liquid Chromatography-Mass Spectroscopy (LC-MS), Gas Chromatography-Mass Spectroscopy (GC-MS) or Raman spectroscopy.

Claim 16. The method of any of claims 1-15, wherein said anticancer agent is selected from the group consisting of a Non-Specific Chemotherapeutic Agent and a Target Specific Chemotherapeutic Agent.

Claim 17. The method of any of claims 1-15, wherein said anticancer agent is an Immunotherapeutic Agent, and is selected from the group consisting of an antibody, a molecule that comprises an epitope-binding fragment of an antibody, and a diabody.

Claim 18. A method of treating cancer in a cancer patient, wherein said method comprises administering to said cancer patient a pharmaceutical composition comprising:

(A) an anti-folate anticancer agent; and

(B) one or more metabolic compounds selected from the group consisting of thymine, a molecule that comprises a thymine moiety, formate, a molecule that comprises a formate moiety, glycine and a purine; and

(C) a pharmaceutically acceptable excipient, carrier or diluent;

wherein said composition contains said anti-folate anticancer agent in an amount sufficient to treat said cancer and contains said metabolic compound(s) in amount(s) sufficient to remediate attenuation of the concentration of said metabolic compound(s) by said anti-folate anticancer agent or to attenuate an adverse side effect caused by said administered anti-folate anticancer agent.

Claim 19. The method of claim 18, wherein said one or more metabolic compounds is thymidine.

Claim 20. The method of any of claims 1-18, wherein said tumor cells are tumor cells of: an adrenal gland tumor, an AIDS-associated cancer, an alveolar soft part sarcoma, an astrocytic tumor, bladder cancer, bone cancer, a brain and spinal cord cancer, a metastatic brain tumor, a breast cancer, a carotid body tumor, a cervical cancer, a chondrosarcoma, a chordoma, a chromophobe renal cell carcinoma, a clear cell carcinoma, a colon cancer, a colorectal cancer, a cutaneous benign fibrous histiocytoma, a desmoplastic small round cell tumor, an ependymoma, a Ewing's tumor, an extraskeletal myxoid chondrosarcoma, a fibrogenesis imperfecta ossium, a fibrous dysplasia of the bone, a gallbladder or bile duct cancer, gastric cancer, a gestational trophoblastic disease, a germ cell tumor, a head and neck cancer, hepatocellular carcinoma, an islet cell tumor, a Kaposi's sarcoma, a kidney cancer, a leukemia, a lipoma/benign lipomatous

tumor, a liposarcoma/malignant lipomatous tumor, a liver cancer, a lymphoma, a lung cancer, a medulloblastoma, a melanoma, a meningioma, a multiple endocrine neoplasia, a multiple myeloma, a myelodysplastic syndrome, a neuroblastoma, a neuroendocrine tumors, an ovarian cancer, a pancreatic cancer, a papillary thyroid carcinoma, a parathyroid tumor, a pediatric cancer, a peripheral nerve sheath tumor, a phaeochromocytoma, a pituitary tumor, a prostate cancer, a posterior uveal melanoma, a rare hematologic disorder, a renal metastatic cancer, a rhabdoid tumor, a rhabdomysarcoma, a sarcoma, a skin cancer, a soft-tissue sarcoma, a squamous cell cancer, a stomach cancer, a synovial sarcoma, a testicular cancer, a thymic carcinoma, a thymoma, a thyroid metastatic cancer, or a uterine cancer.

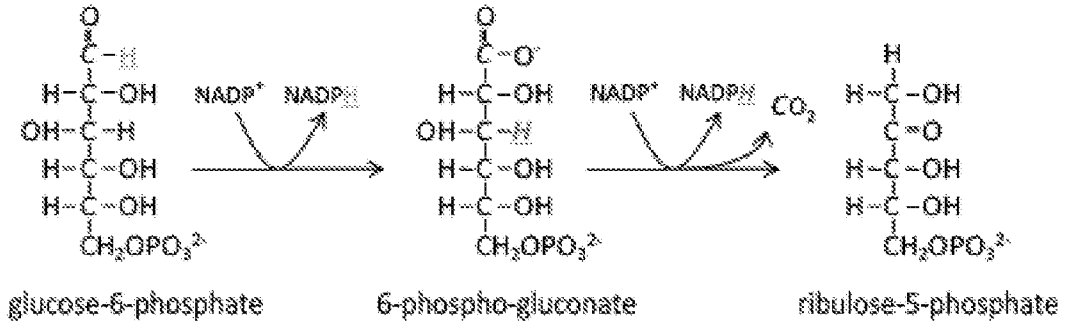

Figure 1A

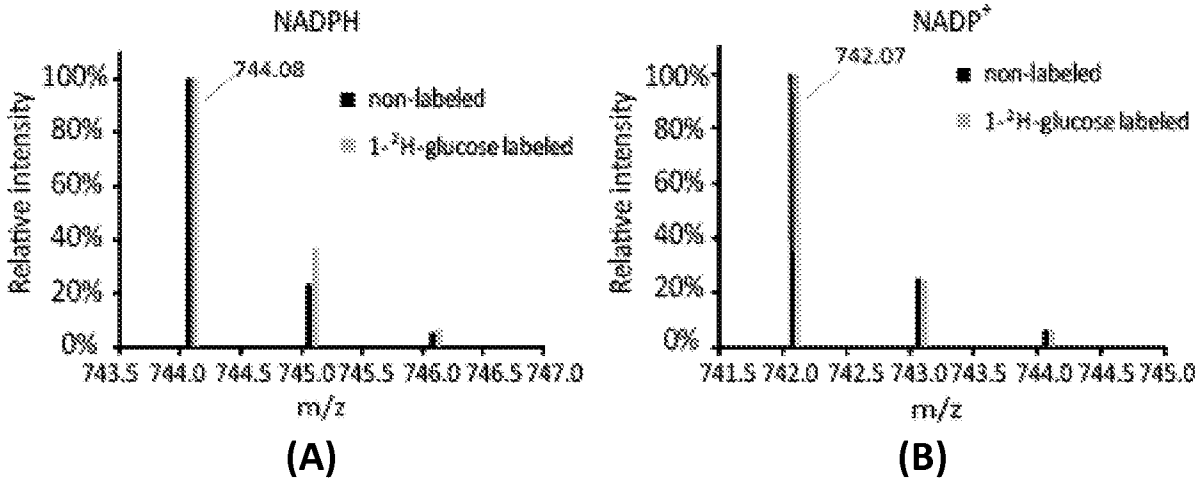

Figure 1B

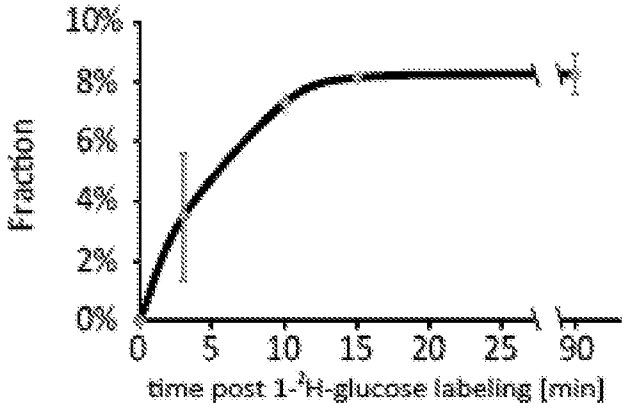

Figure 1C

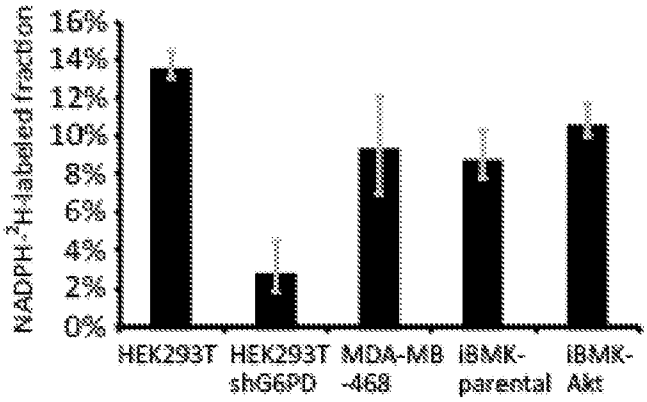

Figure 1D

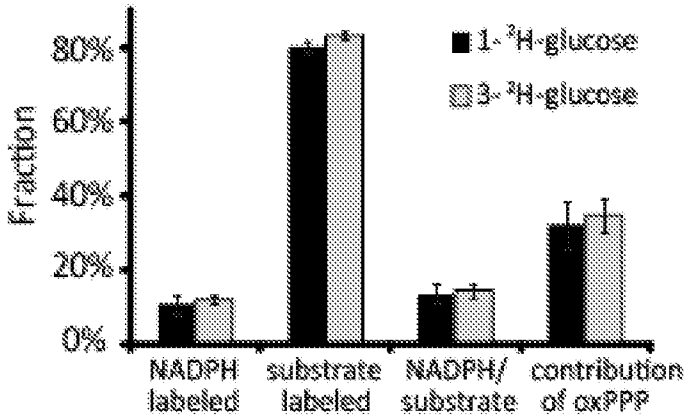

Figure 1E

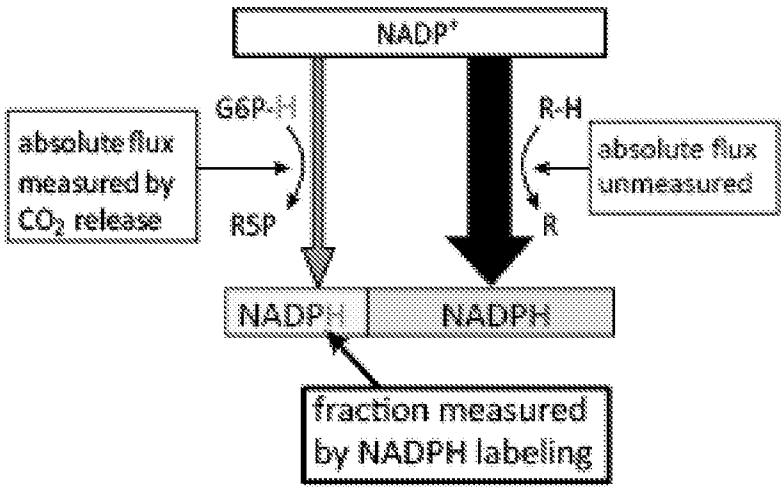

Figure 1F

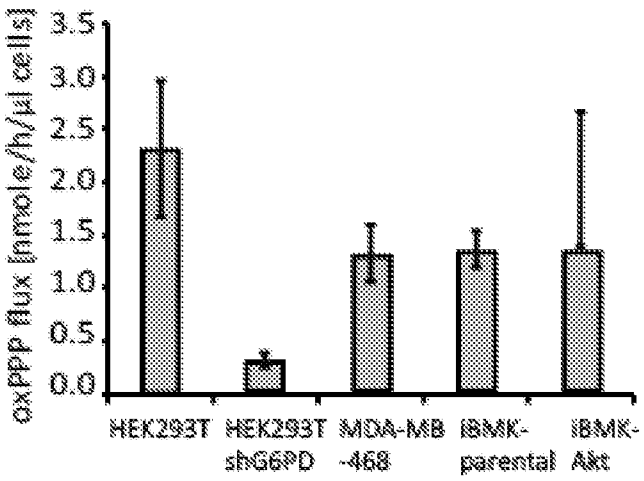

Figure 1G

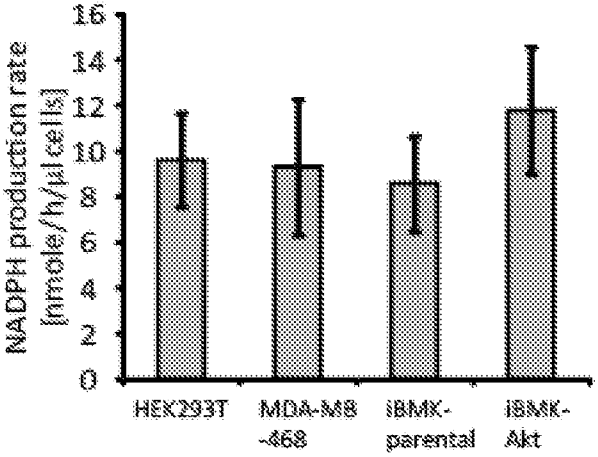

Figure 1H

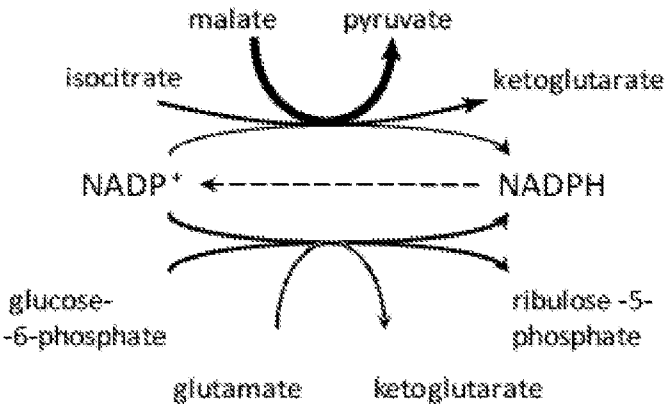

Figure 2A

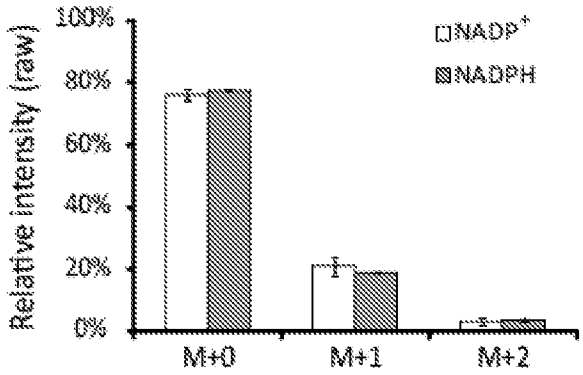

Figure 2B

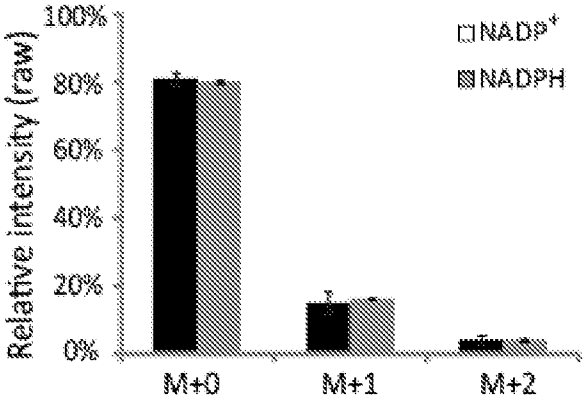

Figure 2C

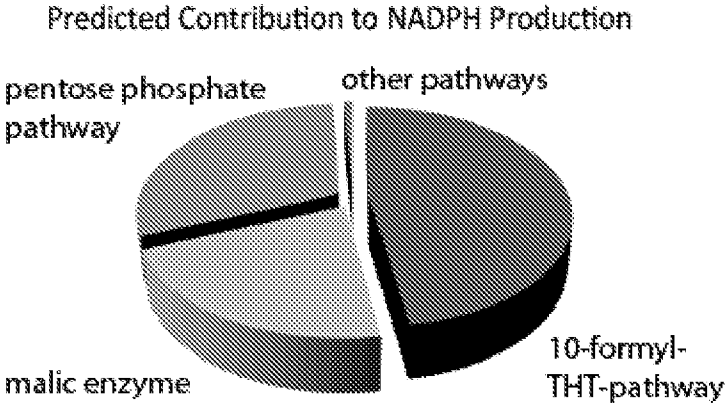

Figure 2D

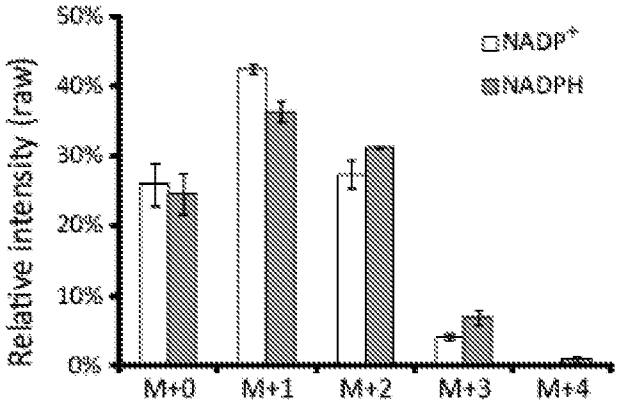

Figure 2E

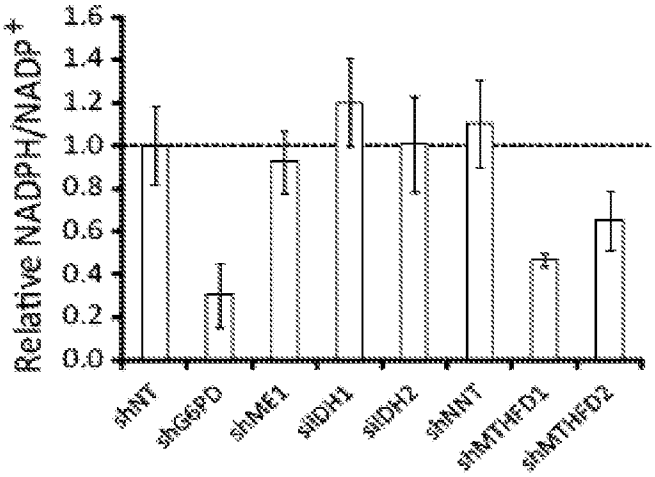

Figure 2F

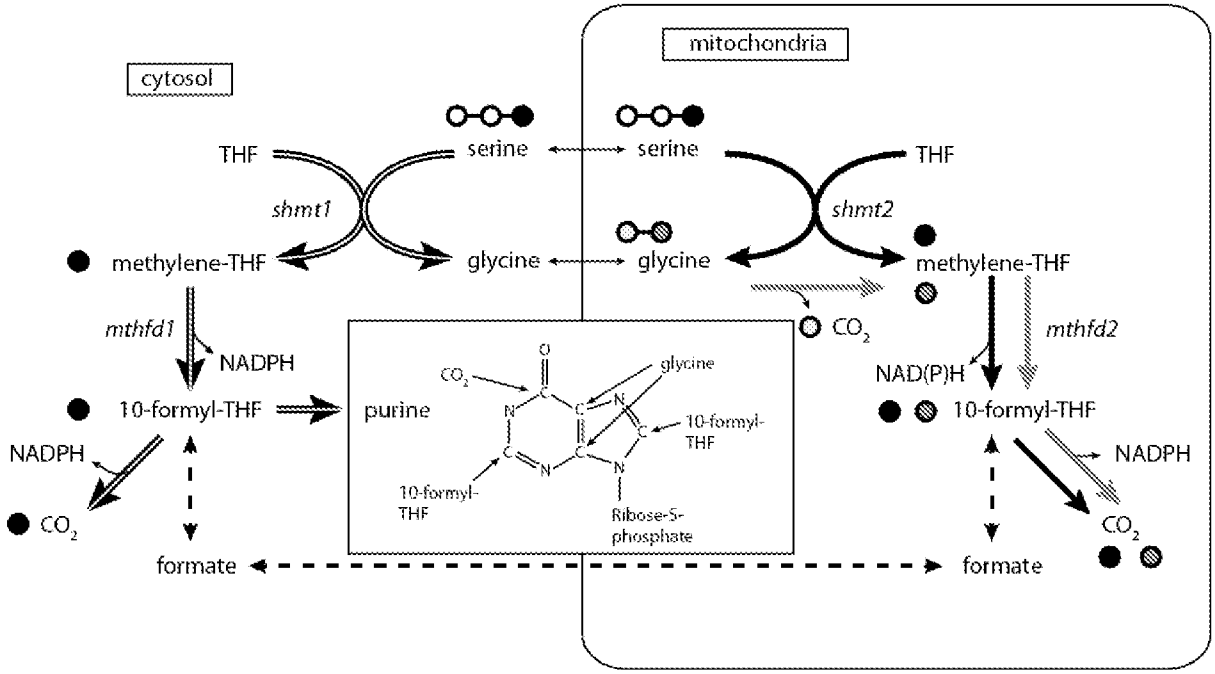

Figure 3A

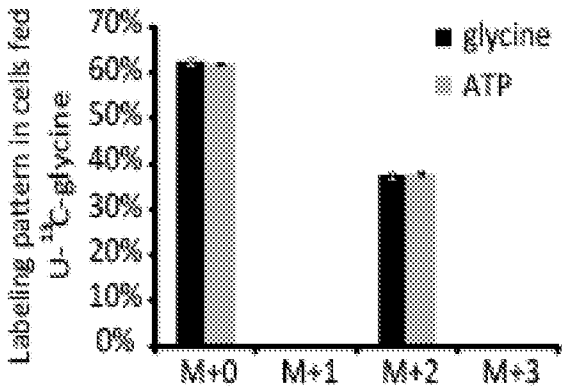

Figure 3B

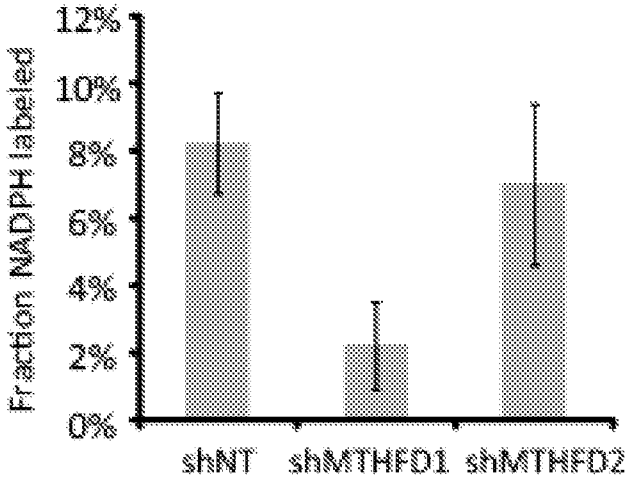

Figure 3C

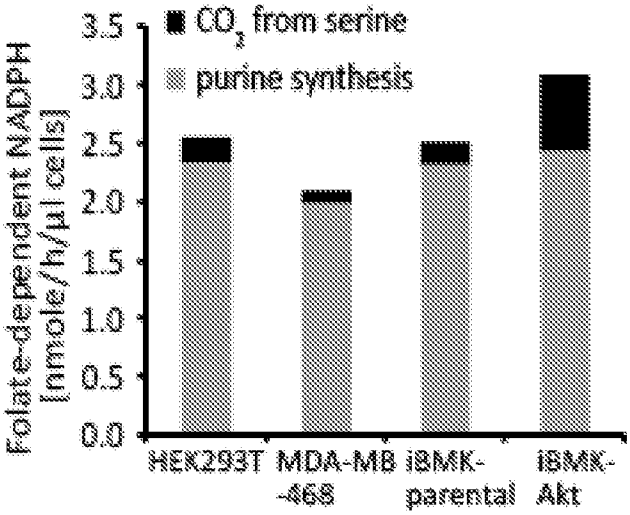

Figure 3D

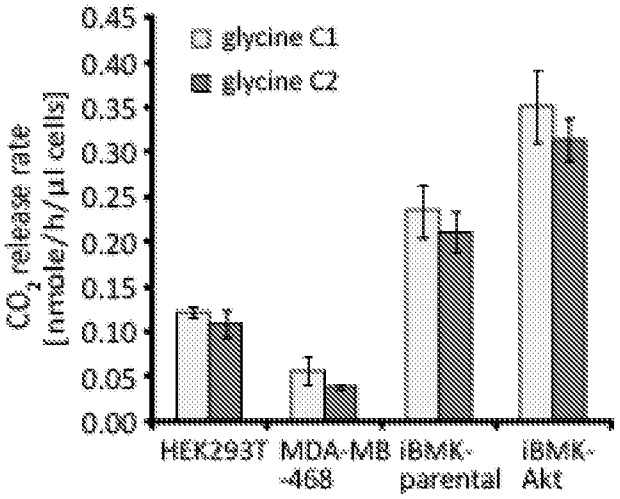

Figure 3E

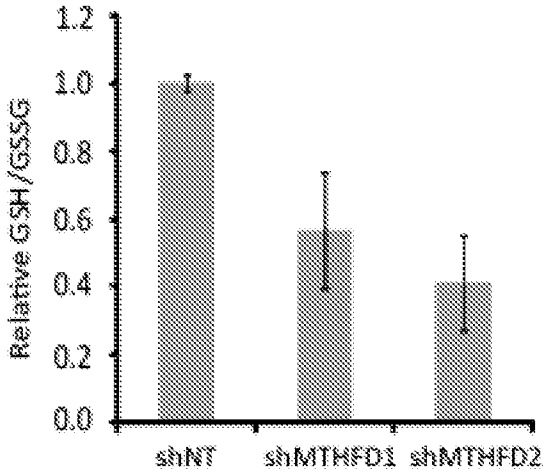

Figure 3F

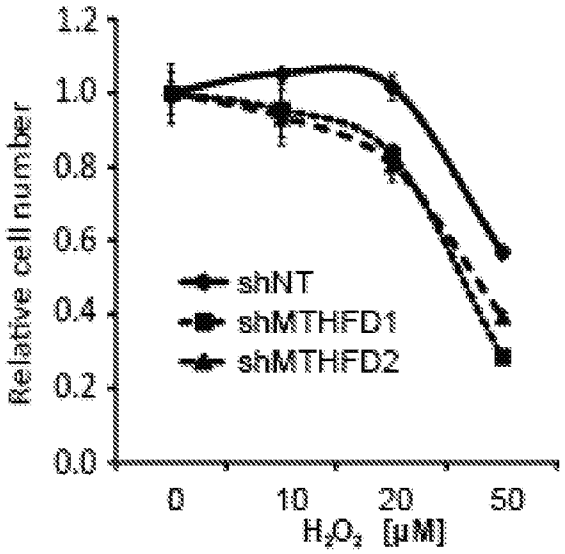

Figure 3G

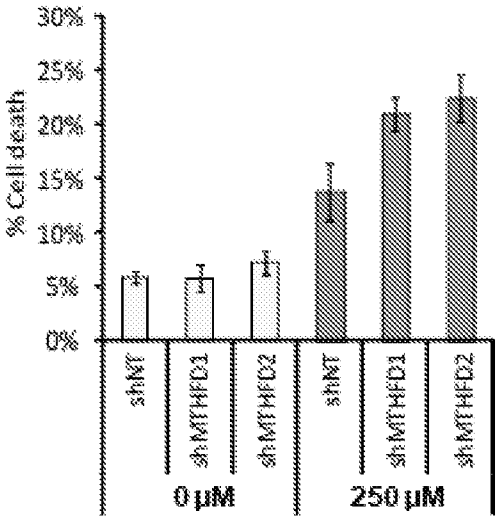

Figure 3H

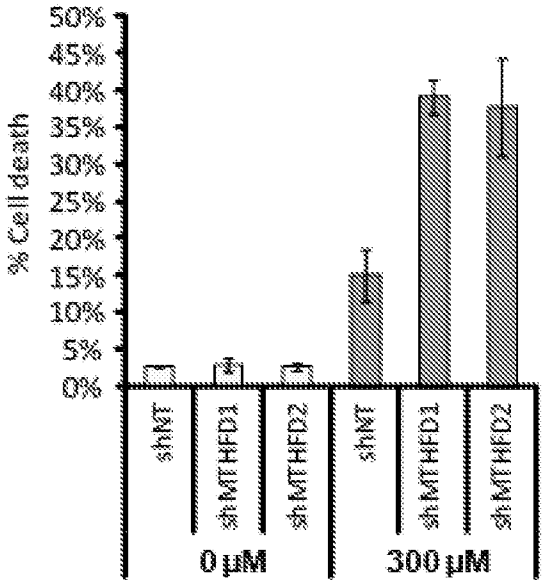

Figure 3I

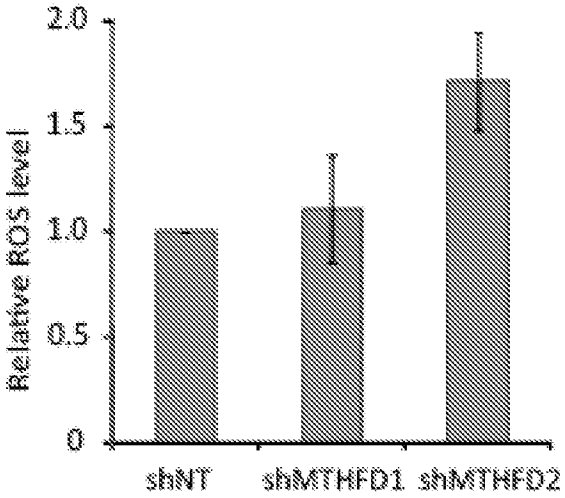

Figure 3J

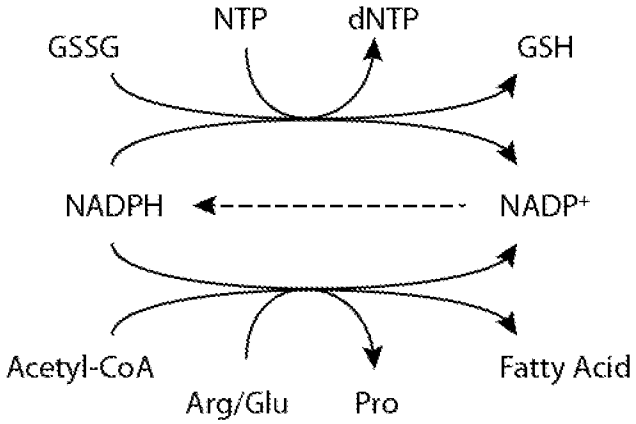

Figure 4A

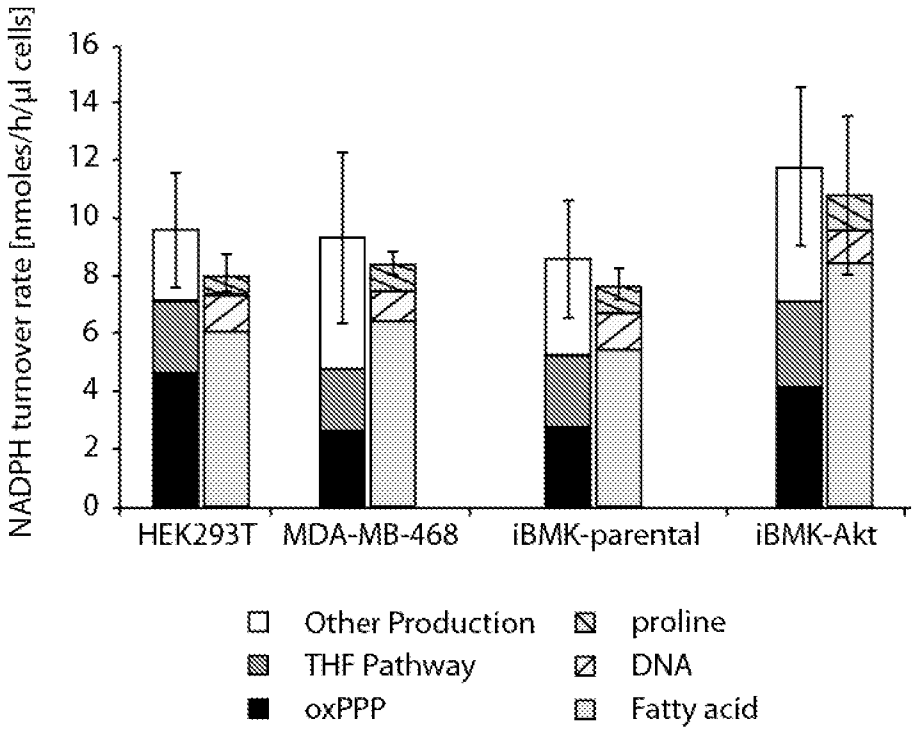

Figure 4B

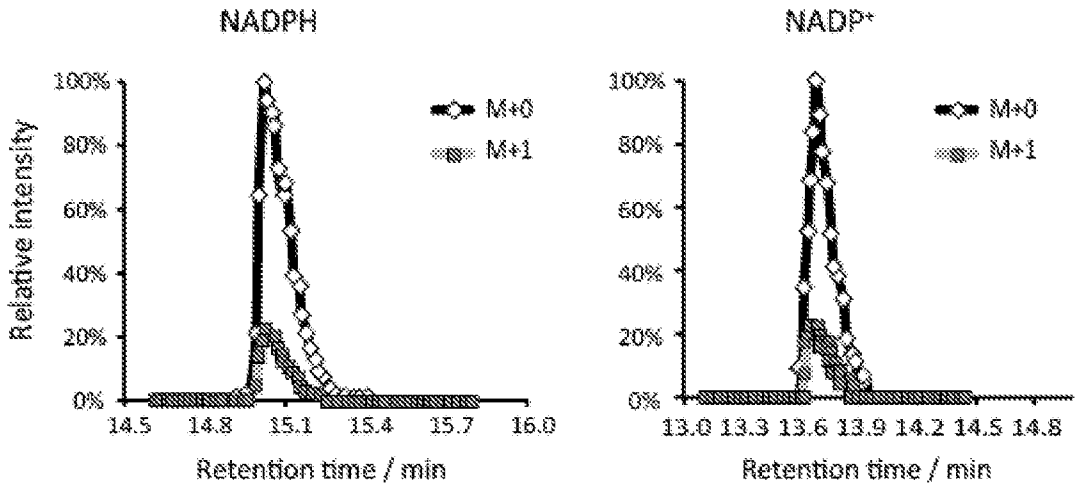

Figure 5A

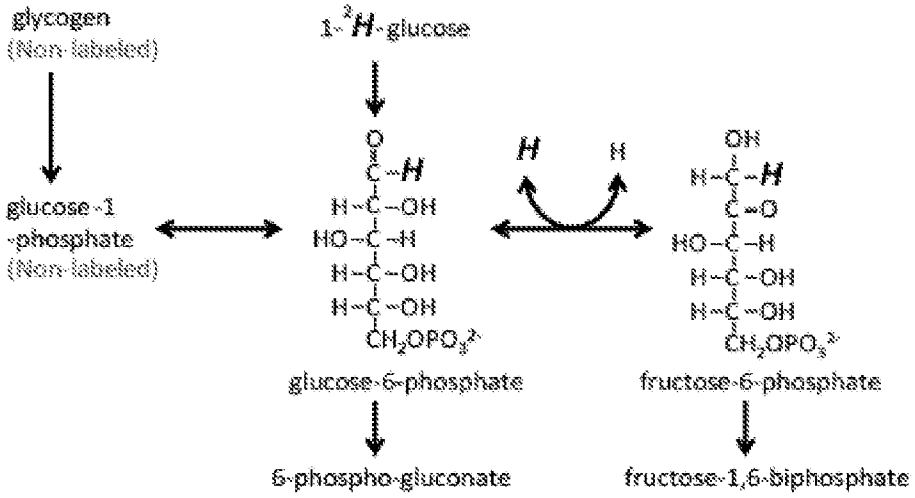

Figure 5B

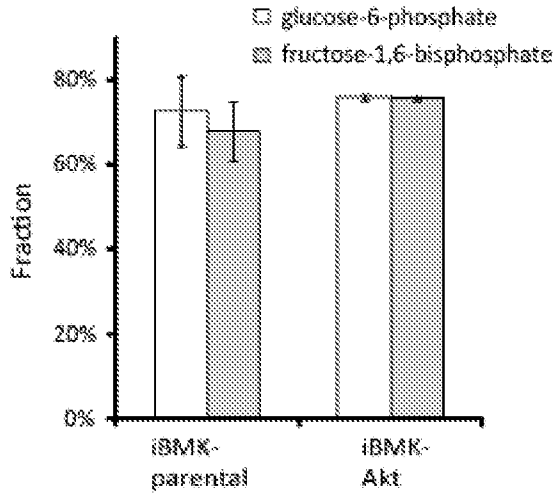

Figure 5C

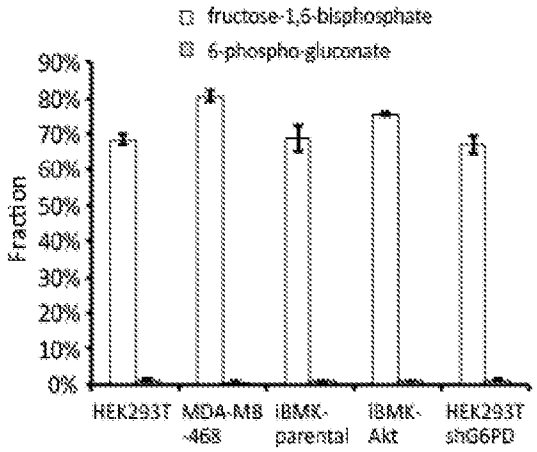

Figure 5D

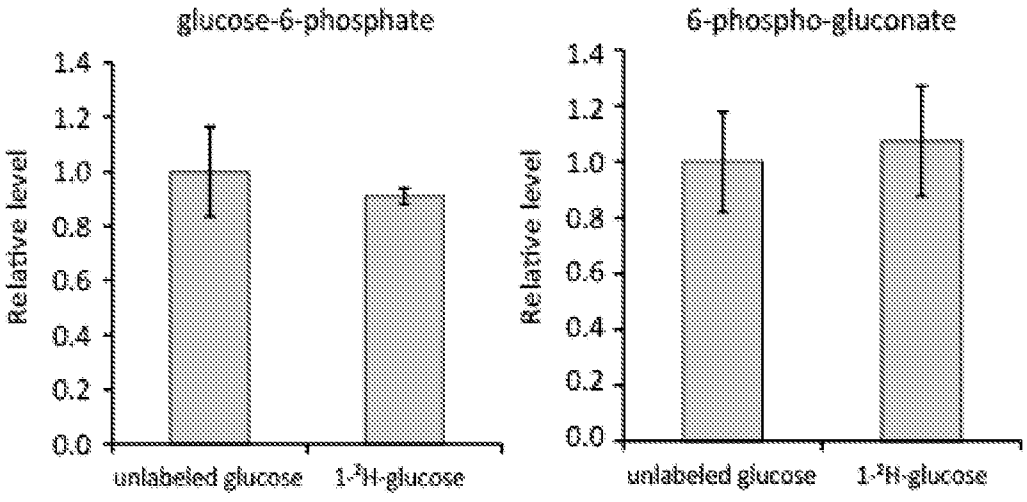

Figure 5E

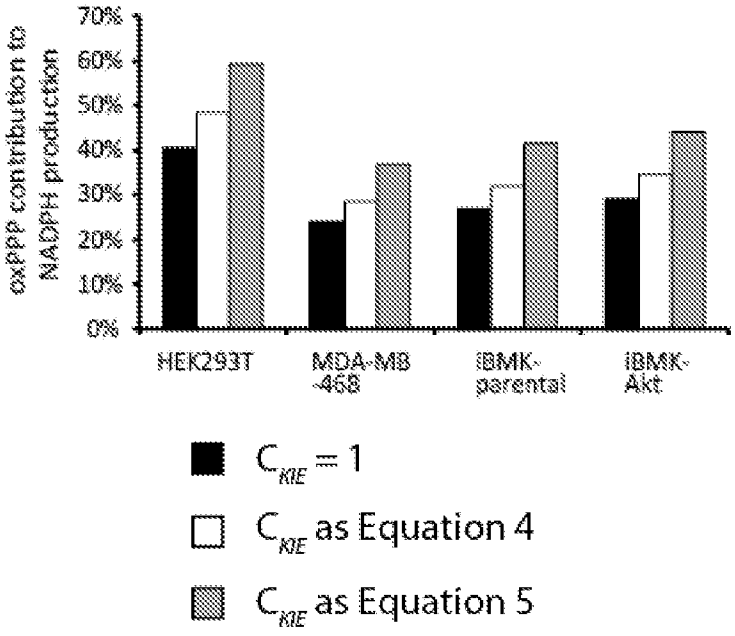

Figure 5F

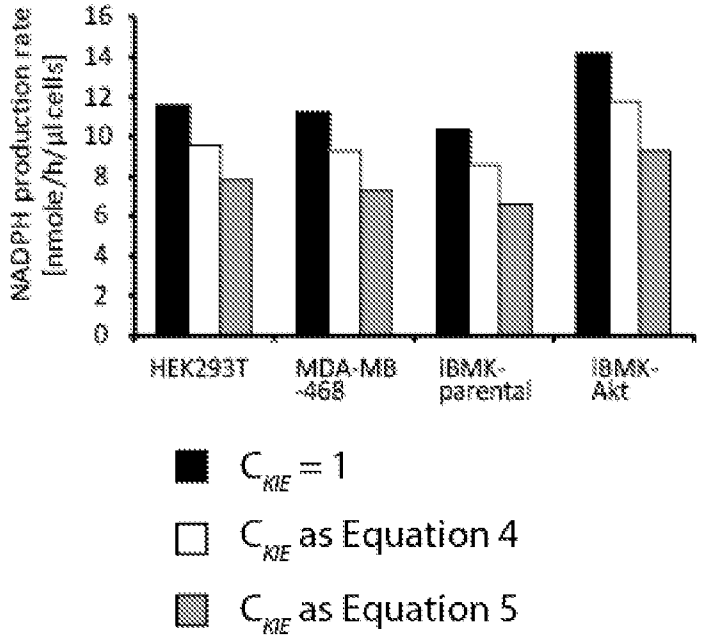

Figure 5G

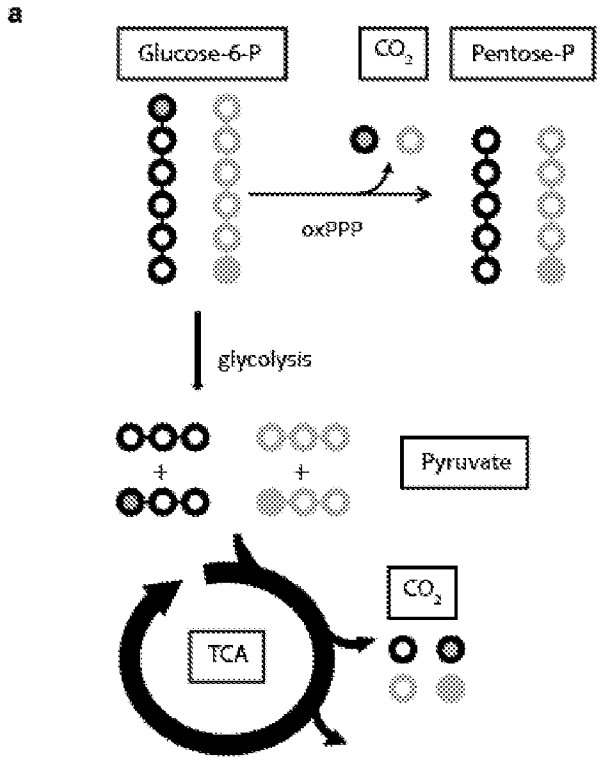

Figure 6A

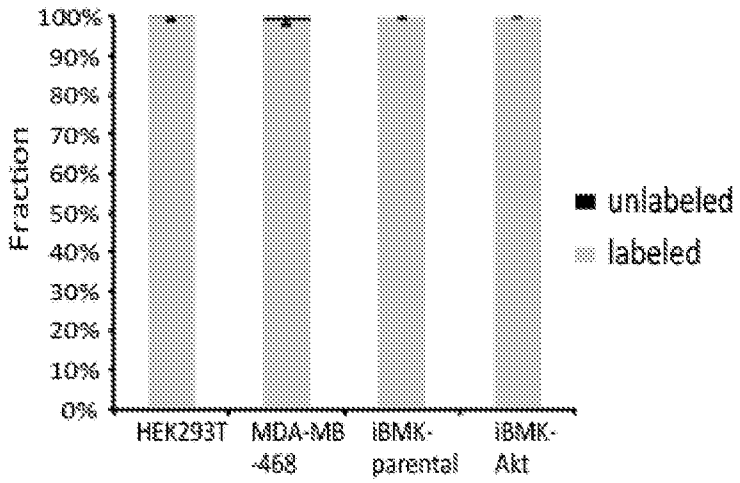

Figure 6B

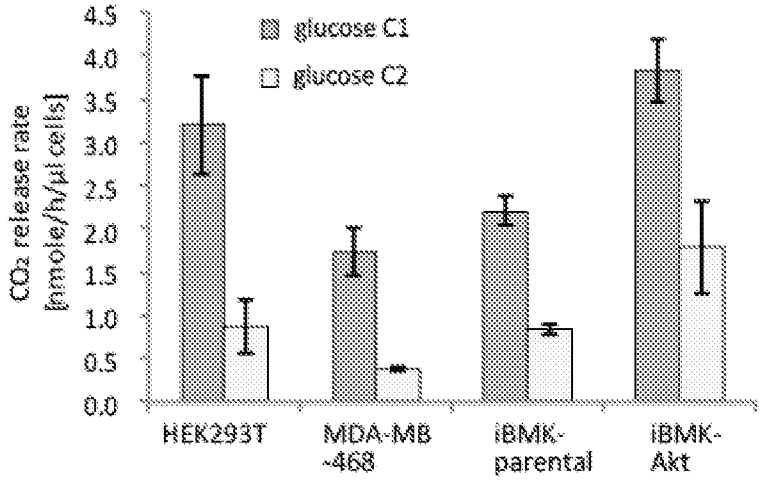

Figure 6C

Pool Size of 6-pjosphogluconate [pmole/µl cells]

HEK293T	MDA-MB-468	iBMK-parental	iBMK-Akt
23±6	16±7	12±3	15±4

Figure 6D

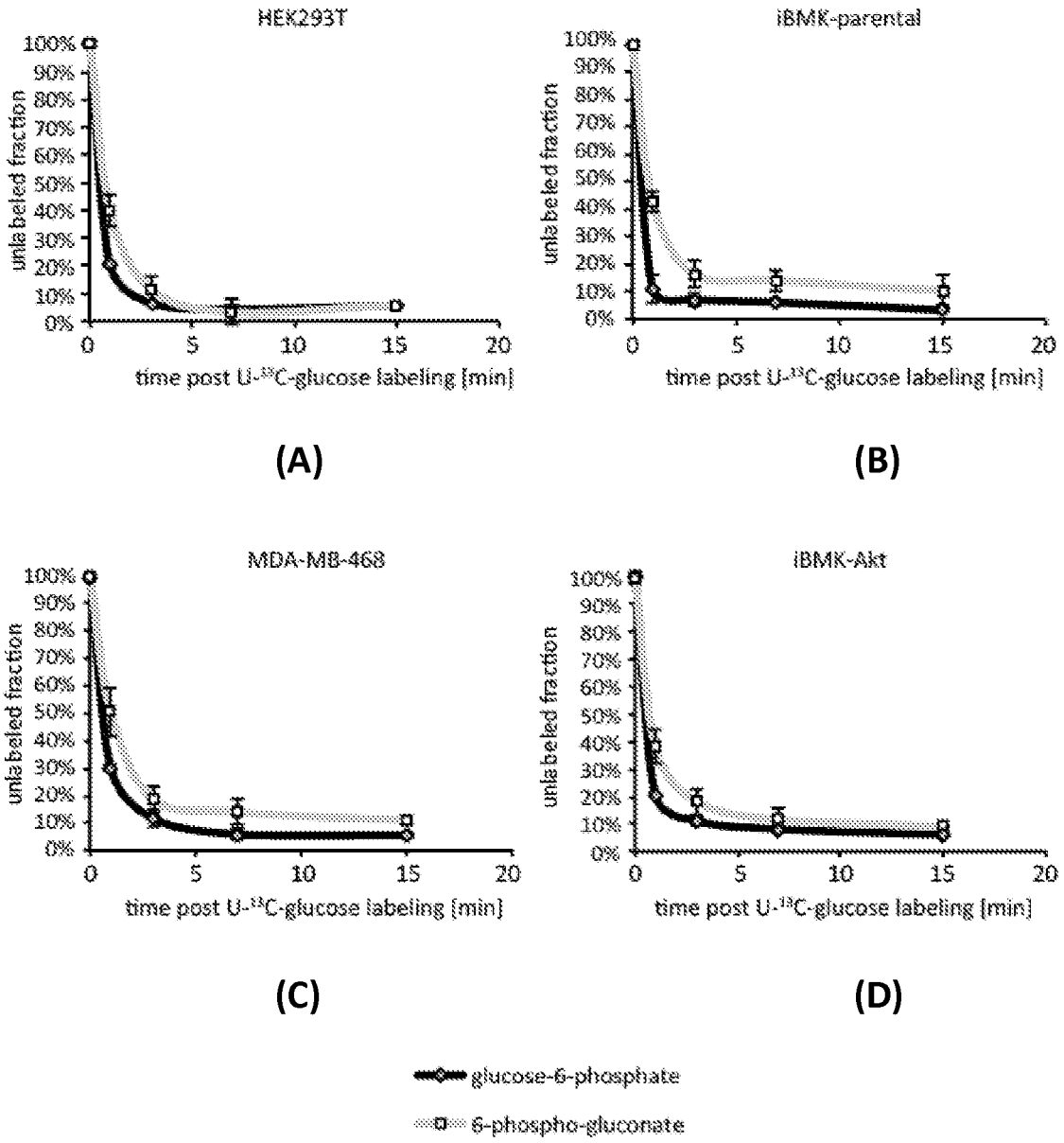
HEK293T
iBMK-parental
MDA-MB-468
iBMK-Akt
unlabeled fraction
time post U-13C-glucose labeling (min)
(A)
(B)
(C)
(D)
glucose-6-phosphate
6-phospho-gluconate

Figure 6E

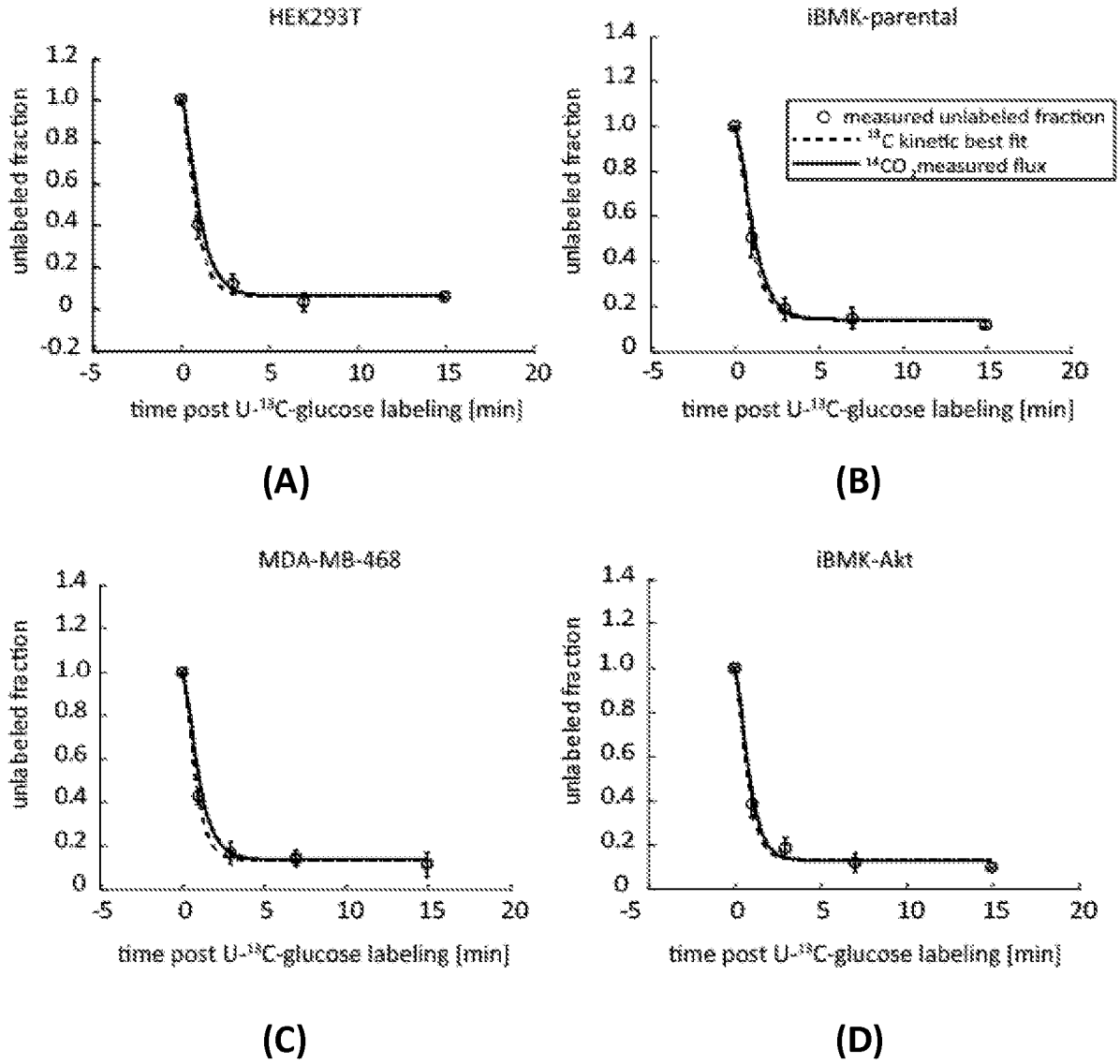

Figure 6F

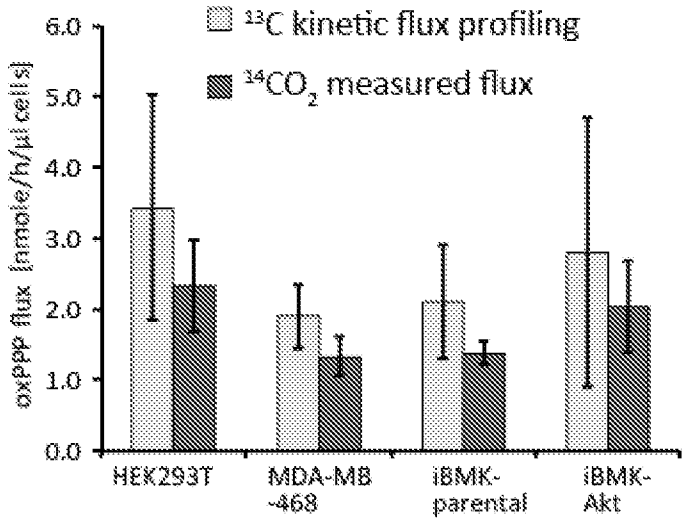

Figure 6G

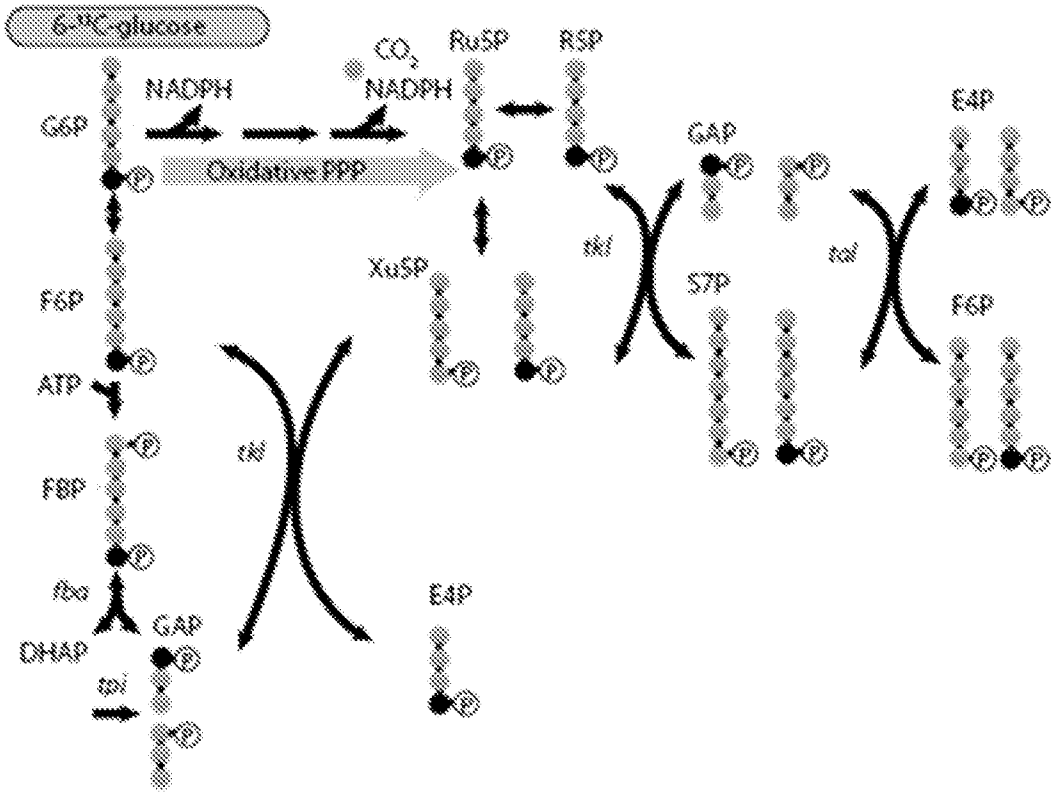
6-^{14}C-glucose
G6P
NADPH
CO_2
NADPH
RuSP
RSP
Oxidative PPP
GAP
E4P
F6P
XuSP
S7P
F6P
ATP
FBP
E4P
GAP
DHAP

Figure 7A

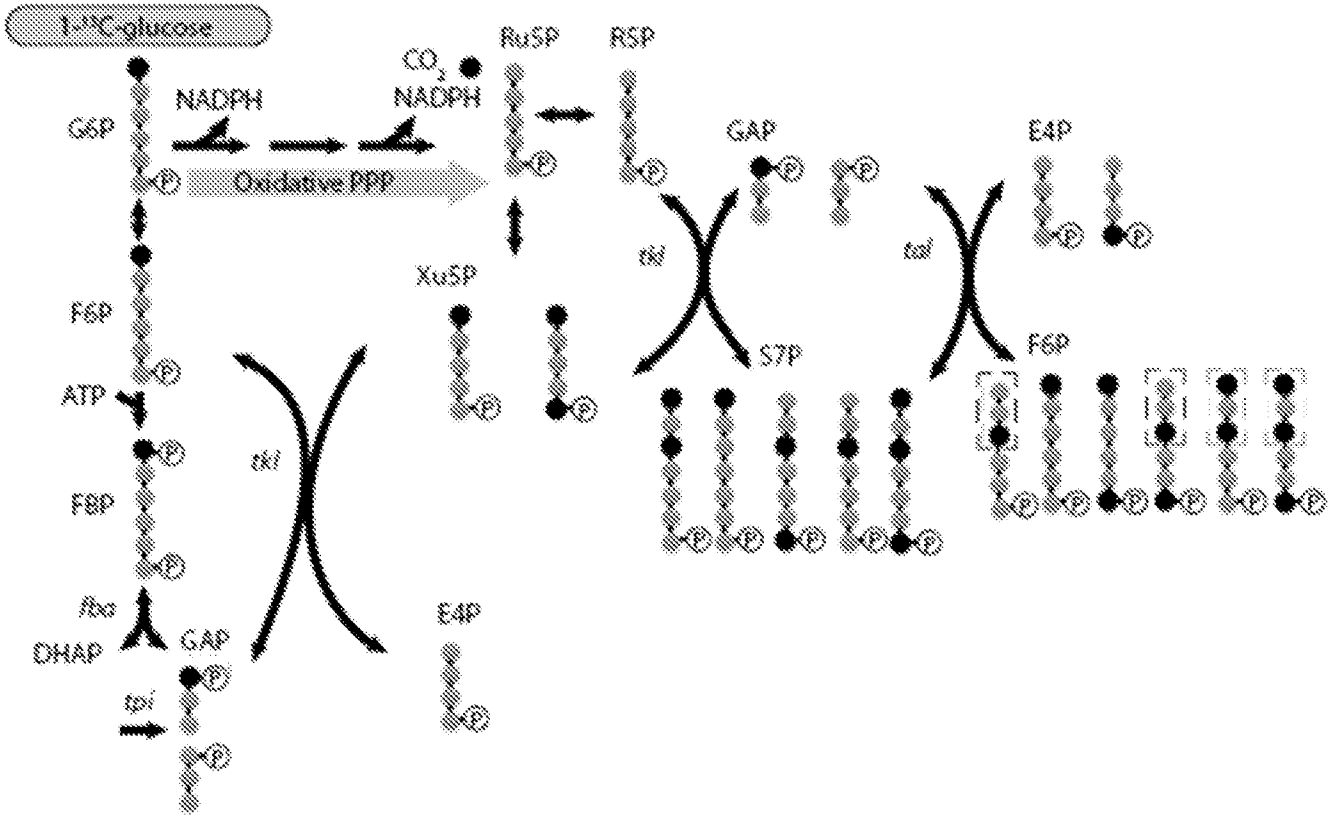

Figure 7B

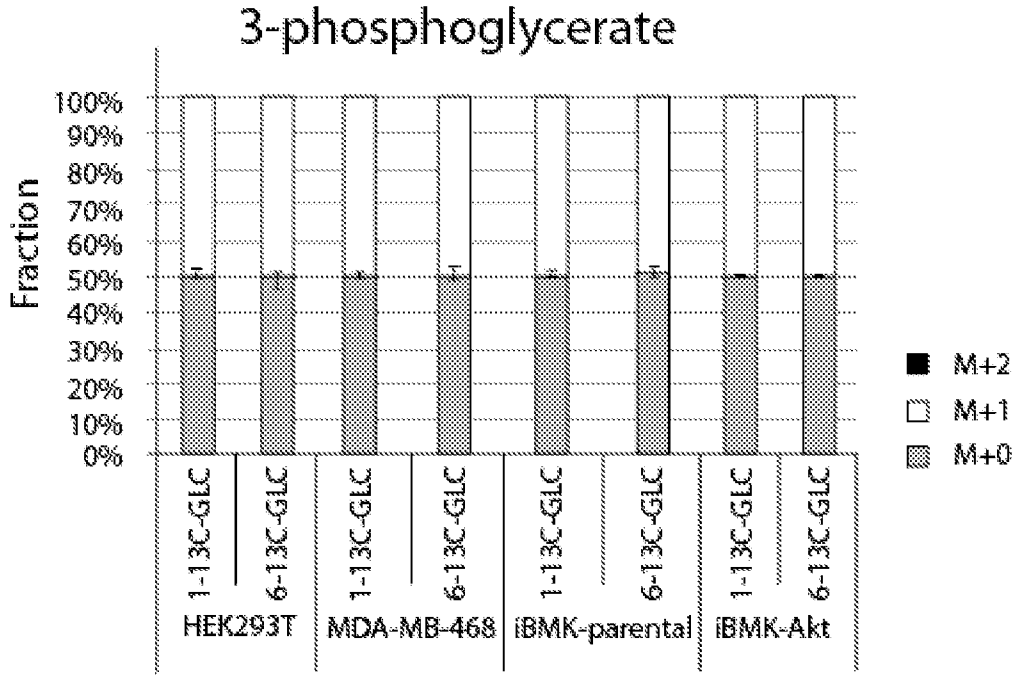

Figure 7C

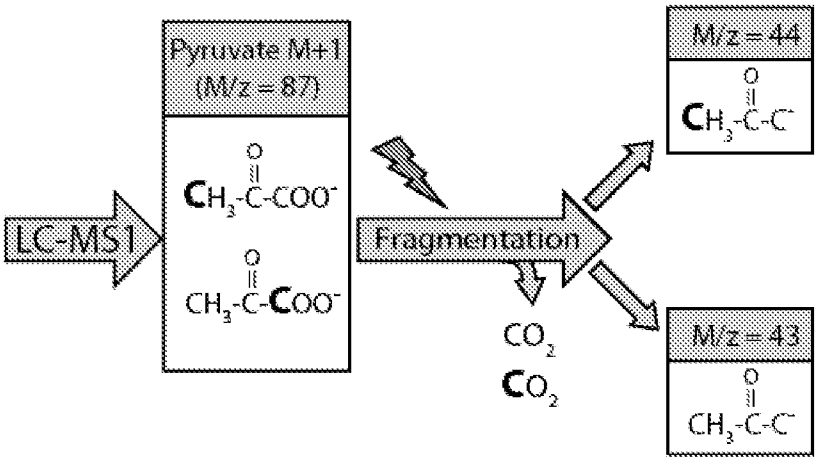

Figure 7D

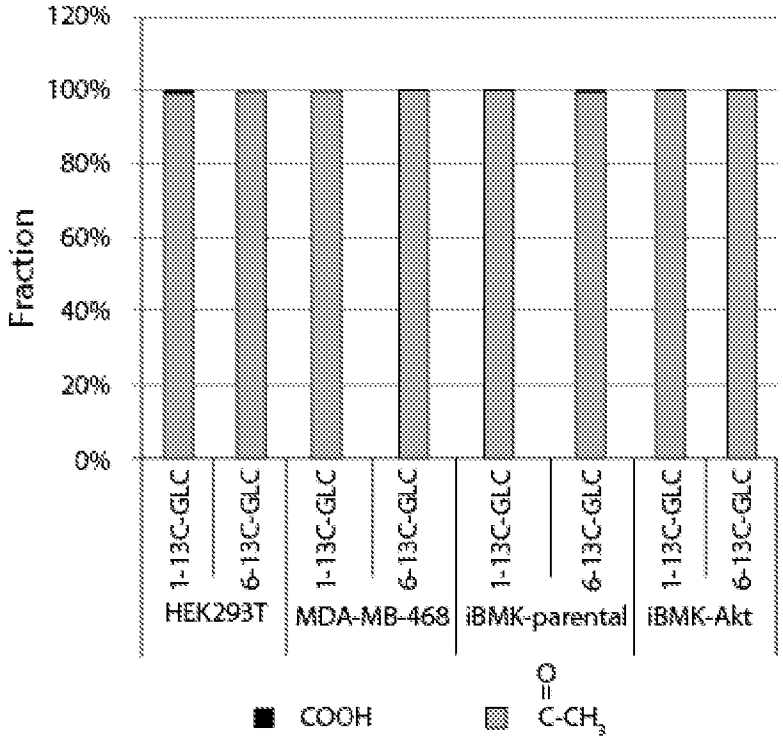

Figure 7E

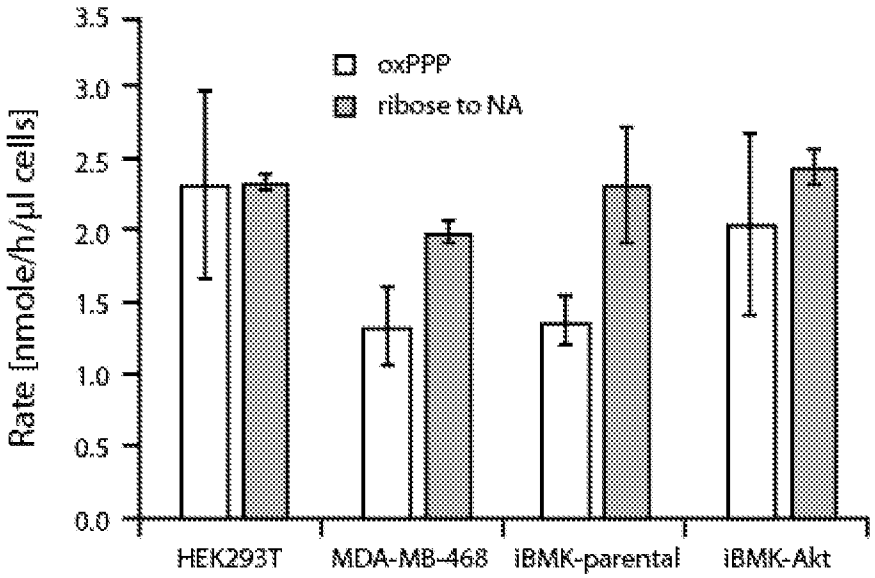
3.5
3.0
2.5
2.0
1.5
1.0
0.5
0.0
Rate [nmole/h/µl cells]
oxPPP
ribose to NA
HEK293T
MDA-MB-468
iBMK-parental
iBMK-Akt

Figure 7F

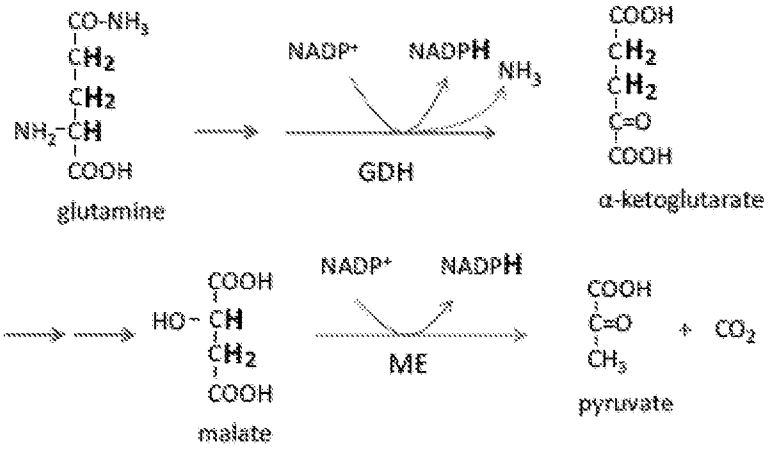

Figure 8A

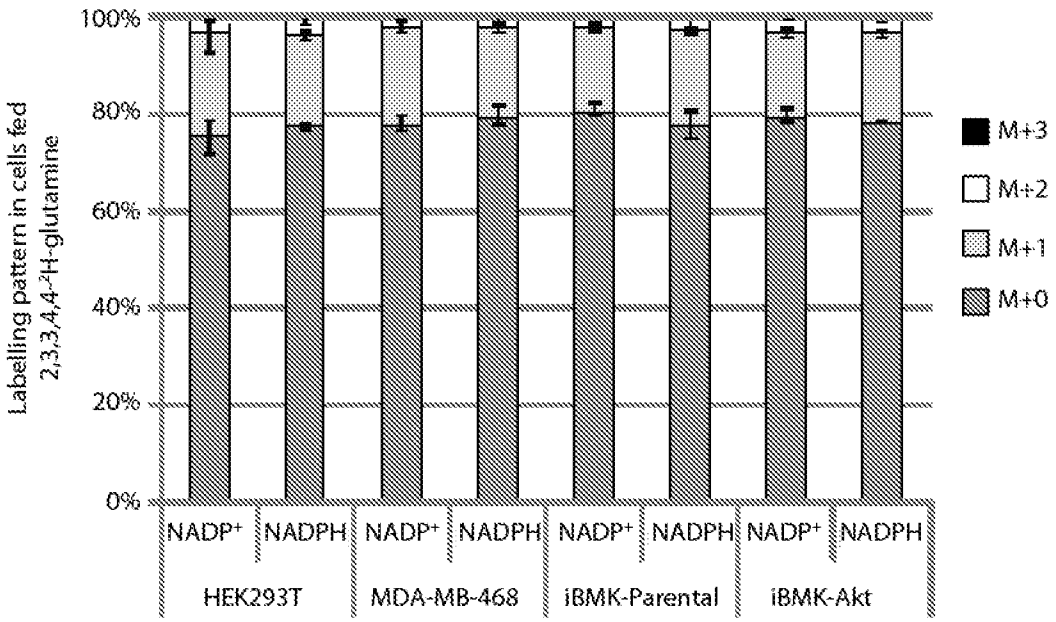

Figure 8B

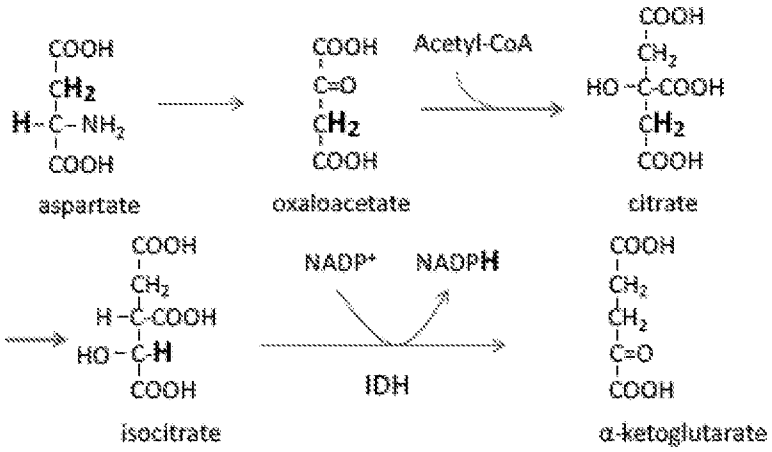

Figure 8C

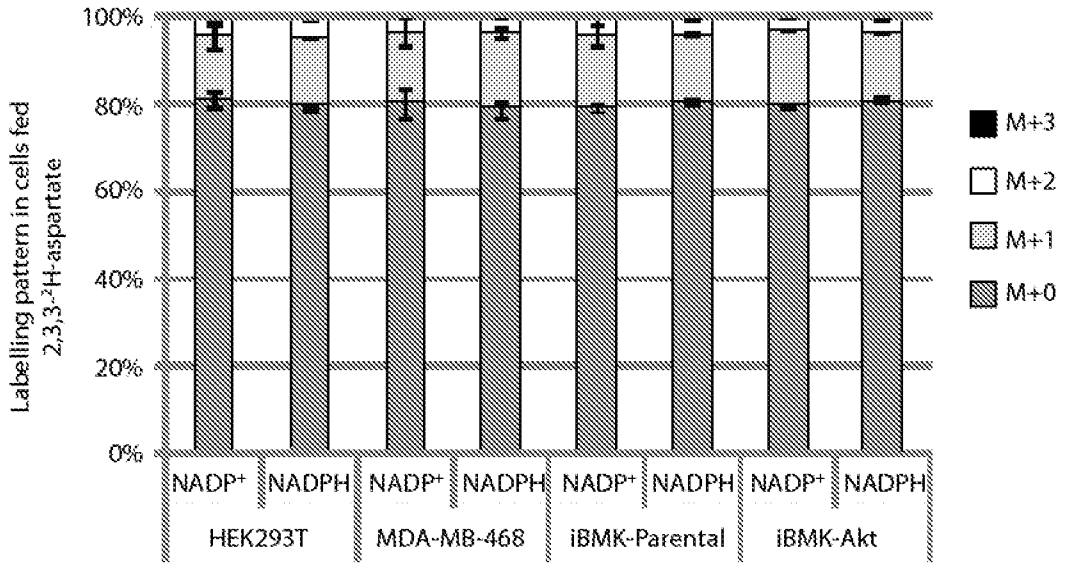

Figure 8D

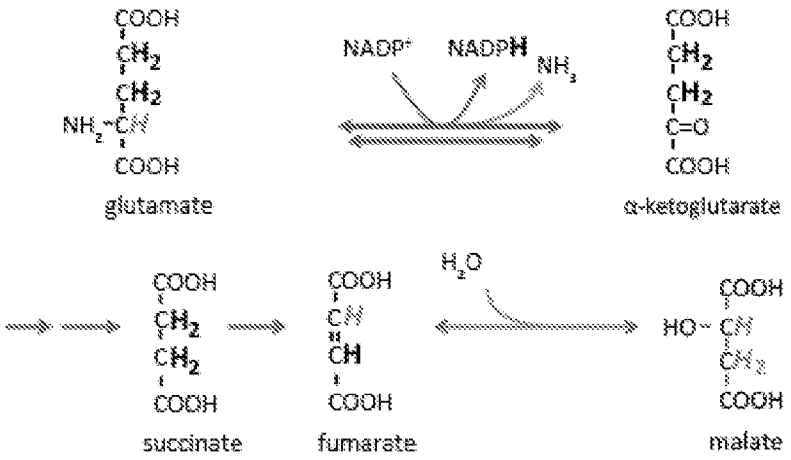

Figure 8E

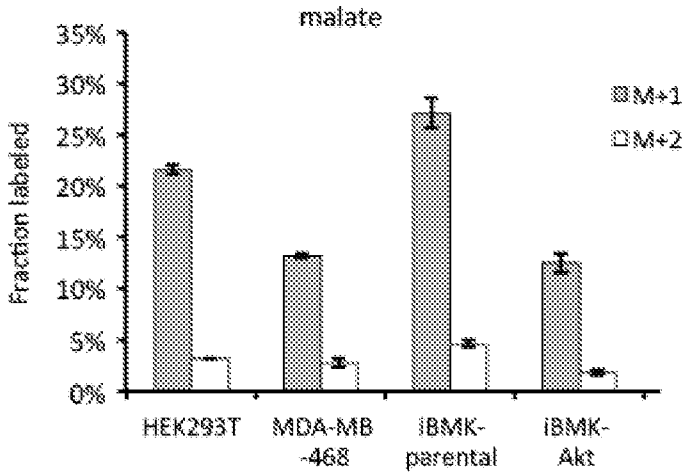

Figure 8F

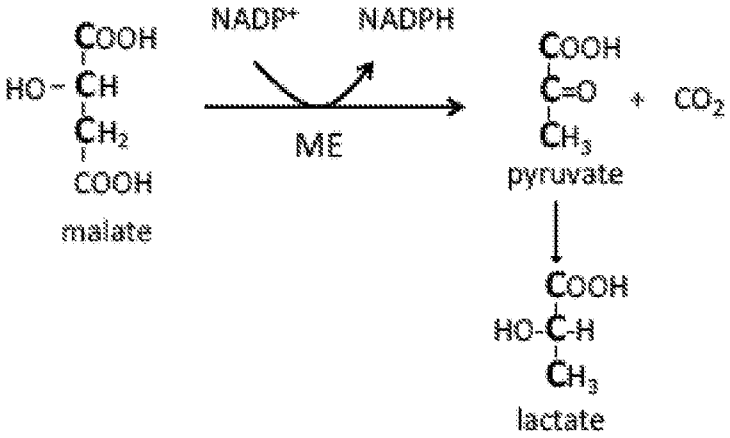

Figure 8G

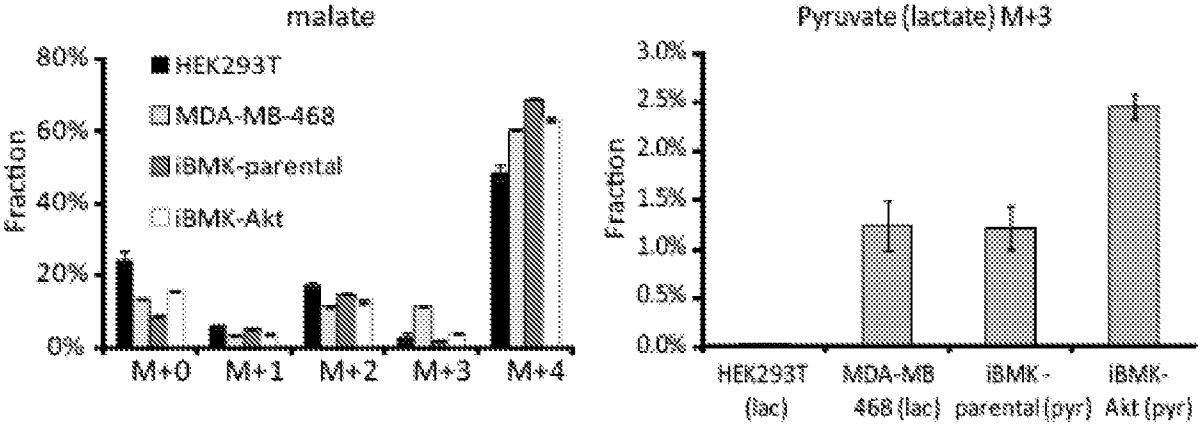

(A) (B)

Figure 8H

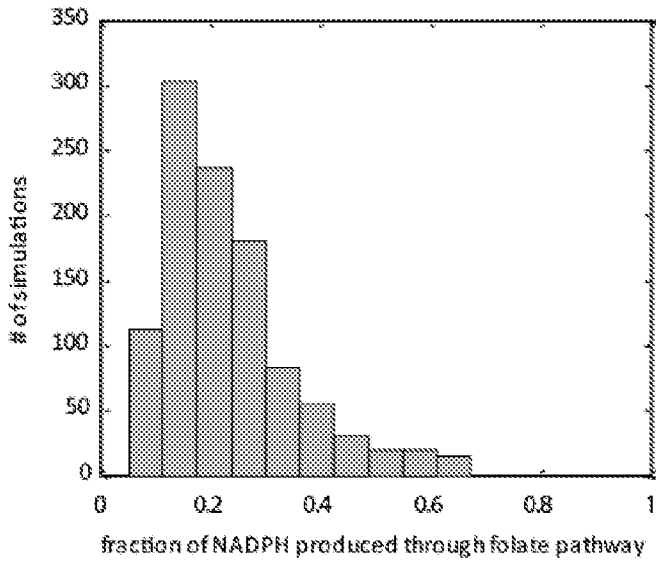

Figure 9A

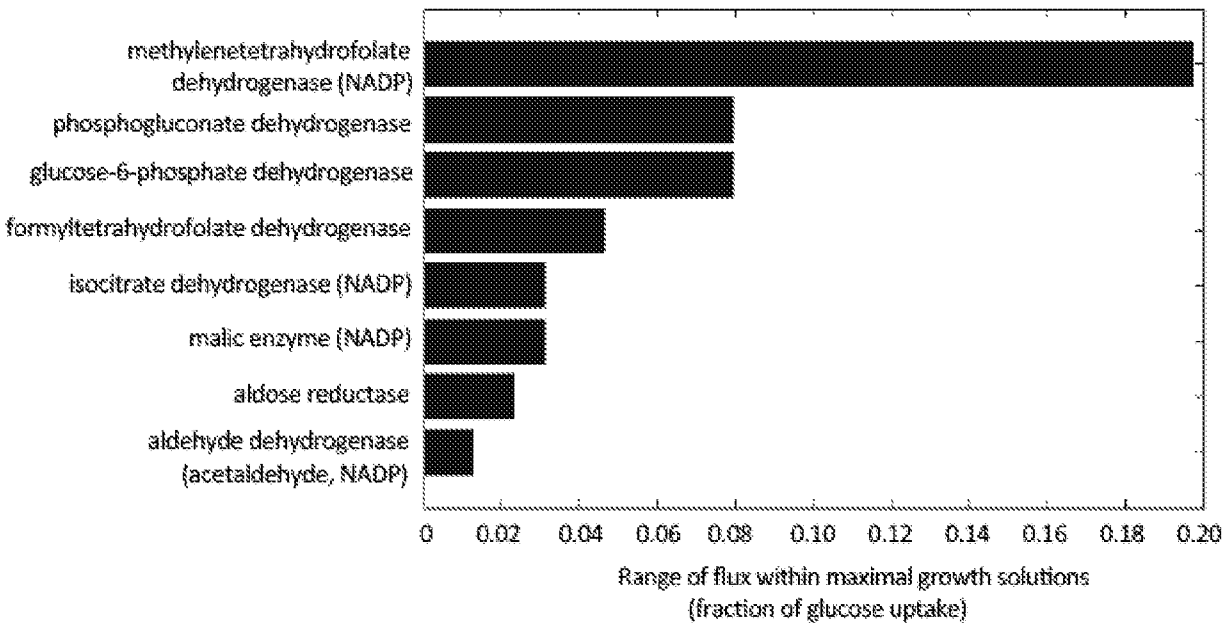

Figure 9B

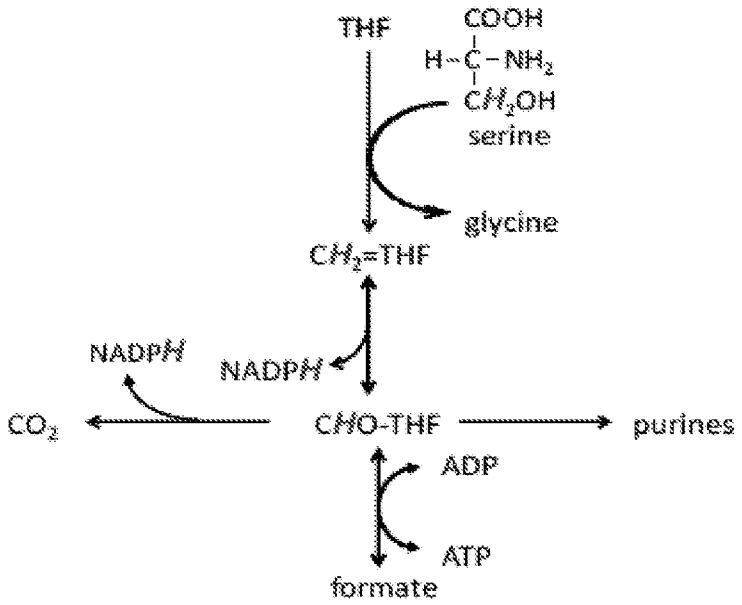

Figure 9C

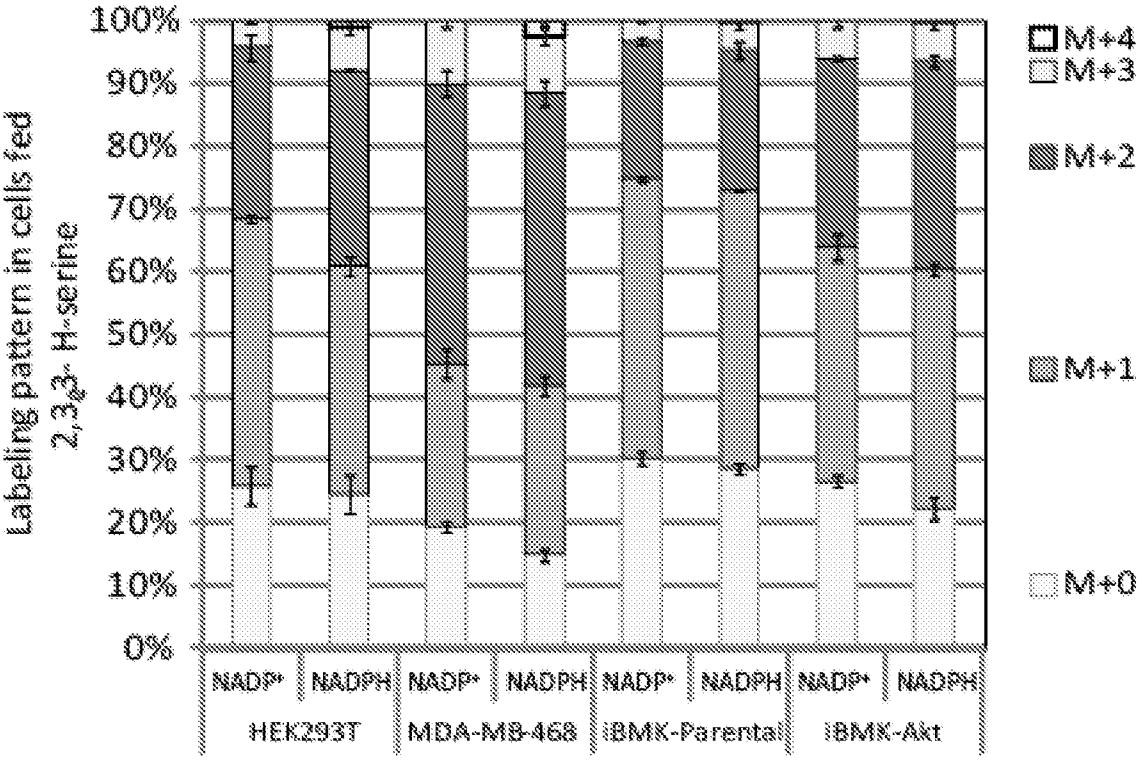

Figure 9D

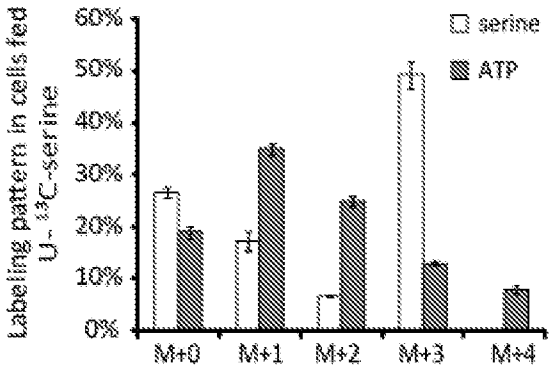

Figure 10A

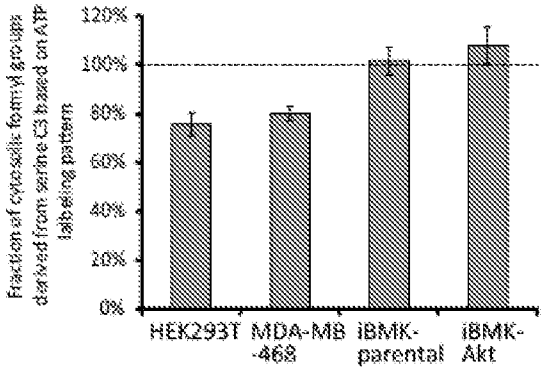

Figure 10B

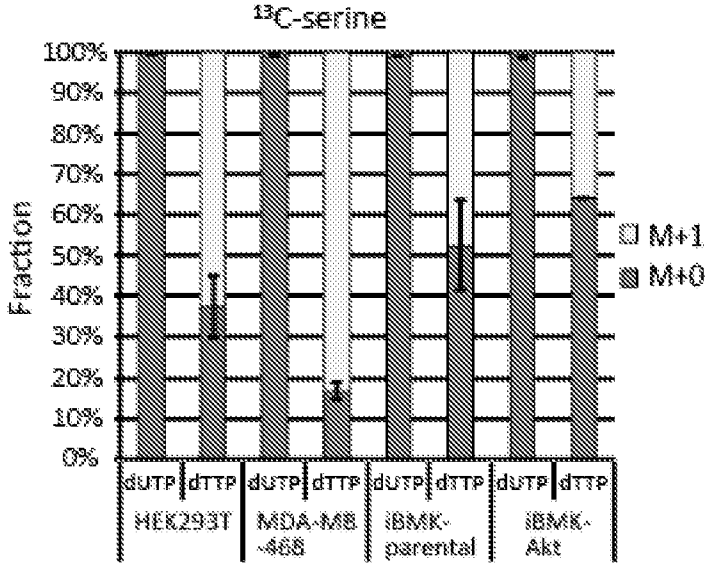

Figure 10C

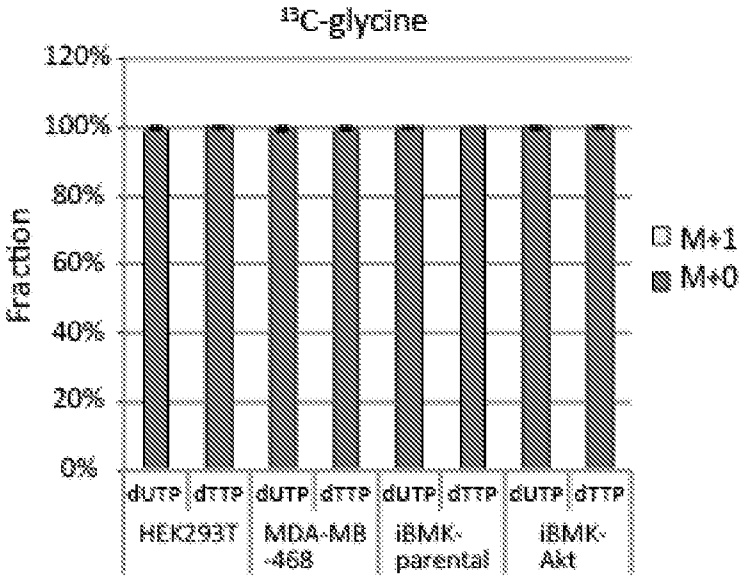

Figure 10D

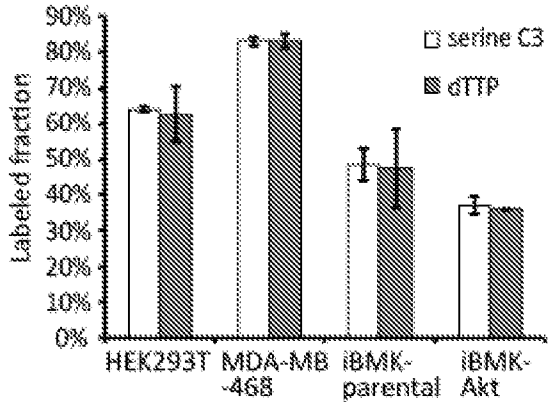

Figure 10E

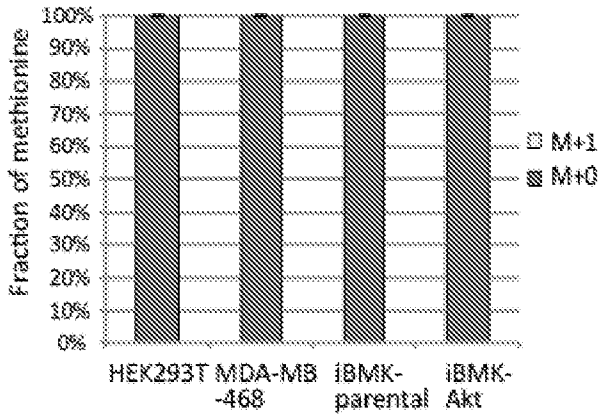

Figure 10F

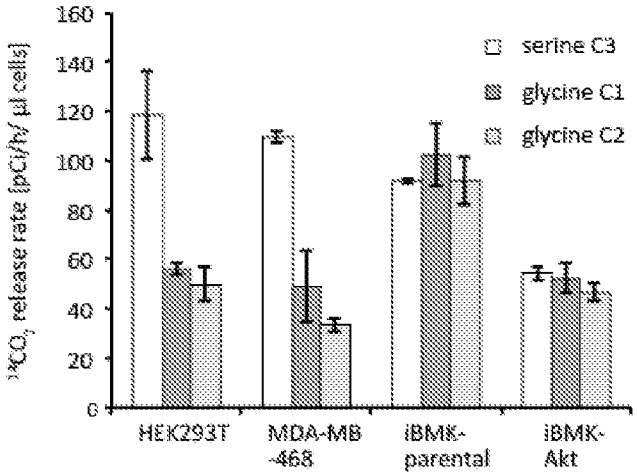

Figure 11A

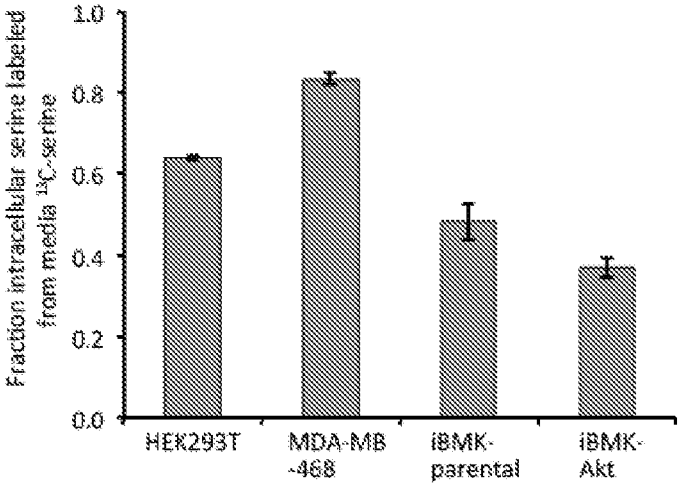

Figure 11B

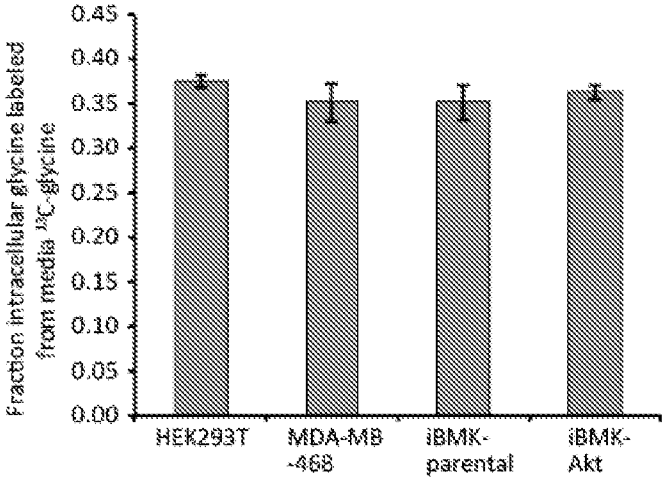

Figure 11C

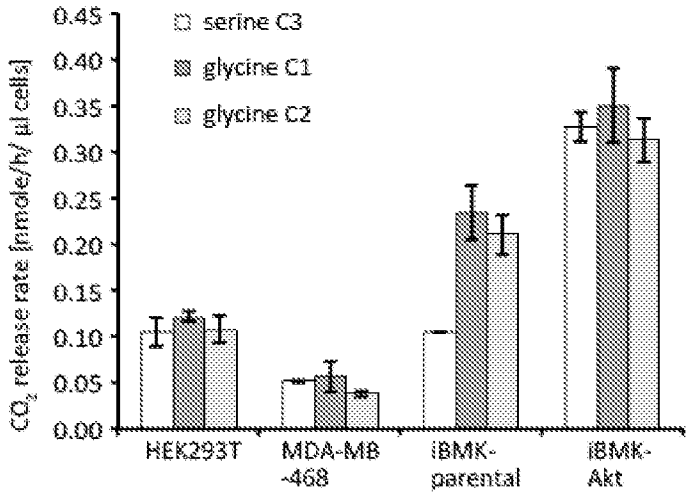

Figure 11D

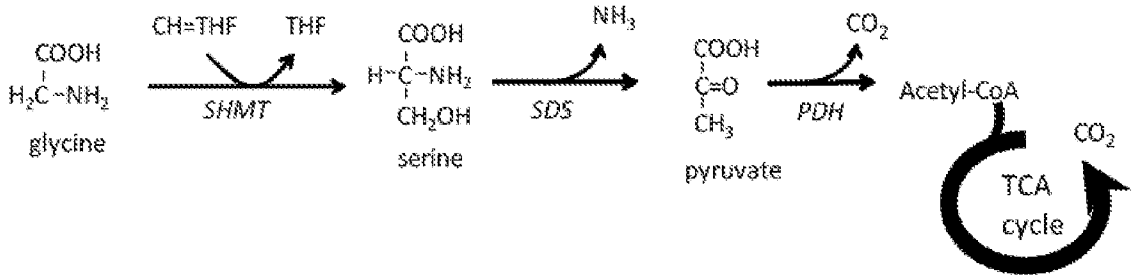

Figure 11E

Tracer	Fraction of Pyruvate Labeled			
	HEK293T	MDA-MB-468	iBMK-parental	iBMK-Akt
U-^{13}C-serine	<0.5%	<0.5%	<0.5%	<0.5%
U-^{13}C-glycine	<0.5%	<0.5%	<0.5%	<0.5%

Figure 11F

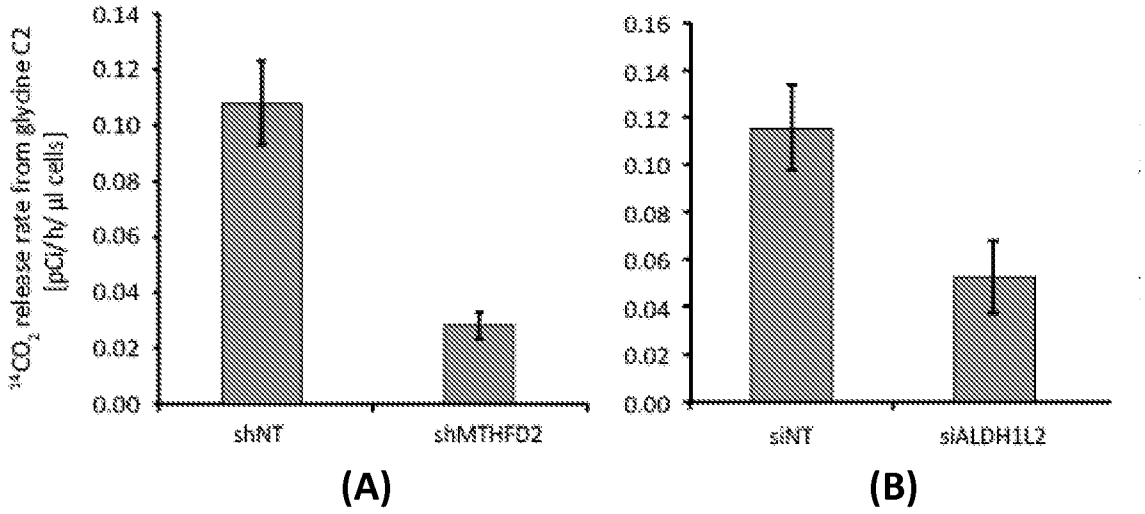

Figure 11G

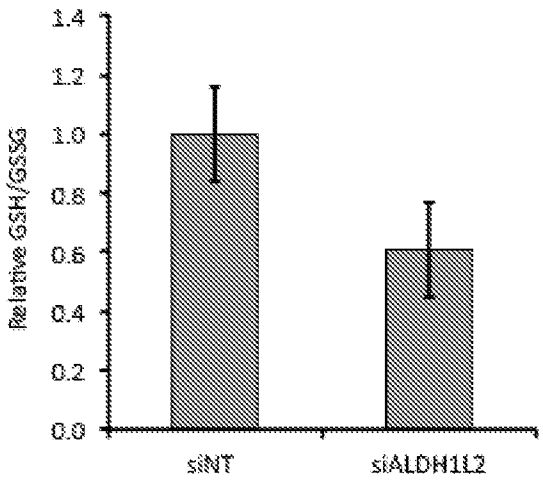

Figure 11H

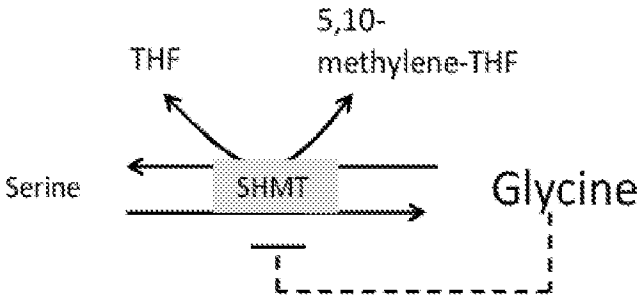

Figure 12A

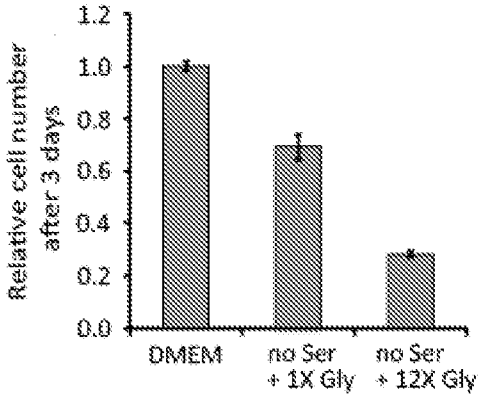

Figure 12B

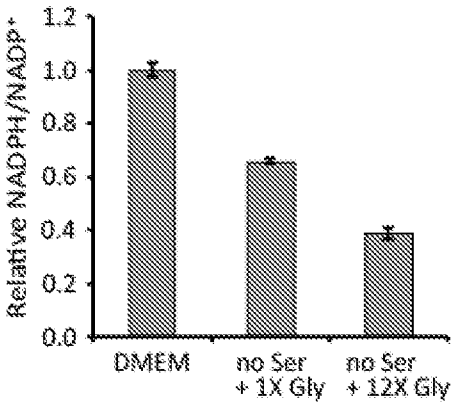

Figure 12C

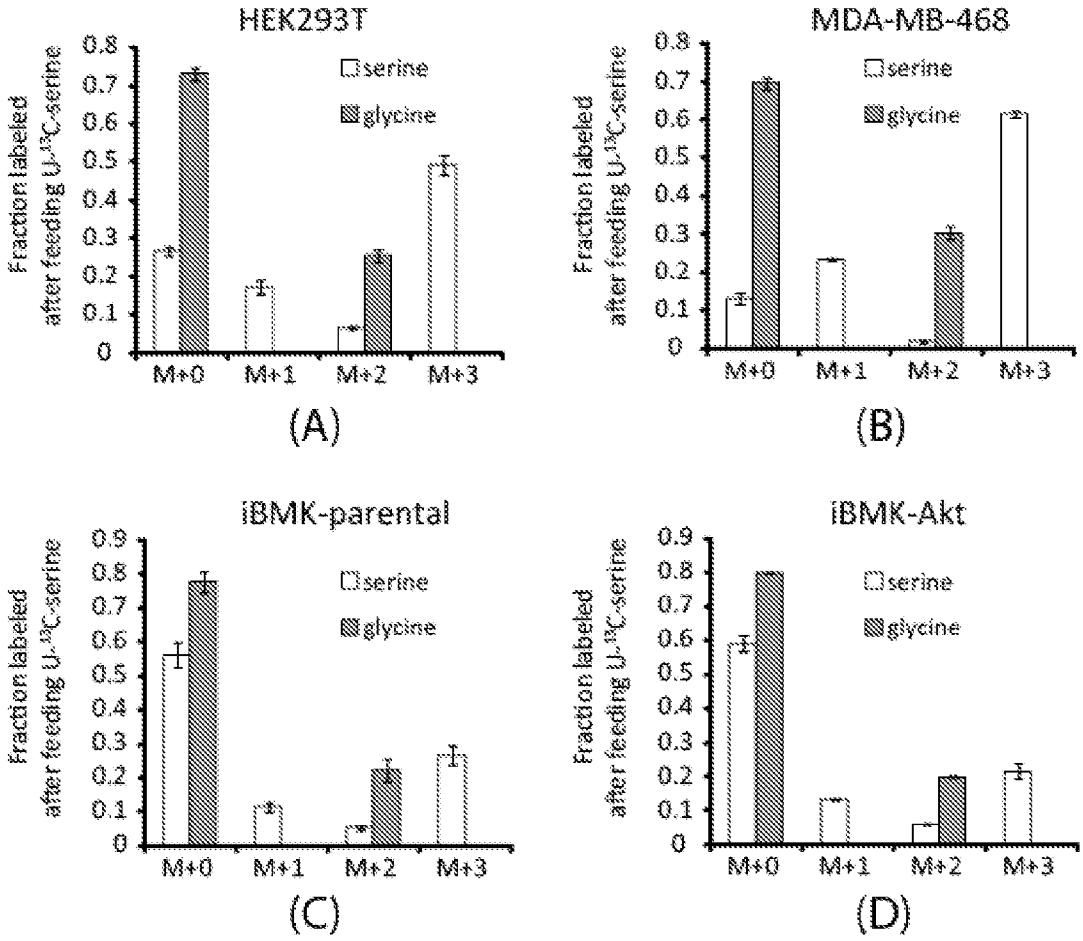
HEK293T
MDA-MB-468
iBMK-parental
iBMK-Akt
serine
glycine
Fraction labeled after feeding U-13C-serine
M+0
M+1
M+2
M+3
(A)
(B)
(C)
(D)

Figure 12D

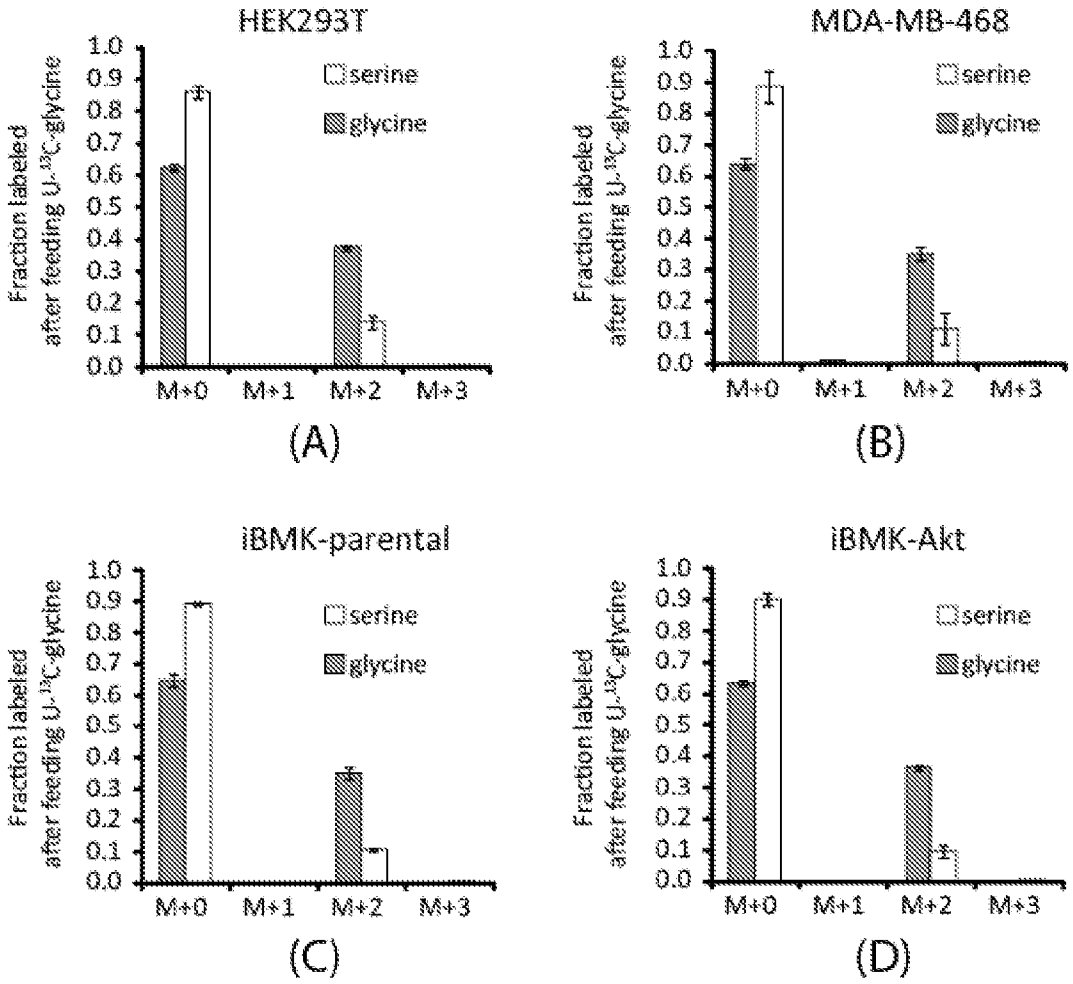
HEK293T
MDA-MB-468
iBMK-parental
iBMK-Akt
serine
glycine
Fraction labeled after feeding U-13C-glycine
1.0
0.9
0.8
0.7
0.6
0.5
0.4
0.3
0.2
0.1
0.0
M+0
M+1
M+2
M+3
(A)
(B)
(C)
(D)

Figure 12E

Cell Doubling Times

HEK293T	MDA-MB-468	iBMK-parental	iBMK-Akt
22 h	25 h	24 h	21 h

Figure 13A

Cellular Protein Content [µg/µl cells]

HEK293T	MDA-MB-468	iBMK-parental	iBMK-Akt
69±5	69±3	71±3	85±1

Figure 13B

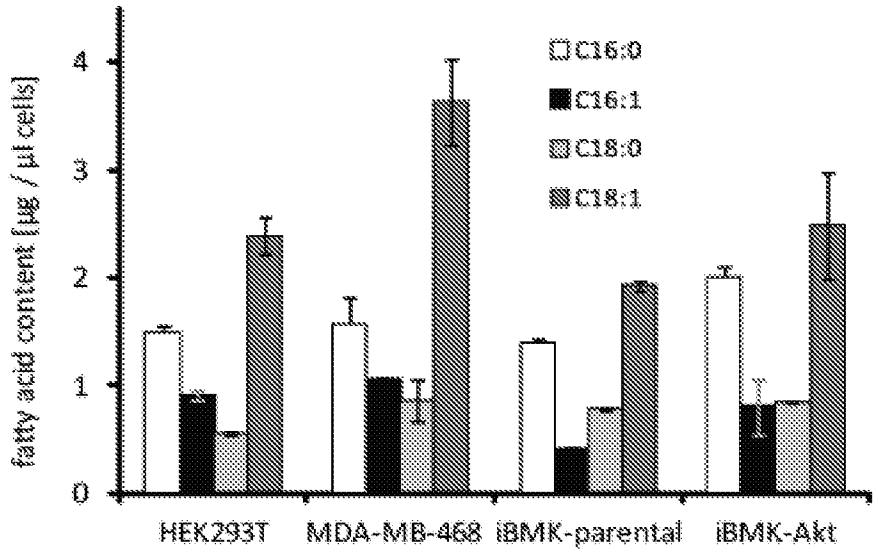

Figure 13C

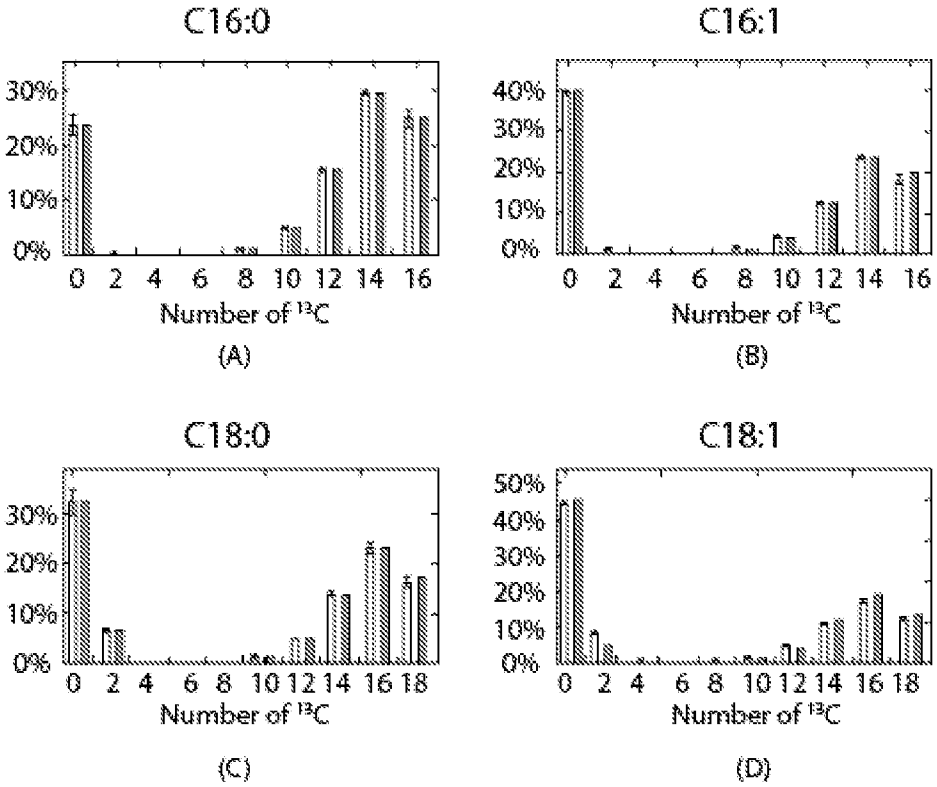

Figure 13D

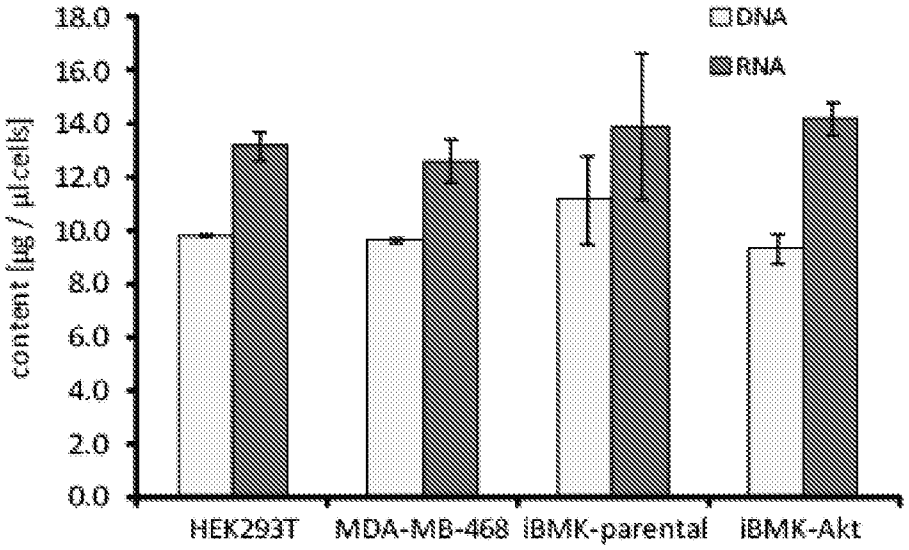

Figure 13E

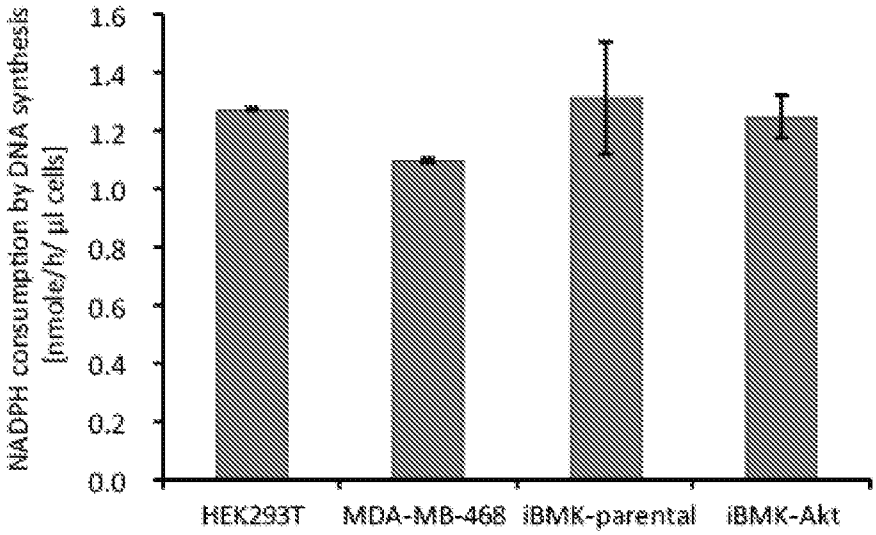

Figure 13F

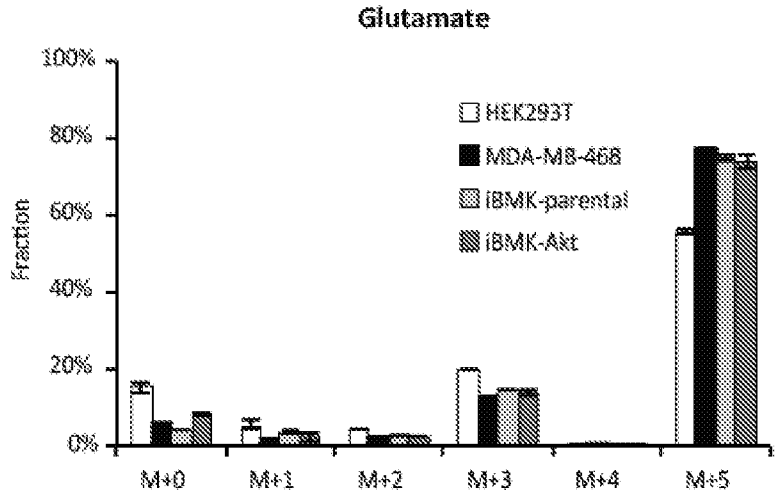

(A)

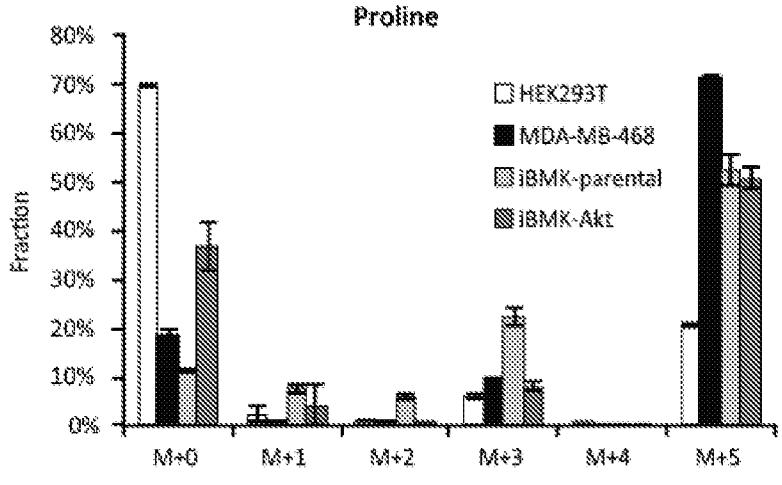

(B)

Figure 13G

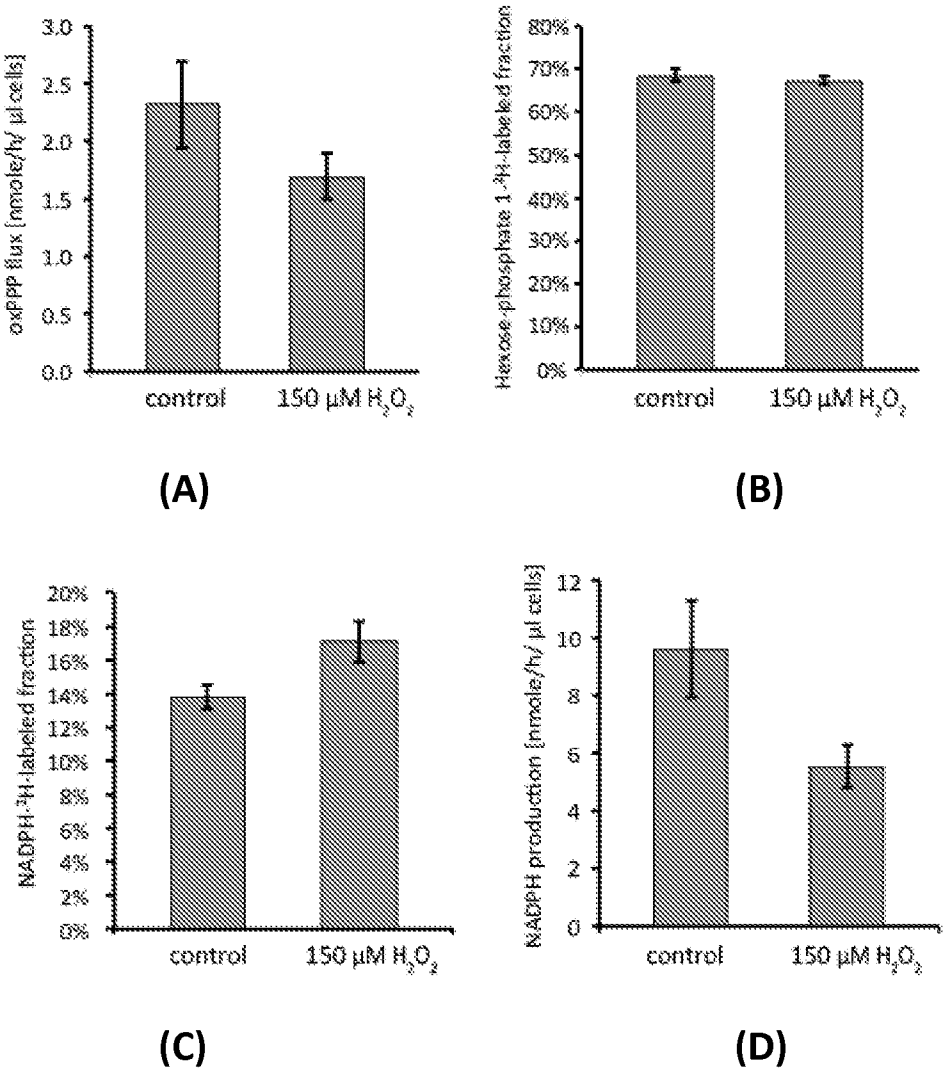
oxPPP flux [nmole/h/ µl cells]
3.0
2.5
2.0
1.5
1.0
0.5
0.0
control
150 µM H_2O_2
(A)
Hexose-phosphate 1-^{3}H-labeled fraction
80%
70%
60%
50%
40%
30%
20%
10%
0%
control
150 µM H_2O_2
(B)
NADPH-^{3}H-labeled fraction
20%
18%
16%
14%
12%
10%
8%
6%
4%
2%
0%
control
150 µM H_2O_2
(C)
NADPH production [nmole/h/ µl cells]
12
10
8
6
4
2
0
control
150 µM H_2O_2
(D)

Figure 13H

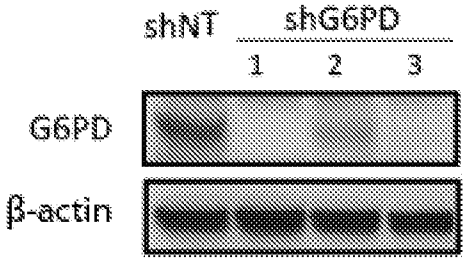

Figure 14A

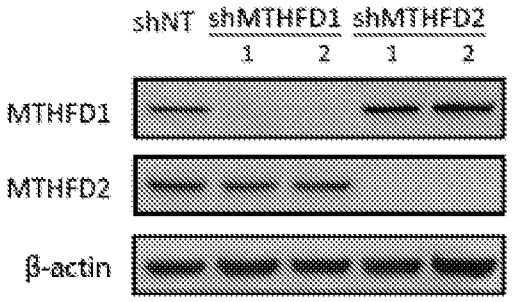

Figure 14B

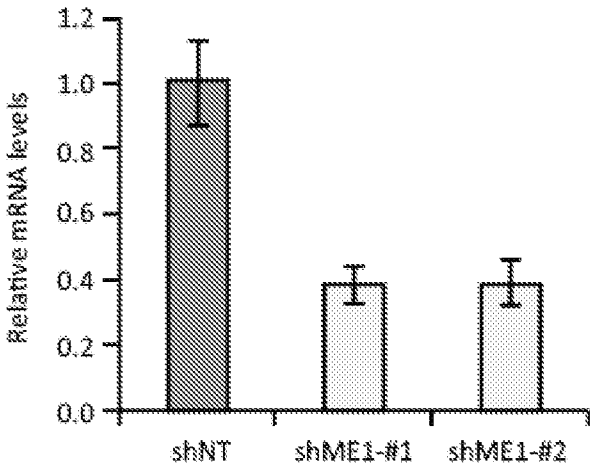

Figure 14C

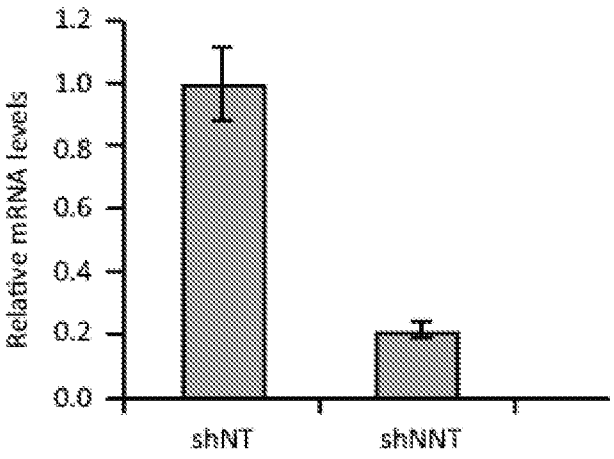

Figure 14D

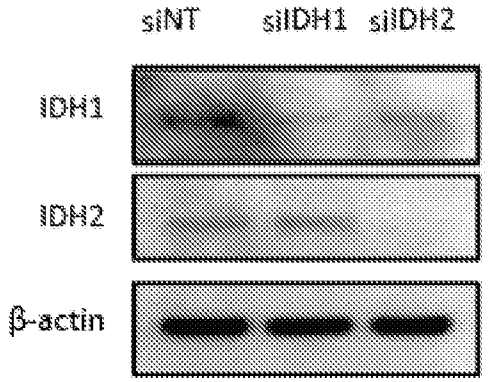

Figure 14E

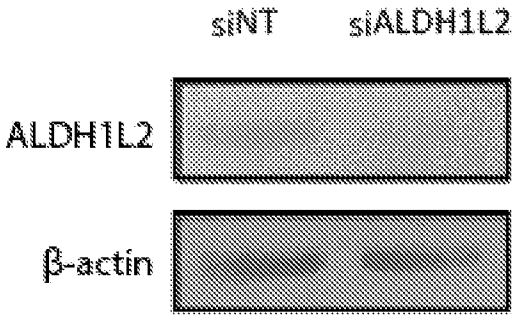

Figure 14F

Cell Doubling Times

shNT	shG6PD	shMTHFD1	shMTHFD2	shME1	shNNT
22 h	38 h	35 h	26 h	24 h	22 h

Figure 14G

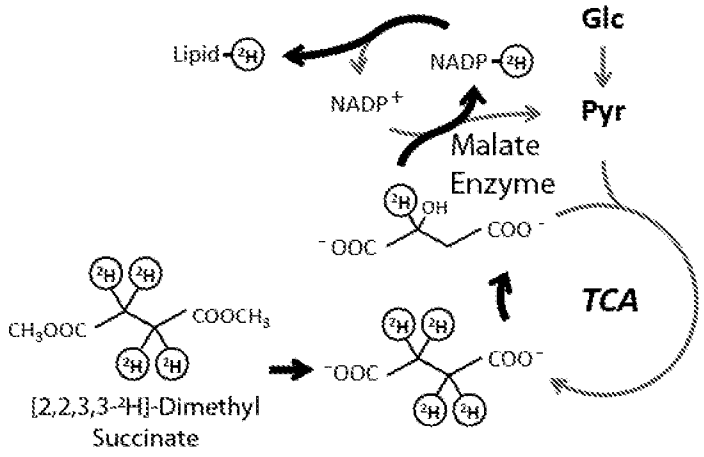

Figure 15A

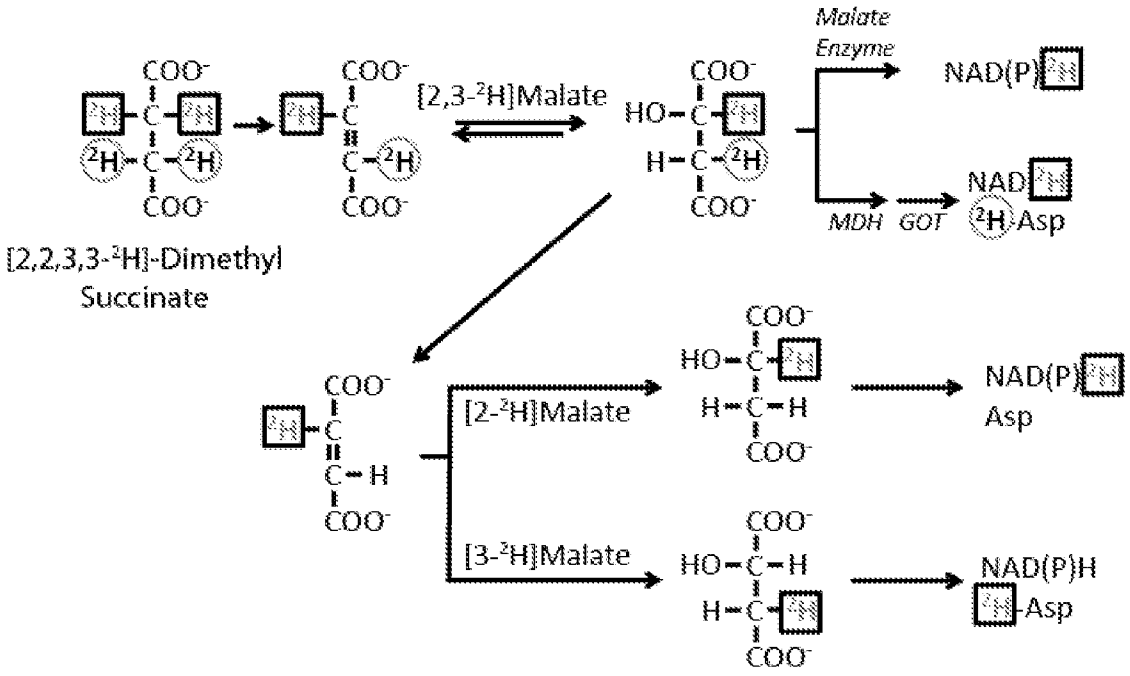

Figure 15B

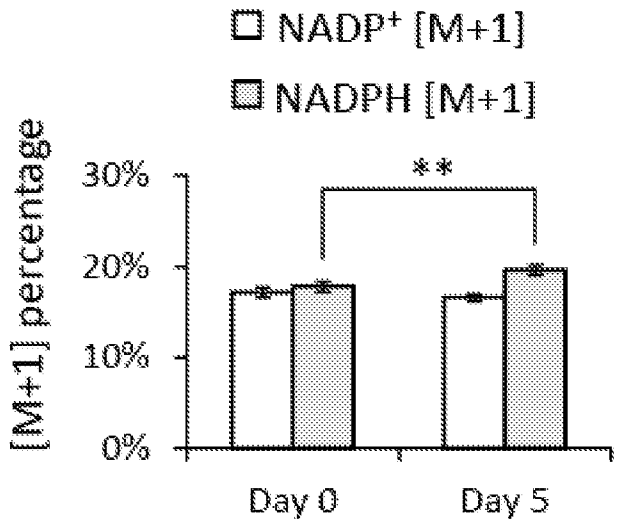

Figure 15C

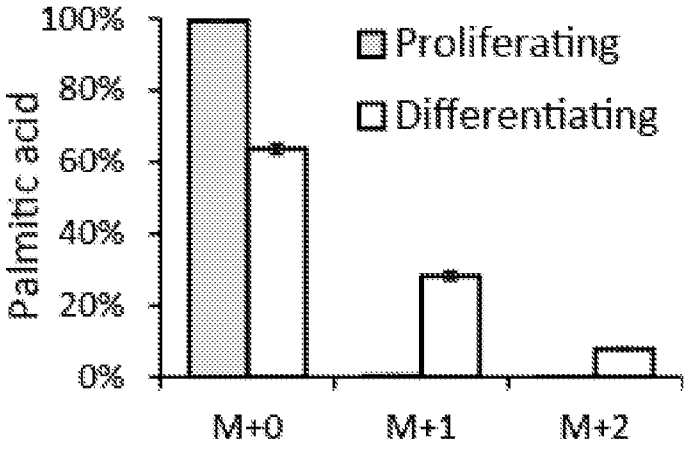

Figure 15D

Isotope	Fraction %
[M+1]Malate	10.9 ± 0.2
[M+2]Malate	1.5 ± 0.1
[M+1]Aspartate	6.0 ± 0.1

Figure 15E

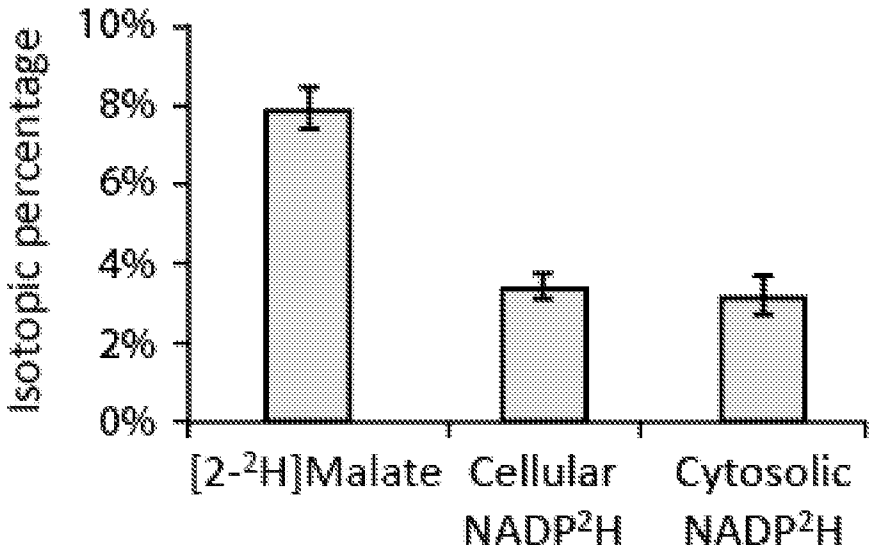

Figure 15F

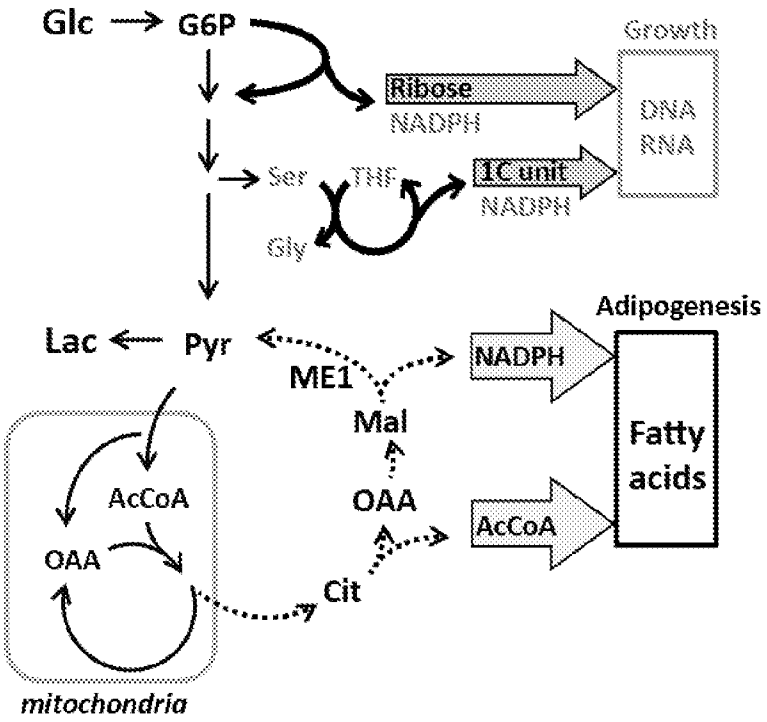
Glc
G6P
Growth
Ribose
NADPH
DNA
RNA
Ser
THF
1C unit
NADPH
Gly
Adipogenesis
Lac
Pyr
ME1
NADPH
Mal
Fatty
acids
AcCoA
OAA
OAA
AcCoA
Cit
mitochondria

Figure 16